



## Durham E-Theses

---

### *Studying the formation of neuromuscular junctions in vitro*

MOBBS, CLAIRE,LOUISE

#### How to cite:

---

MOBBS, CLAIRE,LOUISE (2019) *Studying the formation of neuromuscular junctions in vitro*, Durham theses, Durham University. Available at Durham E-Theses Online:  
<http://etheses.dur.ac.uk/14119/>

#### Use policy

---

The full-text may be used and/or reproduced, and given to third parties in any format or medium, without prior permission or charge, for personal research or study, educational, or not-for-profit purposes provided that:

- a full bibliographic reference is made to the original source
- a [link](#) is made to the metadata record in Durham E-Theses
- the full-text is not changed in any way

The full-text must not be sold in any format or medium without the formal permission of the copyright holders.

Please consult the [full Durham E-Theses policy](#) for further details.



**Studying the formation of neuromuscular junctions *in vitro*.**

Claire Louise Mobbs

A thesis submitted for the degree of Master of Science

Supervisor: Professor Stefan Przyborski

Department of Biosciences

Durham University

DH1 3LE

## **Abstract**

The neuromuscular junction (NMJ) is a specialised structure that acts as a chemical synapse between a motor neuron terminal and muscle fiber end plate. It allows transfer of neural signals resulting in muscular contraction. Although extensively studied, the NMJ still requires investigation, as much remains unknown regarding molecular physiology of the junction in health and in disease. This is in part a result of the challenges faced studying the NMJ in animals and lack of good *in vitro* models.

This project describes the development of a novel co-culture system enabling the potential for the development of neuromuscular junctions *in vitro*. Neurons derived from pluripotent stem cells and an established myoblast lineage were used to produce a robust and reproducible co-culture model whereby neurons and muscle cells developed interactions possessing key characteristics of NMJs. Physiologically relevant structures including terminal boutons and points of co-localisation were observed and subsequently characterised in the model. At these points of co-localisation, acetylcholine receptor clustering and nuclei accumulation was evident. Evidence suggests that certain fundamental aspects of NMJ formation have recapitulated *in vitro*. Building on these observations, preliminary evidence of muscle cell contraction was observed after pharmacological manipulation of cultures. Other developmental aspects were also apparent, including neurite competition at the myotube surface.

In addition, this project investigated the role of Rho A and ROCK signaling during the differentiation of the neurons and myotubes. These molecules are involved in actin cytoskeleton dynamics, but their involvement at the NMJ is poorly understood. This project provides evidence that ROCK-inhibition enhances the growth conditions of neurons and muscle cells whereby C2C12 myotube differentiation and neurite outgrowth was significantly enhanced. Combined, these data provide the potential to increase functional NMJ synapses per unit area, which could prove invaluable in the research of NMJ formation and the evaluation of drugs acting at these synapses.

## **Acknowledgements**

I wish to express complete gratitude to my supervisor Prof. Stefan Przyborski for providing me with the opportunity to work as part of his laboratory whilst providing complete support, patience, and guidance throughout. I would also like to thank Dr. Kirsty Goncalves for her kindness and dedication to helping me succeed, without which, this work would not have been possible.

To all members of the Przyborski group for providing companionship and a lovely working environment: Ben Allcock, for the pre-planned jokes and general disregard for the phonetic alphabet; Henry Hoyle for being Henry Hoyle, a rower and a comedian; Lydia Costello, Nicole Darling and Lucy Smith for always being genuine and accommodating; Steve Bradbury, Amy Simpson, Ariana González, Kelly Choong, and Alex Hidalgo for their positivity and enthusiasm, and Matt Freer for his general persona and love of life. Thank you to Kleo, Eve and Melissa for their friendship and advice.

Also, I would like to thank members of the department including Joanne Robson and Tim Hawkins from Microscopy, for their help in allowing me to produce such a colourful and beautiful thesis.

Finally, I would like to emphasise my gratitude to my parents and my boyfriend Hugh, for always being there and keeping me believing in myself as well as my dreams.

## **Declaration**

This work described herein was carried out in the Department of Biosciences, at Durham University between October 2017 and September 2018. All of the work is my own, except otherwise stated. No part has previously been submitted for a degree at this or other university.

## **Statement of Copyright**

The copyright of this thesis rests with the author. No quotation from it should be published without the prior written consent and information derived from it should be acknowledged.

<b>Abstract</b> .....	<b>i</b>
<b>Acknowledgements</b> .....	<b>ii</b>
<b>Declaration</b> .....	<b>iii</b>
<b>Contents</b> .....	<b>iv-viii</b>
<b>List of figures</b> .....	<b>ix-xi</b>
<b>List of tables</b> .....	<b>xii</b>
<b>Abbreviations</b> .....	<b>xiii-xiv</b>

<b>1.0 Introduction</b> .....	<b>1</b>
1.1 Developmental biology of the central nervous system.....	1
1.1.1 Neural tube formation .....	1
1.1.2 Dorso-ventral patterning during vertebrate neurulation demarcates the developing central nervous system. ....	3
1.1.3 Retinoic acid in development of the central nervous system .....	5
1.1.4 Neuritogenesis .....	7
1.1.4.1 Actin cytoskeleton mobility .....	8
1.1.4.2 Rho / ROCK signalling and neurite outgrowth.....	9
1.1.4.3 Neurite path-finding during neurite outgrowth .....	11
1.2 Mesoderm development and myogenesis .....	12
1.2.1 Mesoderm patterning.....	12
1.2.1.1 Paraxial mesoderm .....	13
1.2.1.2 Myotome development .....	14
1.2.1.3 Genetic network in muscle differentiation.....	14
1.2.2 Myosin heavy chain expression .....	16
1.2.3 Myoblasts and myotubes in forming muscle.....	17
1.2.3.1 Myoblast cell cycle arrest .....	17
1.2.3.2 Myoblast adhesion and alignment .....	18
1.2.3.3 Myoblast fusion .....	18
1.2.3.4 Myotube maturation .....	20
1.2.4 RhoA/ROCK signaling in myotube formation .....	20
1.2.5 Nuclei number and distribution in myotubes.....	22

1.2.6 Acetylcholine receptor distribution in myotubes .....	23
1.2.7 Skeletal muscle innervation .....	24
1.3 The neuromuscular junction .....	24
1.3.1 The presynaptic nerve terminal is a specialized structure .....	26
1.3.1.1 SNARE proteins .....	27
1.3.2 The synaptic cleft .....	29
1.2.3 Post-synaptic membrane specializations .....	29
1.4 Development of neuromuscular junctions .....	30
1.4.1 Acetylcholine receptor (AChR) accumulation .....	31
1.4.1.1 The agrin-MuSk-raspyn-AchR pathway in AChR accumulation .....	32
1.4.1.2 ARIA in AChR accumulation .....	35
1.2.3.2 Nuclei accumulation .....	36
1.4 Investigating the neuromuscular junction .....	36
1.4.1 Diseases involving neuromuscular junctions .....	37
1.4.2 Modeling the NMJ: In vitro vs. in vivo. ....	38
1.4.2.1 <i>In vitro</i> co-culture modeling of the NMJ .....	40
1.4.2.1.1 Homologous vs. heterologous co-culture models .....	40
1.4.2.1.2 C2C12 cell line in co-culture models .....	41
1.4.2.1.3 <i>In vitro</i> co-culture models involving derivatives of pluripotent stem cells .....	42
1.5 Conclusions .....	44
1.5.1 Cell lines used .....	45
1.6 Hypothesis, aims and objectives .....	46
1.6.1 Project hypothesis .....	46
1.6.2 Project aims .....	46
1.6.3 Objectives .....	46
<b>2.0 Materials and methods .....</b>	<b>48</b>
2.1 Cell culture .....	48
2.1.1 Cell line maintenance .....	48
2.1.1.1 TERA2.cl.SP12 .....	48
2.1.1.1.1 Revival and Cryopreservation .....	48
2.1.1.1.2 Maintenance .....	49
2.1.1.2 C2C12 myoblasts .....	50

2.1.1.2.1 Revival and Cryopreservation .....	51
2.1.1.2.2 Maintenance .....	51
2.1.2 Neuron production from stem cells.....	52
2.1.2.1 Neuron production through natural retinoid and dissociation culture ...	52
2.1.2.2 Neuron production through synthetic retinoid and dissociation culture	53
2.1.3 Neurosphere formation .....	54
2.1.4 Induction of neurite outgrowth from neurospheres.....	55
2.1.4.1 Coating of culture plates for neurite outgrowth .....	55
2.1.4.2 Induction of neurite outgrowth.....	55
2.1.4.3 The effect of ROCK signaling on neurite outgrowth.....	56
2.1.5 Myotube formation .....	56
2.1.5.1 The effect of ROCK signaling on myotube formation.....	57
2.1.6 Neuron-myotube co-culture.....	57
2.1.7 Neurosphere-myotube co-culture.....	57
2.1.7.1 Introduction of ROCK inhibitor Y-27632 into co-culture system.....	58
2.1.7.2 Addition of Acetylcholine to the co-culture system .....	59
2.2 Analytical techniques.....	59
2.2.1 Fixation of samples .....	59
2.2.2 Immunofluorescence staining .....	59
2.2.3 Phalloidin staining of F-actin.....	60
2.2.3.1 Phalloidin staining of F-actin in monoculture.....	60
2.2.3.2 Phalloidin staining of F-actin in co-culture .....	61
2.2.4 alpha-bungarotoxin staining.....	61
2.2.4.1 Staining in monoculture.....	61
2.2.4.2 Staining in co-culture .....	61
2.2.5 Summary of antibodies and stained used in analysis.....	62
2.2.6 ImageJ analysis of neurite outgrowth .....	63
2.2.7 ImageJ analysis of myotube number .....	64
2.2.8 MHC quantification.....	65
2.3 Microscopy.....	65
2.3.1 Phase contrast microscopy.....	65
2.3.2 Confocal microscopy.....	65
2.4 Statistical analysis .....	65



<b>3.0 Results .....</b>	<b>67</b>
3.1 Generation of human neurons from TERA2.cl.SP12 stem cells.....	67
3.1.1 Differentiating human neurons from stem cells through exposure to retinoids .....	67
3.1.2 Formation of neurospheres from stem cells through synthetic retinoid exposure.....	68
3.1.3 Neurite outgrowth from neurospheres .....	70
3.1.4 Enhancing neurite outgrowth from neurospheres through ROCK inhibition by Y-27632 .....	72
3.2 Production of myotubes from mammalian C2C12 myoblasts.....	74
3.2.1 Differentiating C2C12 myoblasts into myotubes.....	74
3.2.2 Quantification of the differentiation process .....	77
3.2.3 Assessing contractile apparatus of myotubes .....	79
3.2.4 Enhancement of myogenic differentiation through ROCK inhibition by Y-27632 .....	81
3.2.4.1 Effect of ROCK inhibition on Myosin Heavy Chain expression .....	83
3.2.5 The effect of mitotic inhibitors on myotubes.....	87
3.2.6 Maintaining mature myotubes <i>in vitro</i> .....	88
3.2.7 Acetylcholine receptor distribution in mature myotubes.....	89
3.3 Development of a novel co-culture system for the production of neuromuscular junctions.....	93
3.3.1 Co-culturing dissociated neurons in monolayers on mature myotubes .....	93
3.3.2 Co-culturing neurospheres with myotubes .....	94
3.3.3 Enhancement of neurite outgrowth in co-culture through ROCK inhibition by Y-27632 .....	100
3.3.4 Identification of neuromuscular junctions in co-culture.....	105
3.3.4.1 Fundamental nuclei accumulation .....	105
3.3.4.2 Acetylcholine receptor accumulation.....	106
3.3.4.3 Functional evidence of NMJ formation .....	114
<b>4.0 Discussion .....</b>	<b>116</b>
4.1 Producing human neurons from pluripotent stem cells .....	116
4.1.1 Dissociation culture of human neurons.....	116
4.1.2 Neurosphere formation for neurite outgrowth .....	118
4.1.2.1 ROCK Inhibition enhances neurite outgrowth from neurospheres.....	119

4.2 Producing mammalian muscle from C2C12 myoblasts .....	120
4.2.1 ROCK inhibition enhances C2C12 differentiation .....	123
4.3 Modelling the Neuromuscular Junction <i>in vitro</i> .....	124
4.4 Conclusions .....	134
4.5 Future Directions .....	136
<b>5.0 References .....</b>	<b>139</b>

## List of figures

<b>1.0 Introduction</b> .....	<b>1</b>
Figure 1.1.2: Dorso-ventral patterning in specification of the neural tube. ....	4
Figure 1.1.3: Retinoic acid autocrine signalling mechanism.....	6
Figure 1.1.4.2: Rho A signalling in neurite protrusion and neurite inhibition. ....	10
Figure 1.2.3: Mononucleate myoblasts fuse and elongate to form long, multinucleated myotubes. ....	17
Figure 1.2.4: Hypothesized involvement of Rho A and ROCK signaling in myogenesis .....	22
Figure 1.3: The neuromuscular junction consists of a presynaptic neuron terminal, a synaptic cleft, and a post-synaptic muscle membrane .....	26
Figure 1.3.1.1 SNARE proteins are involved in the trafficking, docking, fusion and exocytosis of synaptic vesicles at the NMJ. ....	27
Figure 1.4.1.1: Hypothesized organization of Agrin-Musk-Raspyn-AChR complex that forms at the developing neuromuscular junction. ....	33
<b>2.0 Materials and methods</b> .....	<b>48</b>
Figure 2.1.1.1.2 – TERA2.cl.SP12 cell population at low (A), medium (B), and high (C) confluence.....	49
Figure 2.1.2.2.2: C2C12 myoblasts at low (A), medium (B), and high (C) confluence..	52
Figure 2.1.4: The Key stages involved in neurite outgrowth for both 2D monoculture and co-culture studies. ....	54
Figure 2.2.6: Neurite quantification was performed using ImageJ. ....	63
<b>3.0 Results</b> .....	<b>67</b>
Figure 3.1.1: TERA2.cl.SP12 stem cells can be differentiated into human neurons through exposure to retinoids using cell dissociative culture method .....	69
Figure 3.1.2: TERA2.cl.SP12 stem cells can be cultured to form neurospheres capable of producing neurites through retinoic acid exposure. ....	71
Figure 3.1.3: Neurites radiate outwards from the central mass of cells of the neurosphere.....	73
Figure 3.1.4-1: The effect of RhoA/ROCK signalling on neurite outgrowth from TERA2.cl.SP12 neurospheres. ....	75
Figure 3.1.4-2: Neurite outgrowth from TERA2.cl.SP12 neurospheres is enhanced in vitro through ROCK inhibitor Y-27632. ....	76

Figure 3.2.1: C2C12 myoblasts fuse and elongate to form multinucleate myotubes upon serum withdrawal.....	78
Figure 3.2.2: Quantification of C2C12 myotubes per day during differentiation. ....	80
Figure 3.2.3: Myosin heavy chain (MHC) expression increases during C2C12 differentiation.....	82
Figure 3.2.4: ROCK inhibitor Y-27632 appears to enhance differentiation of C2C12 myoblasts. ....	84
Figure 3.2.4.1: ROCK inhibitor Y-27632 appears to enhance differentiation of C2C12 myoblasts. ....	85
Figure 3.2.4.1-2: MHC expression increased earlier in differentiation process when myoblasts are differentiated with ROCK inhibitor. ....	86
Figure 3.2.6: C2C12 myotubes can be maintained in vitro following differentiation ..	91
Figure 3.2.7: .....	92
Figure 3.3.1 Neuron endings co-localise with myotubes in co-culture when neurons differentiated from TERA2.cl.SP12 are co-cultured with mature C2C12 myotubes for 5 days. ....	95
Figure 3.3.2-1: TERA2.cl.SP12 derived neurospheres can be co-cultured with mature C2C12 myotubes for 10 days. ....	97
Figure 3.3.2-2: Neuron terminals co-localise with myotubes showing evidence of sites of contact in neurosphere-myotube co-cultures. ....	98
Figure 3.3.2-3: Some neurite branching can be observed in co-culture as well as more than one neurite contacting particular myotubes. ....	99
Figure 3.3.3-1: ROCK inhibitor appears to enhance neurite outgrowth in co-culture. ....	102
Figure 3.3.3-2 –Neurite outgrowth is enhanced in co-culture through ROCK inhibition using 10 $\mu$ M Y-27632. ....	103
Figure 3.3.3-3: ROCK inhibitor Y-27632 enhances both neurite outgrowth and neurite density in monoculture as well as co-culture, although not as effectively in co-culture. ....	104
Figure 3.3.4.1: Neuron terminals co-localise with myotubes at points where nuclei aggregation in myotubes is evident, a key feature of neuromuscular junctions.....	107
Figure 3.3.4.2-1 Positive $\alpha$ -bungarotoxin staining depicts acetylcholine receptor clustering at points of co-localization between neuron terminal and myotube in co-culture.....	109
Figure 3.3.4.2-3: Positive $\alpha$ -bungarotoxin staining depicts acetylcholine receptor clustering at points of co-localization between neuron terminal and myotube in co-culture between dissociative TERA2.cl.SP12 derived neurons and mature myotubes. ....	112

<b>4.0 Discussion .....</b>	<b>116</b>
<b>5.0 References .....</b>	<b>139</b>

## List of tables

<b>1.0 Introduction</b> .....	<b>1</b>
<b>2.0 Materials and methods</b> .....	<b>48</b>
Table 2.2.5-1 – Summary of primary antibodies used in immunofluorescence .....	62
Table 2.2.5-2 – Summary of secondary antibodies used in immunofluorescence. ....	62
Table 2.2.5-3 – Summary of stains used in fluorescence analysis of cultures. ....	62
<b>3.0 Results</b> .....	<b>67</b>
<b>4.0 Discussion</b> .....	<b>116</b>
Figure 4.4: Terminal neuron bouton contacting myotube surface where nuclei accumulation is evident. ....	136
<b>5.0 References</b> .....	<b>139</b>

## List of Abbreviations

°C	Degrees Celsius
ACh	Acetylcholine
AChE	Acetylcholinesterase
AChR	Acetylcholine Receptor
ATRA	All-Trans Retinoic Acid
BDNF	Brain Derived Neurotrophic Factor
BMP	Bone Morphogenetic Protein
CAMKII	Calmodulin Kinase II
ChAT	Choline Acetyltransferase
CO <sub>2</sub>	Carbon Dioxide
DMSO	Dimethyl Sulfoxide
Dkk-1	Dockkopf-1
DMEM	Dulbecco's Modified Eagle's Medium
FBS	Foetal Bovine Serum
EC	Embryonal Carcinoma
ECM	Extracellular Matrix
EC23	Synthetic retinoid
EPP	End-Plate Potential
ES	Embryonic Stem Cell
FGF2	Fibroblast growth Factor 2
FGF7	Fibroblast Growth Factor 7
GAP4	Growth Associated protein 4
IGF	Insulin like Growth Factor
MEF-2	Myocyte Enhancer Factor-2
MHC	Myosin Heavy Chain
mM	Millimolar
MRF	Myogenic Regulatory Factor

MT	Microtubule
NFG	Nerve Growth Factor
NMJ	Neuromuscular Junction
NT-4	Neutrophin 4
OCT	Optimal Cutting Compound
RA	Retinoic acid
RARE	Retinoic acid response element
RARE	Retinoic-acid Response Element
RBB1	Retinol-Binding Protein 1
RBP4	Retinol-Binding Protein 4
RXR	Retinoic-x-Receptor
Shh	Sonic hedgehog
TEM	Transmission Electron Microscopy
Y-27632	ROCK Inhibitor
µg	Microgram
µL	Microlitre
µm	Micrometer
µM	Micromolar



## 1.0 Introduction

### 1.1 Developmental biology of the central nervous system

During early embryogenesis, the three organized germ layers begin to form: the mesoderm, ectoderm and endoderm.<sup>1</sup> These three tissue layers are the fundamental foundation of all of the tissues in the body.

#### 1.1.1 Neural tube formation

The central nervous system, which is comprised of the brain and the spinal cord, is derived from one of the three organized germ layers during early embryogenesis; in particular, this specific outer germ layer, termed the ectoderm, is responsible for giving rise to the central nervous system as well as the epidermis. A function of the nervous system is to collect and process sensory information from the peripheral nervous system in order to coordinate appropriate motor responses.

Formation of the brain and spinal cord begins as a level plate of neuroepithelial cells which later fold to form a neural tube during neurulation. Changes in the shape and distribution of cells at specific locations along the plate allows for tissue bending until closure of the tube. This tube then separates from the overlying ectoderm, followed by specialization of cells to become neural and glial cell precursors.<sup>214</sup> Primary and secondary neurulation lead to the formation of the neural tube in the developing embryo.<sup>1</sup> In primary neurulation, the cells surrounding the neural plate cause the surrounding cells to proliferate and invaginate before these are pinched off to form a hollow tube. Following this, during secondary neurulation, the neural tube arises from a cord of cells that sinks and cavitates in the embryo.

Signaling and expression of certain transcription factors during development of the ectoderm is responsible for the acquisition of coherent neuronal phenotypes.<sup>2</sup> The

ectoderm is responsible for three major processes: formation of the neural plate (which later gives rise to the neural tube and thus, the central nervous system), formation of the epidermis, and formation of the neural crest.<sup>3</sup> These three ectodermal regions become physically and functionally distinct from one another throughout primary and secondary neurulation, during which stage the embryo is termed a neurula. This specification is primarily achieved through finely tuned gradients of signaling activity.<sup>3</sup>

Over recent years, neural tube patterning has been the core of many investigations, elucidating the patterning process along its two major axis: anterior-posterior and dorsal-ventral.<sup>4,5</sup> The first patterning process is the anterior-posterior patterning, which is then followed by dorso-ventral patterning. The exact position of cell within the neural tube determines its fate – defined by the unique signaling gradient specific to that exact location within the neural tube. These signals determine cell fate through activation and repression of transcriptional genes and regulators, ultimately controlling the transcriptional profile of the cell, and thus cell function.<sup>5</sup> Expression profiles consist of overlapping and unique combinations of regulations within a given area, generating discrete populations with a specific cell fate.<sup>6</sup>

The dorsal side of the neural tube gives rise to the neural crest cells – a group of cells that relocate upon closure of the neural tube, whereas the ventral portion of the neural tube gives rise to cells of an epidermal fate.<sup>7</sup> The cells of the neural plate are subject to Sox transcription factors that activate genes involved in the specification of cells to be neural plate, whilst simultaneously inhibiting BMP transcription and signaling.<sup>8</sup> Inductive signals that act on the neural tube can also arise in surrounding tissues, for example from mesodermal or endodermal tissue.

### **1.1.2 Dorso-ventral patterning during vertebrate neurulation demarcates the developing central nervous system.**

A process of neural patterning allows for cell fate determination in the developing nervous system. With regard to the dorsal-ventral axis, a neural cell fate determination occurs during and after neural tube closure based upon two different signaling pathways and their respective expression gradients (Figure 1.1.2). These signaling pathways, namely the Sonic Hedgehog (Shh) and bone morphogenetic protein (BMP) signaling pathways emanate from two opposing signaling centers.<sup>9</sup>

During gastrulation, those cells that reside closest to the ventral part of the ectoderm are subject to sonic hedgehog signaling from the notochord, which promotes a neural fate.<sup>9</sup> These signals have an inhibitory effect on BMPs. Sonic hedgehog inhibits expression of homeodomain transcription factor Pax7, and the gradient of Shh regulates expression of another homeodomain transcription factor, Pax6, in progenitor cells, influencing the phenotype of the developing neurons.<sup>10</sup>

Conversely, in the ventral portion of the ectoderm, the cells are not subject to these inhibitory signals and thus acquire an epidermal fate as a result of BMP and Wnt signaling.<sup>11</sup> In the spinal cord, the most ventral cells are those of the floor plate. Adjacent to these floor plate cells are the motor neurons. The signaling determining cell fate arises from the notochord, a structure which itself is also induced through sonic hedgehog signaling factors.<sup>12</sup> The initial induction of the floor plate is contact-dependent whereas motor- neuron induction is non-contact dependent.<sup>12</sup> This is due to the fact sonic hedgehog exists as a membrane bound protein and as a soluble secreted factor involved in motor neuron differentiation.<sup>13</sup> As a ventralising factor, Sonic hedgehog functions by inducing or repressing the expression of transcription factors within the nucleus of developing cells.<sup>14</sup>

In the neural tube for example, Pax3 and Pax7, as well as Msx1 and Msx2 are inhibited

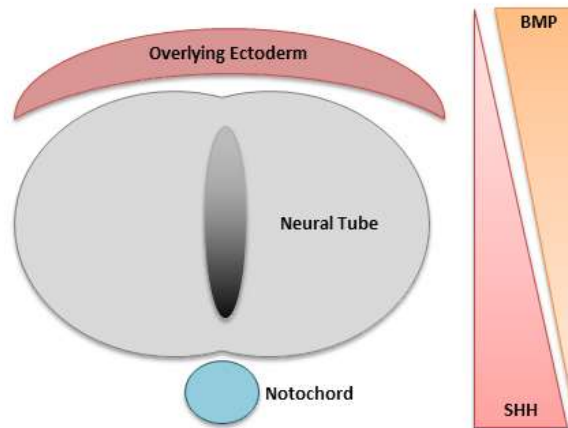


**Figure 1.1.2: Dorso-ventral patterning in specification of the neural tube.** The neural tube is influenced by two key signalling centres, including Shh from the notochord and BMP's (BMP4 and BMP7) from the overlying ectoderm. Neurons of the spinal cord are subjected to a gradient of these paracrine factors, determining their cell fate.

whereas nkx2.1 and nkx2.2 are up-regulated by Shh, thus impacting neural fate.<sup>15</sup> Conversely, the most dorsal cells are those of the roof plate, with the adjacent cells being of a sensory neuron phenotype. The epidermis immediately adjacent to the neural plate produces signaling capable of inducing cell differentiation of both roof plate and neural crest cells. BMP induces a signaling cascade. Sonic hedgehog not only acts as an inducer of a ventral phenotype, but also aids in specifying neurons of a motor phenotype.<sup>16</sup>

Changes in the expression of patterning genes are essential for the identity and function of the cells the ectoderm gives rise to. Dorsoventral patterning thus influences the pluripotency and differential state of cells.<sup>17</sup> Retinoic acid contributes to both dorsoventral and anteroposterior patterning of the neural plate along with Wnts and fibroblast growth factors.<sup>18</sup> The relative quantities of morphogens such as RA, Shh and BMP in the developing neural tube give rise to specific cell types that develop from

resident stem cells.<sup>18</sup> Therefore, fully understanding the signaling pathways activated by such morphogens, can help elucidate the mechanisms behind neural differentiation of stem cells and can be used *in vitro* to generate populations of cells.

### **1.1.3 Retinoic acid in development of the central nervous system**

Retinoic acid (RA) is a metabolic derivative of Vitamin A. There are many important signaling molecules involved in nervous system development including RA. It is an important signaling molecule during embryonic development with a plethora of effects *in vivo*; these include influencing neural tube development and patterning of the nervous system, contributing to both antero-posterior and dorsoventral patterning of the neural plate and neural tube as well as neuronal differentiation.<sup>19</sup>

Retinoic acid cannot be synthesized by the mammalian body, and thus requires obtainment through diet. RA is stored as retinoids in the liver as well as the lungs, bone marrow, and kidneys until required. At this point, retinoids are transported by retinol bound to retinol-binding protein 4 (RBP4), which is then taken up by target cells through membrane receptors RBP4 and STRAT6.<sup>20</sup> Here, in the cytosol, retinol binds retinol-binding protein 1 (RBP1), resulting in its metabolism into all-*trans* retinoic acid (ATRA). RA can then act in autocrine or paracrine fashion.

In autocrine signaling, the mechanism of action of RA is dependent on specific nuclear ligand-activated transcription factors consisting of a heterodimer comprising the RA-receptor (RAR), and the retinoic-X-receptor (RXR) – see Figure 1.1.3. These receptors bind a DNA-sequence termed the retinoic acid response element (RARE).<sup>21</sup> As a result of ligand-receptor binding, induction of expression of over 500 genes can occur, changing the identity of the cell and thus influencing differentiation.<sup>21</sup> Following activation of transcription, ATRA exits the nucleus, where it is catabolized by CYP26 enzymes.<sup>22</sup>

In antero-posterior patterning, retinoic acid induces posterior hindbrain and anterior spinal cord organization.<sup>23</sup> In the absence of RA signaling, hindbrain formation is perturbed as well as spinal cord formation, emphasizing its importance in antero-posterior patterning.<sup>24</sup> Studies into the absence of retinoic acid during embryonal development also demonstrate its importance in dorso-ventral patterning.<sup>25</sup> Along with the Shh and BMP gradients in the developing central nervous system, retinoic acid is involved in induction of a subset of ventral interneurons as well as the specification of motor neuron subtypes. RA induces induction of a neuronal phenotype through inductive expression of transcription factors (NFkB, SOX1 and SOX6), structural proteins, cell surface receptors, as well as signaling proteins.<sup>16</sup> Additionally, RA has a suppressive role in signaling pathways through inducing expression of Dkk-1, an inhibitor of the Wnt signaling pathway, resulting in neuronal differentiation.<sup>16</sup>

Consequently, RA has been in many *in vitro* investigation involving stem cells, utilizing its

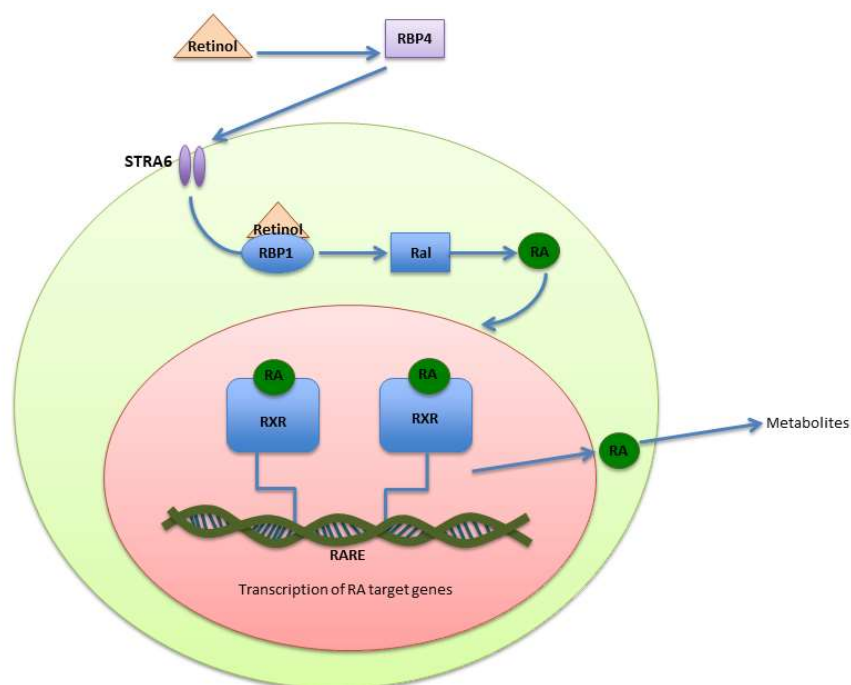


**Figure 1.1.3: Retinoic acid autocrine signalling mechanism.** Retinol binding protein 4 (RBP4) transports retinol to cells where they enter via a specific transmembrane receptor – STRA6. Retinol becomes bound to RBP1, where it is metabolised to Ral and then to RA by specific enzymes Retinaldehyde dehydrogenases before it moves into the nucleus. Inside, it binds retinoic acid receptors (RXRs), which then form a heterodimer that binds to retinoic-acid response element (RARE) on DNA. This results in the transcription of target genes.

ability to induce a neural phenotype. RA has been used in neurogenesis studies using both embryonic stem cells and embryonal carcinoma cells as a patterning and neuronal inducing factor.<sup>26, 27</sup> In the case of nerve regeneration in the central nervous system, it has been proven that RA is capable of inducing neurite outgrowth and thus can mediate production of differentiated neurons.<sup>28</sup>

### **1.1.4 Neuritogenesis**

The function of the nervous system is dependent upon the complex neurite circuitry that comprises it. Despite the heterogeneity of neuronal phenotypes in the developing nervous system, they all develop in a similar step-wise, dynamic process. First, budding occurs, followed by neurite extension, followed by axon/dendrite maturation.<sup>28</sup> During the neuritogenesis stage, the process by which cytoskeletal processes called neurites extend from the cell body of the developing neuron, occurs in three distinct stages: neurite induction; formation of primary neurites; followed by axon/dendritic polarization.<sup>29</sup> Neurites extend from the cell body of the developing neuron, directed from the distal tip, otherwise known as the growth cone, leading to the formation of a mature axon. This process requires neuronal cell polarity and is strongly influenced by biochemical and extracellular components, particularly extracellular matrix proteins. This extension involves cellular movement and migration, which itself critically depends on membrane turnover, actin reorganization, adhesion molecules and cytoskeletal dynamics.<sup>30</sup>

*In vitro* studies have elucidated the influence of these extracellular influences, along with signaling cascades such as WNT signaling on neuritogenesis. Extracellular matrix proteins heavily influencing neuritogenesis include tenascins, collagen, laminin, and Slit proteins.<sup>31</sup> These molecules have extensive influence on the growth and migration of neurites; the signaling emitted by the extracellular environment can be of a positive, negative or guiding in nature. Early morphology and orientation of neurites is regulated

by HB-GAM (heparin-binding growth-associated molecule), as well as adhesive glycoproteins and glycosaminoglycans.<sup>29</sup> Soluble molecules are also involved in early neuronal differentiation – including fibroblast growth factors, FGF2 and FGF7, insulin like growth factor (IGF), and neurophins.<sup>29</sup>

The neurophin family, including nerve growth factor (NGF), brain-derived neurotrophic factor (BDNF), neurotrophin-3 (NT-3), and neurotrophin 4 (NT-4), interact with specific receptors including tropomyosin-related kinase and p75 receptors.<sup>29</sup> This causes activation TRk receptors, triggering intracellular signaling cascades that ultimately result in growth and survival of neurites.<sup>29</sup> Cell adhesion molecules drive precise axonal path finding and targeting during neuritogenesis, including N-cadherin, L1 and NCAM.<sup>32</sup> Studies have shown that there is heterophilic interaction between L1 and axonin-1 during the process of targeting involved in neurite outgrowth.<sup>33</sup>

Neurite outgrowth also entails the activity of the tyrosine kinase receptor function of FGFR. Studies showing FGFR knockout demonstrate that neuritogenesis ceases and thus FGFR is required in this process.<sup>34</sup> The signaling cascade triggered upon FGFR activation involves  $Ca^{2+}$  and MAP-kinase whereby  $Ca^{2+}$  is essential for growth cone assembly.<sup>33</sup> This calcium dependent signaling is known to activate calmodulin kinase II (CAMKII) and growth-associated protein-4 (GAP-3), which are required for neuritogenesis.<sup>33</sup>

#### **1.1.4.1 Actin cytoskeleton mobility**

For neurite extension to occur, actin reorganisation is essential for driving morphological change of the neurite. Investigation into actin turnover rates showed that this influences the basis of neurite outgrowth or quiescence.<sup>35</sup> Neurite extension occurs when actin remodelling occurs within the neuronal cell body, producing filopodia or lamellipodia that function as the growth cone in neurite extension.<sup>36</sup> The growth cone at the distal tip has abundant actin fibrils. This actin framework has intrinsic adhesion function necessary for growth cone extension and thus extension of the neurite. This



actin framework undergoes polymerisation at the leading edge and depolymerisation at the lagging end, a process that drives neurite projection.<sup>35</sup>

The process of actin polymerisation and depolymerisation is regulated by actin-binding proteins; these proteins control the nucleation as well as the distribution of actin within the neuron.<sup>38</sup> Actin filaments polymerise from existing filaments resulting in a branched framework of actin, a phenomenon believed to involve the evolutionarily conserved Arp2/3 branched nucleator complex. Arp2/3 nucleates polymerization of these new axon filaments and requires nucleation promoting factors including members of the WASP family. Specifically, N-WASP binds Arp2/3, resulting in conformational changes allowing the complex to bind to existing actin filaments and initiating new actin filament outgrowth.<sup>37</sup> VEGF has recently been postulated to mediate activation and colocalisation of cofilin and Arp2/3 to the actin cytoskeleton.<sup>37</sup> However, controversial evidence remains for the exact role of the complex in neurite extension. Proteins involved in microtubule stabilization, for example, MAP1B as well as destabilizing proteins including stathmin-like-2 are involved in actin motility and thus neurite outgrowth. MAP1B is also involved in microtubule nucleation.<sup>38</sup>

#### **1.1.4.2 Rho / ROCK signalling and neurite outgrowth**

Although much remains unknown regarding the intracellular dynamics of the neurite during neuritogenesis, certain pathways pivotal to the actin dynamics have been elucidated. One such actin-regulating pathway of particular importance is the Rho A / ROCK signaling pathway. Actin polymerisation and depolymerisation is a process that is dependent upon Rho GTPases and thus the Rho signaling pathway.<sup>39</sup> The Rho family of proteins are low molecular weight guanine nucleotide binding proteins, including Rho A,

Rac1 and Cdc42, all of which are involved in neurite outgrowth and guidance.<sup>40</sup> Through loss- and gain- of function experiments, it was found that Rho A and downstream effector, ROCK, are involved in negative regulation of the initial sprouting stages of neuritogenesis.<sup>41</sup>

It is thought that a membrane receptor becomes activated, resulting in the transmission of signals via guanine-activating-proteins (GAPs) to effector proteins.<sup>40</sup> Activation of the Rho signaling pathway is shown to negatively affect neurite outgrowth by affecting actin stability.<sup>42</sup> During neurite inhibition and retraction, a growth-discouraging signal is conveyed by a series of intracellular events. This occurs following an intracellular signaling cascade whereby it is believed that Rac and downstream effector Wasp are

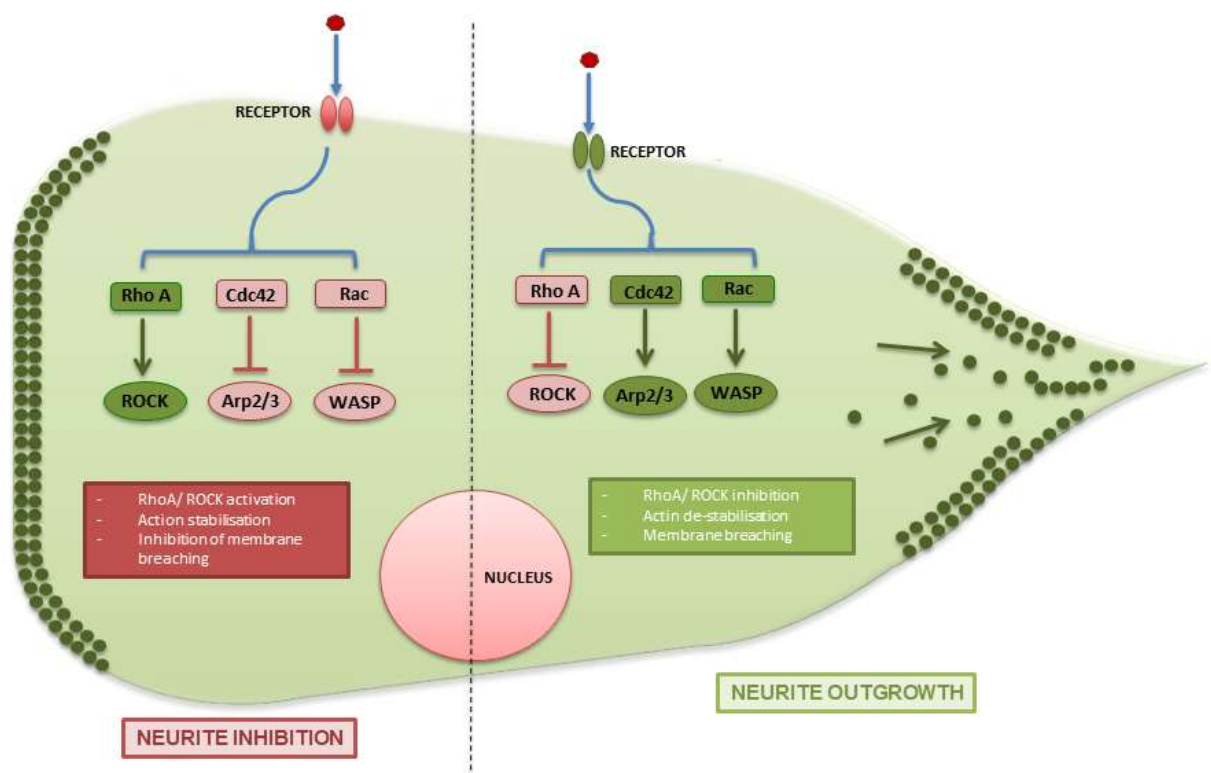


**Figure 1.1.4.2: Rho A signalling in neurite protrusion and neurite inhibition.** Extracellular signals result in the activation of Rho GTPases including Cdc42 and Rac and inhibition of Rho A. Activation of downstream molecules Arp2/3 and WASP, with downstream effector ROCK inhibited results in instability of actin microtubules, membrane breaching and neurite outgrowth. Upon Rho A activation, the opposite occurs, with subsequent promotion membrane stability and neurite inhibition.

deactivated, as well as Cdc42 and its downstream effector complex Arp2/3, whilst Rho A and downstream effector ROCK are activated.<sup>35</sup> This intracellular cascade results in actin stability and inhibition of membrane breaching. As such, studies have shown that constitutive or increases expression of RhoA is responsible for neurite arrest and retraction.<sup>43</sup> Conversely, when a growth favoring stimuli is encountered, a different intracellular signaling cascade is initiated. Instead, RhoA and downstream effector ROCK are inhibited, whereas Rac and Cdc42 are activated, along with their respective effectors.<sup>35</sup> Ultimately, this causes instability of the actin network at the leading edge of the neurite, allowing for membrane breaching and neurite extension through microtubule penetration of the membrane. Through exploitation of the aforementioned intracellular events, some studies of neurite outgrowth have investigated the potential of certain molecules to enhance neurite outgrowth *in vitro*. C3 transferase, an inhibitor of RhoA has commonly been used to increase neurite outgrowth from neural stem cells.<sup>44</sup>

#### **1.1.4.3 Neurite path-finding during neurite outgrowth**

As already mentioned, the ECM plays a crucial role in the neurite outgrowth process, through providing points of adhesion, neurite growth cues, as well as a favorable environment for the growing neurite.<sup>45</sup> Integrin receptors located on the developing growth cone have been postulated to be involved in the transmission of ECM cues to the developing neurite. ECM components, including laminin, collagens, tenascins, fibronectin among many others, creating a heterogeneous mixture consisting of proteoglycans and glycoproteins that provide a scaffold supporting cellular adhesion.<sup>45</sup> Laminins represent the most commonly studied ECM component, and are thought to be one of the strongest promoters of neurite growth and is therefore found in abundance in the nervous system, especially during development.<sup>46</sup> These heterotrimeric proteins consist five  $\alpha$ , three  $\beta$ , and three  $\gamma$  chains have been identified, giving rise to the many different laminin isoforms.<sup>47</sup> Furthermore, specific integrins propagate the effects of each laminin isoform.<sup>48</sup> Tenascins are oligomeric glycoproteins that can have inhibitors

or promoting influences on neurite outgrowth.<sup>49</sup> Specifically, FN-II domain is thought to be adhesion promoting.<sup>49</sup>

## **1.2 Mesoderm development and myogenesis**

The mesoderm is also one of the three germ layers produced following gastrulation. It is responsible for the generation of many organs and systems in the mammalian body, including the musculoskeletal tissues. The mesoderm is divided into four sections as a result of patterning events: the axial mesoderm (notochord), lateral-mesoderm (cardiac), paraxial mesoderm (somites), and the extraembryonic mesoderm, each giving rise to different cell types and tissues.<sup>50</sup>

On either side of the notochord, lies paraxial mesoderm, otherwise called the somatic mesoderm.<sup>51</sup> The tissues that emanate from this region will be located at the back of the organism. The cells of the somatic mesoderm form somites, blocks of mesodermal cells that produce muscle as well as connective tissues of the back. These somatic tissue blocks are initially pseudo-stratified epithelial progenitors, but as they mature, they receive specific signals from the notochord, neural tube, lateral-mesoderm and ectoderm.<sup>52</sup>

### **1.2.1 Mesoderm patterning**

The mesoderm is also specified by signaling gradients, similar to that of the ectoderm. The mesodermal subdivisions are believed to be patterned through mediolateral patterning – from the centre to the side - through increasing concentrations of bone-morphogenetic-proteins.<sup>51</sup> Elucidation of this BMP signaling using chick embryos has revealed that the more central areas of the mesoderm express less BMP4 than the more lateral mesoderm.<sup>53</sup> As well as this, by changing the expression levels of BMP within the mesoderm, it is possible to alter the phenotypic profile of the resulting cells produced.<sup>54</sup> It is believed that BMP expression affects Fox expression, as different Fox transcription factors are expressed in different regions of the mesoderm. For example, Foxc1 and

Foxc2 are found to be expressed in paraxial mesoderm, whereas Fox1 expression can be observed in extraembryonic and lateral mesoderm areas.<sup>55</sup>

### 1.2.1.1 Paraxial mesoderm

Paraxial mesoderm specification appears to be the result of Noggin antagonisation of BMPs, which is synthesized in the presomitic mesoderm.<sup>56</sup> The formation of somites within the paraxial mesoderm occurs along an anterior-posterior axis.<sup>56</sup> This is determined by numerous signaling gradients including Notch/Wnt signaling, FGF and retinoic acid signaling.<sup>57</sup> Notch/Wnt signaling in particular, is important for determining positional identity of somite formation.

Somites divide into three compartments: sclerotome, myotomes and dermamyotomes. The sclerotome is responsible for formation of vertebrae and the cartilage of the ribcage, the myotome is responsible for producing muscle of the back, and the dermamyotome is responsible for skeletal musculature progenitor cells.<sup>52</sup>

Paired homeobox genes, (Pax genes) are a highly conserved set of genes containing a DNA-binding domain termed a paired domain (PD).<sup>58</sup> Pax genes comprise a family of genes pivotal to specification and maintenance of progenitor cells.<sup>52</sup> Pax3 and Pax7 are expressed in somitic cells, and are involved in the specification of muscle progenitors.<sup>59</sup> Pax3 in particular is expressed in dorsal cells of the neural tube, where it has been shown through mutation studies to be involved in the regulation of hepatocyte-growth factor, ultimately playing a role in muscle progenitor migration to the limb bud during myogenesis.<sup>60</sup> Pax3 is also involved in the direct activation of *Myf5* and *FoxC2*. The function of Pax3 largely depends on the presence of two highly conserved DNA binding domains.<sup>60</sup>

### **1.2.1.2 Myotome development**

The skeletal muscle mass found in the vertebrate body emanates from the dermamyotome.<sup>61</sup> The Myotome resides laterally of the dermamyotome. Skeletal muscle forms from progenitor cells that originate in dermamyotome, later emigrating to the limb bud, where they proliferate and lead to differentiation through expression of myogenic determination factors.<sup>62</sup>

Induction of the myotome in the somite occurs at two distinct areas of the somite.

The hypaxial myotome is patterned through BMP4 and Wnt7a signaling from the overlying ectoderm.<sup>63</sup> In the medial myotome, factors of the neural tube such as Wnt1 and Wnt3a act upon the cells as well as low levels of Shh from the floor plate of the neural tube and the notochord.<sup>63</sup>

Migrating neural crest cells appear to affect the development of the myotome. These delta-expressing neural crest cells migrate and make contact with primaxial mesoderm cells, aiding in the expression of myogenic regulatory factors.<sup>59</sup> Moreover, the migrating cells secrete neuregulins, neuregulin-1 in particular, which is involved in myoblast phenotype maintenance.<sup>64</sup>

### **1.2.1.3 Genetic network in muscle differentiation**

This multistep process is controlled by muscle specific transcriptional regulators involved in cell fate determination, as well as external signals that pair the process of myogenic differentiation to the development and growth of the mammal.

At the molecular level, the major transcriptional determinants of muscle differentiation are myogenic regulatory factors (MRFs – often referred to as bHLH proteins), including Myf5, myogenin, MyoD and myogenic regulatory factor-4 (MRF4).<sup>65</sup> These myogenic regulatory factors are basic helix-loop-helix transcription factor family members involved in the proliferative, precursor cell irreversible cell cycle arrest and withdrawal,

and muscle specific gene activation, ultimately resulting in production of a muscle phenotype. These MRF proteins form heterodimers with ubiquitously expressed E proteins. Following this, they bind specific DNA sequences termed an E-box (CANNTG), which is found in the promoter sequence of almost all muscle regulatory protein genes.<sup>66</sup>

The importance and potency of the MRF family has been demonstrated in *in vitro* studies whereby induction of their expression in non-myogenic fibroblastic cell lines is enough to induce differentiation into myoblastic cell types.<sup>67</sup> Each MRF is responsible for the activation of other MRF family members, and thus a powerful positive feedback mechanism exists, allowing for a defined sequence of expression.<sup>68</sup> Genetic studies involving mice have shown that Myf-5 and MyoD are expressed in the proliferating, undifferentiated cell, thus shown to be involved in muscle progenitor specification. (m) Interestingly, MRF4 is expressed in both proliferative and differentiated cell stages. Conversely, myogenin expression can be observed in differentiated cell types.<sup>69</sup> It appears that MyoD is responsible for the direct activation of the muscle-specific-creatine-phospho-kinase gene, as well as acting as a positive activator of itself.<sup>70</sup>

As well as MRF's, the MADs-box myocyte enhancer-binding factors, part of the MEF2 family, are involved in myogenic determination.<sup>71</sup> The function of the MRF family is dependent upon this second family of proteins – the myocyte enhancer factor-2 proteins (MEF2).<sup>72</sup> These proteins are indispensable for muscle differentiation, although lack the ability to induce differentiation by themselves, unlike the MRF family.<sup>66</sup> They are also found in other tissue types, and are therefore not exclusive to skeletal muscle. MRFs and MEF2 transcription factors interact, forming a complex and hence synergistic regulation of transcription in myogenesis.<sup>73</sup> The myogenic program activated by the two families is very tightly tuned, through activation and repression of each other's transcription.<sup>73</sup> For example, MyoD is involved in the expression of MEF2c, and myogenin is involved in activation of MEF2 expression; therefore these two families of

proteins function combinatorially in the differential process.<sup>74</sup> MyoD is also involved in the negative regulation of expression of myoblastic genes, and studies show that for differentiation to occur, MyoD function switches from a repressor to an activator.<sup>59</sup> MRFs are secreted by myoblasts, progenitor cells committed to a muscle lineage.

### 1.2.2 Myosin heavy chain expression

Myosin heavy chain (MHC) is a motor protein of skeletal muscle thick filaments, constituting part of their contractile apparatus.<sup>75</sup> Myosin heavy chains are alpha-helical rods consisting of an N-terminal head domain and a C-terminal tail, two of which form a coiled-coil dimer, holding the chains together. The protruding head binds to actin on the thin filament, and is responsible for actin-based, ATP-dependent motility of skeletal muscle contraction as a result of conformational changes.<sup>76</sup>

Although there exists slight variation between different isoforms, myosin heavy chain is expressed late in myogenesis.<sup>77</sup> *In vitro* muscle differentiation studies using C2C12 myoblasts, a murine cell line, have showed that MHC expression, generally, increases significantly around day 4 of differentiation; this is late on in the differentiation phase, as mature myotubes can be observed around day 5 of differentiation.<sup>77</sup> Quantification saw a rise of MHC as a percentage of total cellular protein content from 2.62% in dividing myoblasts, increasing to 6.37% in early myotubes.<sup>78</sup>

Much remains unknown about the regulated expression of each MHC isoform. *In vitro* and *In vivo* studies have suggested that many cellular processes are involved, some of which occurring at the myoblast stage, but mostly in microtubule stage.<sup>79, 80</sup> In the mammalian muscle however, extrinsic factors are also involved; these include hormone levels, and local innervation.<sup>81</sup> It is not yet known if expression of myogenic regulatory factors, as discussed in the previous section, are involved in MHC expression.



### 1.2.3 Myoblasts and myotubes in forming muscle

Muscles consist of cells that work as a unit, rather than individual cells like that of the rest of the body. These units consist of cytoskeletal systems comprising microfilaments, intermediate filaments, and microtubules. These three cytoskeletal components are required for muscle cell viability and shortening to develop force during contraction.<sup>82</sup>

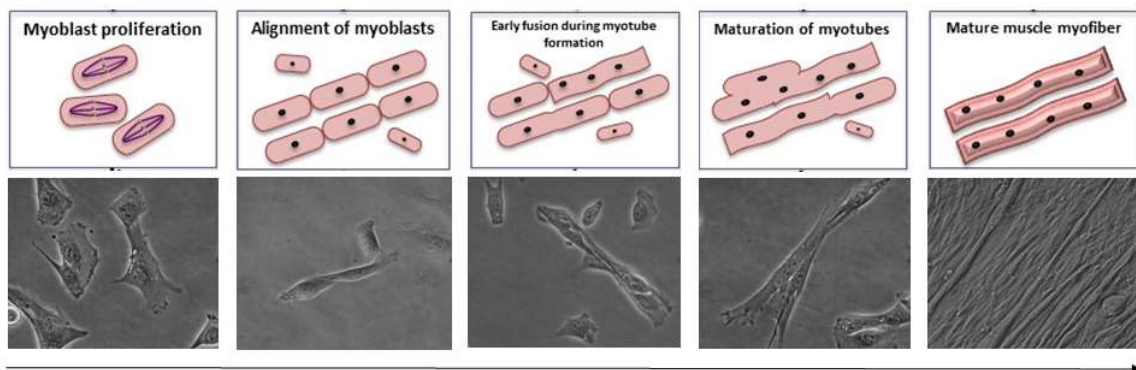


**Figure 1.2.3: Mononucleate myoblasts fuse and elongate to form long, multinucleated myotubes.** Myoblasts exist as mononucleate single cells. Upon initiation of differentiation, myoblasts withdraw from the cell cycle and initiate their myogenic process. These cells align into rows and fuse their membranes, and elongate longitudinally, eventually becoming long, multinucleated myotubes. Nuclei distribute along the length of the myotube. The process of differentiation is illustrated here using murine C2C12 cell line.

The dramatic morphological change during myogenesis is largely a result of actin remodeling and reorganization; during which, mononucleate myoblasts migrate, align, perform target recognition, and fuse their membranes - forming a single, continuous, multinucleated cell.<sup>83</sup>

#### 1.2.3.1 Myoblast cell cycle arrest

Before myoblast fusion occurs, the myoblasts irreversibly withdraw from the cell cycle to become post-mitotic, a process involving Shh signaling.<sup>82</sup> During this, cell cycle inhibitor p21 expression is increased, and is pinpointed to be involved in the coupling of cell cycle withdrawal and initiation of myogenic differentiation; this increase in p21 correlates with decreased cyclin-dependent kinase activity, a molecule crucial in cell

cycle regulation.<sup>84</sup> Furthermore, the upregulated p21 is known to be involved in protecting differentiated cells against apoptosis, and thus differentiated myotubes exhibit decreased propensity for undergoing apoptosis.<sup>82</sup>

### **1.2.3.2 Myoblast adhesion and alignment**

Following exiting the cell cycle, proteins are secreted by myoblasts into the extracellular matrix (ECM), including fibronectin. Here, fibronectin acts as a substratum for adhesion, and binding occurs through alpha-5-beta-1 integrin, a pivotal ECM receptor.<sup>253</sup> In particular, *in vitro* studies demonstrate that fibronectin is required for attachment of myoblasts to collagen.<sup>252</sup> This fibronectin secretion can be visualized microscopically, where fibronectin fibrillar networks extend into ‘footprints’ at abutting surfaces of myoblasts.

Next, the myoblasts align in a linear array. This step involves glycoproteins, including cadherins – calcium dependent cell adhesion molecules (CAM) involved in the formation of cell-cell junctions.<sup>85</sup> Only myoblasts are able to fuse with each other, and prior to stimulation of fusion, the cytoplasm is reorganized before actin reorganization begins.<sup>85</sup>

### **1.2.3.3 Myoblast fusion**

The stimulating this fusion process is unknown, but it is known that calcium influx is essential.<sup>86</sup> Upon stimulation, calcium transporters are activated, including A23187 – these transport calcium ions into the myoblasts.<sup>85</sup> Many molecules are involved in this process, including transcription factors, membrane proteins and secreted molecules.<sup>87</sup> Much of the molecular biology behind myoblast fusion however, remains unknown.

Matrix metalloproteinases (MMPs) are a group of enzymes that selectively digest ECM components.<sup>88</sup> They have been subject of *in vitro* studies – whereby they have been shown to be implicated in myoblast migration and fusion.<sup>89</sup> MMP-1 for example, is upregulated in the myoblast before migration, and C2C12 myoblasts treated with MMP-

1 exhibit increased migrational capacity.<sup>89</sup> Investigation into MMP involvement in fusion events suggests that they may function to eliminate ECM components between potential fusing myoblasts.<sup>89</sup> Meltrins are a group of MMPs, and recent reports outline the involvement of meltrin- $\alpha$ , meltrin- $\beta$  and meltrin- $\gamma$  in myoblast fusion.<sup>90</sup>

Studies have shown that phosphatidylserine is involved in this fusion process.<sup>91</sup> It is found to be transiently expressed at the cell surface of skeletal myoblasts as well as at cell-cell junctions, but its mechanism of action remains unknown. Phosphatidylserine function was shown to be facilitated by proteins including Stabilin-2 (Stab-2), a type-I protein transmembrane receptor that is expressed by myoblasts during myogenesis.<sup>91</sup> Stab-2 is regulated by calcineurin signaling, and is proven to be pivotal to membrane fusion in mutation studies whereby stab-2 deficiency results in formation of small, thin myotubes, and few nuclei as a result of reduced phosphatidylserine-dependent fusion.<sup>91</sup> Conversely, through forced increased Stab2 expression, myotubes form with an increased cross-sectional area as a result of increased myoblast fusion.<sup>91</sup>

The actin reorganization and myoblast fusion process is tightly regulated, ensuring fusion occurs in a linear arrangement parallel with the long axis of the cell, rather than forming spherical masses.<sup>92</sup> During this alignment process, non-muscle-myosin-II interacts with actin at the periphery of the myoblast, potentially being involved in the elongation process.<sup>93</sup> Interestingly, it was found that myoblasts still maintain ability to move during the fusion process.<sup>94</sup> Stress-fibre like actin bundles can be observed in these mobile myoblasts, but this phenotypic characteristic is lost upon cessation of locomotion.<sup>95</sup>

Myoblast fusion to form myotubes concludes with sealing of the membranes to become one. Proteins involved in this final step include myoferlin and dysferlin, and is similar to that of a resealing membrane following neurotransmitter release at the neuromuscular

junction.<sup>96</sup> Cells lacking myoferlin in murine studies fail to fuse and large myotubes are lacking.<sup>96</sup>

#### **1.2.3.4 Myotube maturation**

Once fused and entering a state of maturation, myotubes begin to secrete paracrine factors that aid in their maturation. Interleukin-4 (IL4), is one such paracrine factor – a complex glycoprotein that is involved in the migration of myoblasts to mature myotubes.<sup>97</sup> Concomitant with this, is the appearance of the type II IL4 receptor, found to be expressed on myoblasts around 72hours into differentiation.<sup>97</sup> Data suggests the involvement of IL4 in recruiting myoblasts with pre-fused myotubes to form larger, mature myotubes. Fitting with this, upon addition of an IL4 blocking antibody, myotubes formed appeared thinner and had less nuclei.<sup>97</sup>

Conversely, other molecules are involved in the negative regulation of myotubes. Myostatin for example, as a member of the transforming growth factor- $\beta$  (TGF-  $\beta$ ) family, is involved in controlling myoblast number, and restricting myoblast proliferation and differentiation.<sup>98</sup> Myostatin is responsible for inhibiting growth of the muscle fibre when it reaches normal size.<sup>98</sup>

#### **1.2.4 RhoA/ROCK signaling in myotube formation**

Rho signaling plays a very important role during myogenesis. Members of the Rho family of small GTPases - RhoA, RAC1 and Cdc42, proteins involved in actin cytoskeleton regulation – are also found to be involved in migration of myoblasts, cell cycle progression, as well as transcriptional profile expression of myogenic regulatory genes.<sup>99</sup> RhoA is involved in the activation of serum-response factors crucial for *myoD* and *alpha-actin* expression, thus involved in the promotion of gene expression pivotal to myogenesis.<sup>100</sup>

Conversely, Rac1 and Cdc4 have been identified as negative regulators of myogenesis.<sup>101</sup> Studies into the levels of Rho A and downstream effector ROCK at different time-points in the myogenic differentiation process reveal that levels and the activity of Rho A are down regulated in myoblasts undergoing differentiation and that a fine-tuned regulation is pivotal. Rho A is required at the onset of myogenesis and functions as a positive regulator of induction.<sup>102</sup> However, forced expression of Rho A in quail myocytes results in altered muscle-specific protein expression and disruption of cell fusion.<sup>98</sup> Findings indicate that Rho A and ROCK function independently in myoblasts, and that ROCK may receive signaling input from Raf-1 kinase, rather than Rho A only.<sup>98</sup> Other studies support this finding, proving that Rho A has to be down regulated in order for myoblast fusion to occur; elucidation of the mechanisms underpinning this reveal that Rho A GTPase activity regulates M-cadherin activity, and as previously mentioned in section 1.2.2.4, cadherins are involved in the fusion process.<sup>102</sup> M-cadherin in particular, is abundantly expressed in myoblasts as they begin their fusion process.<sup>103</sup> Where a form of constitutively expressed Rho A (RhoAV14) is found in myoblasts, fusion is completely inhibited; findings show that M-cadherin levels are significantly increased, but not other molecules crucial for myoblast fusion such as N-cadherin, suggesting the importance of both a tightly tuned Rho A signaling cascade and cadherins in fusion.<sup>102</sup> Furthermore, Rho A mediates ubiquitination and degradation of M-cadherin, a process involving a lysosomal-dependent pathway.<sup>104</sup>

Interestingly, recent studies have investigated the effect of ROCK inhibitor, Y-27632, on myotube formation from myoblasts; Conclusive results were obtained showing ROCK inhibition significantly enhanced myoblast fusion *in vitro*, postulating this a causative effect of nuclear accumulation of FKHR, a direct substrate of ROCK.<sup>100, 105</sup> Thus, results concur RhoA/ROCK down regulation an essential aspect of myoblast fusion and as a result, terminal myogenesis.

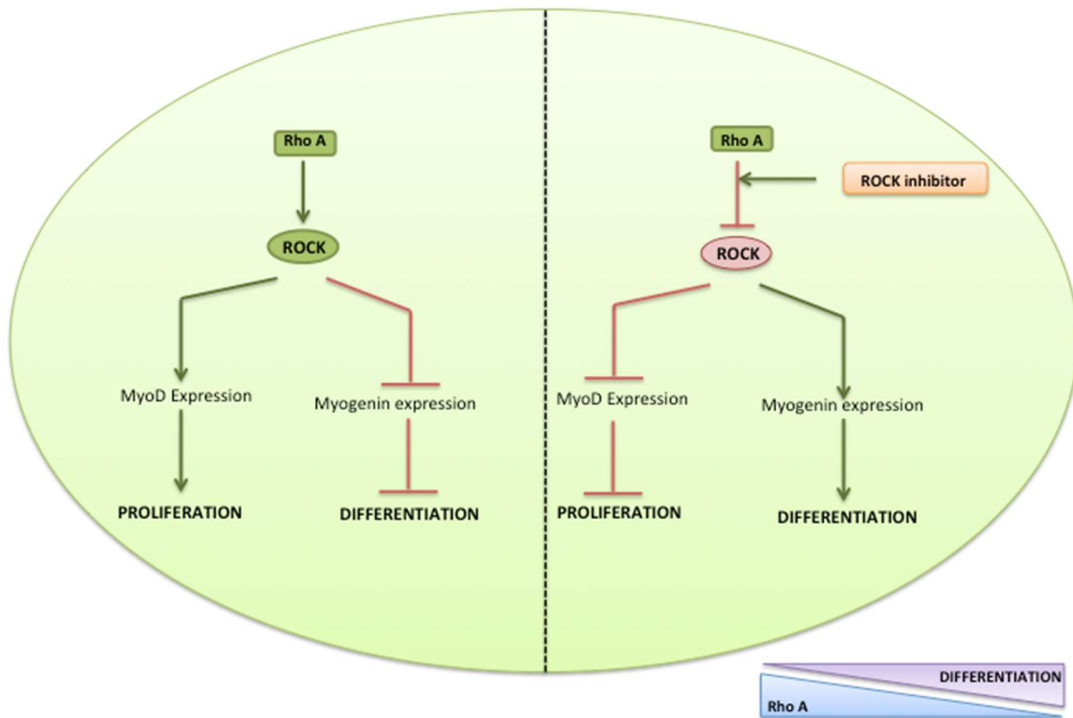


**Figure 1.2.4: Hypothesized involvement of Rho A and ROCK signaling in myogenesis.** Upon activation of Rho A and downstream effector ROCK, myoblast phenotype is promoted and maintained. Conversely, when Rho A/ROCK are inhibited, differentiation is promoted, although exact signaling mechanisms remain unclear.

### 1.2.5 Nuclei number and distribution in myotubes

Muscle fibers and myotubes, as previously mentioned, are large cells formed by the fusion of smaller cells, and thus are more of a unit than a cell. They differ in shape, and size to other mammalian cells, which are usually more spherical and mononucleate. It is not surprising then, that the myotube requires the functional capacity of multiple nuclei – to provide the transcriptional output and DNA necessary to maintain such a large cell volume viable.<sup>106</sup> This way, mRNA and synthesized proteins do not have to travel far to their destination.<sup>107</sup> One study into the distribution of nuclei within myotubes of 40 different mammalian species found them to be distributed in an orderly manner in order to minimize any potential transport issues.<sup>107</sup> Furthermore, although previous

literature has suggested that nuclei in myotubes are of a 'random' distribution, the aforementioned study found a significant difference in positions of nuclei from those that would be expected if they were of a random distribution.<sup>107</sup> Therefore, even though nuclei appear distributed evenly throughout myotubes, it is not of a random organization, instead, of intrinsic design.

Multiple nuclei migration events occur during myotube development, a phenomenon unveiled through time-lapse evidence, showing the migration of nuclei to the centre-point of a myotube following fusion of myoblasts - a process termed centration. Following this, nuclei spread out along the length of the myotube – a process termed spreading.<sup>108</sup> Improper nuclei positioning results in altered muscle function, potentially contributing to the pathophysiology of certain skeletal muscle disorders, including centronuclear myopathies.<sup>109</sup> This nuclear migration process is not well understood; it is thought to be modulated by myotubules, motor proteins and a dynein/dynactin protein complex, a process regulated by Cdc42, Par3 as well as Par6.<sup>109</sup> Following maturation of myotubes into myofibers or during muscle regeneration, nuclei migrate again from the centre to the periphery of the myotube through a N-Wasp-dependent mechanism.<sup>108</sup>

### **1.2.6 Acetylcholine receptor distribution in myotubes**

Acetylcholine receptors (AChRs), ligand gated ion channels that consist of binding site receptors for acetylcholine (ACh) as well as ion binding domains required to initiate a response, and thus usually defined by their function as a mediator of an electrophysiological response. The acetylcholine receptor consists of four subunits:  $\alpha$ ,  $\beta$ ,  $\gamma$ , and  $\delta$ , each of which encoded by a separate gene. These genes are activated during the myogenic program, beginning at the point of myoblast cell cycle withdrawal.<sup>110</sup>

Although usually found clustered in high concentrations at the neuromuscular junction, as will later be described, they also exist extrasynaptically, and can be found in skeletal

muscle fibres, where they are thought to play a role in the myogenic process. They can be found distributed at a low density across myotube surfaces prior to innervation.<sup>111</sup> The exact function of acetylcholine receptor existence during myotube formation is not yet understood, although several hypotheses exist.

Terminal differentiation involves the fusion of myoblasts in myotubes, and studies suggest that the presence of acetylcholine receptors favor myotube fusion (a25). One paper suggests the function of acetylcholine receptors in the developing myotube as a method of contributing to myotube survival – especially in the absence of nerve activity.<sup>112</sup> Spontaneous contraction is a phenomenon that can be observed in many developing myoblast cell lines, and this ability is attributed to the presence of acetylcholine receptors in the developing myotubes. One study in particular outlines evidence showing the presence of ChAT, and Ach-Ic in developing myotubes derived from a murine cell line; these are crucial for the spontaneous contraction observed during myotube formation, and hypothesise this as a way of keeping uninnervated myotubes alive.<sup>113</sup> Another laboratory found the presence of acetylcholine receptors to be linked to myotube size *in vitro*.<sup>114</sup>

### **1.2.7 Skeletal muscle innervation**

Innervation represents the final step in myogenesis in which motor neuron and skeletal muscle interact and form junctions, termed neuromuscular junctions.

## **1.3 The neuromuscular junction**

Synapses between motor neurons and skeletal muscle are essential relay stations critical for coordination of information. The chemical synapse found here is called the neuromuscular junction (NMJ).<sup>115</sup> For simplicity, as seen in Figure 1.3, the neuromuscular junction can be split into three areas: the presynaptic terminal, the synaptic cleft, and the postsynaptic terminal. At the presynaptic terminal, the motor axon divides into numerous branches ending in a bouton that synapses with the surface



of a muscle fiber, the postsynaptic terminal. In between these two structures, exists the synaptic cleft – the gap. The post-synaptic membrane, also termed the end-plate, consists of active zones whereby a high density of nicotinic acetylcholine receptors reside.

A brief summary of transmission at the neuromuscular junction involves depolarization of the presynaptic membrane, causing opening of voltage-gated calcium ion channels in the membrane, allowing an influx of  $\text{Ca}^{2+}$  into the presynaptic bouton. This calcium binds to synaptic vesicles, which contain the neurotransmitter acetylcholine, causing them to fuse with the presynaptic membrane, later exocytosing their contents into the synaptic cleft. This acetylcholine then diffuses across the synaptic cleft to ligand-gated ion channels containing acetylcholine receptors found on the post-synaptic membrane, where it binds, causing them to open, and allowing an influx of sodium into the postsynaptic terminal. This causes depolarization, which leads to depolarization and an end-plate potential, and consequent muscle contraction. Choline acetyltransferase (ChAT) is an enzyme involved in the synthesis of the neurotransmitter acetylcholine at these cholinergic junctions, catalyzing the movement of an acetyl group from acetyl-coA to choline.<sup>116</sup> Another enzyme, acetylcholinesterase (AChE), is the enzyme responsible for the breakdown of acetylcholine in the synaptic cleft in order to terminate synaptic transmission. The resulting compounds, choline and acetyl-coA can then be transported back into the pre-synaptic nerve terminal, where they can be recycled.

At rest, in the absence of neural depolarization, multiple small end-plate potentials are spontaneously evoked at the postsynaptic membrane; these are called miniature end-plate potentials (MEPPs).<sup>117</sup> These are a result of small quantal releases of ACh from the presynaptic membrane. To fulfill the complex task of transmission, the neuromuscular junction is well equipped with specialized cells and surfaces, as well as an abundance of specialized proteins, and all occurrences are under extreme regulation.

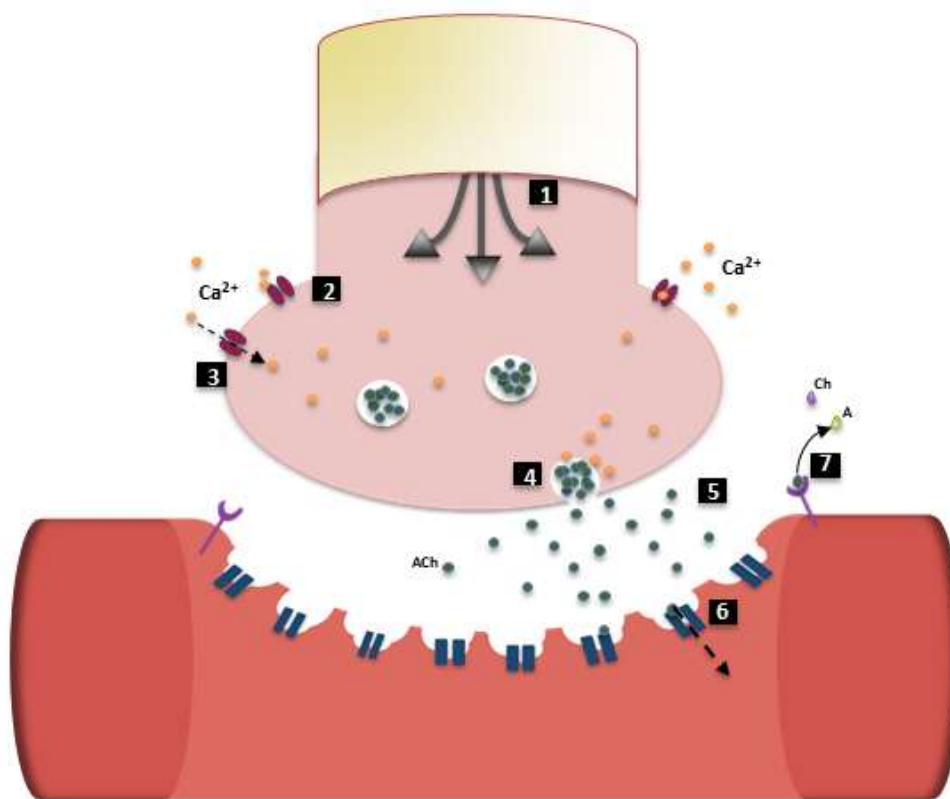


**Figure 1.3: The neuromuscular junction consists of a presynaptic neuron terminal, a synaptic cleft, and a post-synaptic muscle membrane.** A brief overview of signal transduction includes (1) depolarization of the terminal nerve. (2)  $\text{Ca}^{2+}$  voltage-gated ion channels open. (3) Influx of  $\text{Ca}^{2+}$  into presynaptic bouton stimulates synaptic vesicle movement and docking. (4) Synaptic vesicles containing neurotransmitter dock and exocytose acetylcholine into synaptic cleft. (5) Acetylcholine binds ligand gated ion channels containing acetylcholine receptors, causing them to open. (6) Sodium enters post-synaptic terminal, leading to depolarization and subsequent muscle contraction. (7) Acetylcholine is broken down by acetylcholinesterase.

### 1.3.1 The presynaptic nerve terminal is a specialized structure

The motor bouton terminal is a structure specialized for neurotransmitter synthesis, release, incorporation, synaptic vesicle docking, neurotransmitter reuptake, as well as ion transport; thus, the crucial starting events mediating neurotransmission at the NMJ are mediated by this nerve terminal. All of the aforementioned processes are energy demanding. Consequently, a large population of mitochondria exists in the presynaptic terminal, supplying the energy in the form of ATP to fuel these processes.<sup>118</sup>

This is a demyelinated part of the motor nerve axon, and it itself contains cholinergic, nicotinic receptors that function to increase the quantal output of neurotransmitter through binding of acetylcholine.<sup>117</sup> The docking, fusion and exocytosis of synaptic vesicles containing the neurotransmitter are extremely complex processes, and a lot remains to be elucidated. Most of the recent elucidation emanates from *in vitro* models as *in vivo* counterpart systems are difficult to access and study.<sup>119</sup>

### 1.3.1.1 SNARE proteins

A family of membrane-associated proteins called soluble N-ethyl-maleimide-sensitive factor attachment protein receptor's, or SNAREs are involved in the trafficking, docking, and fusion of vesicle docking at the presynaptic membrane of the NMJ and therefore neurotransmitter release. Both synaptic vesicle protein and calcium channel migration

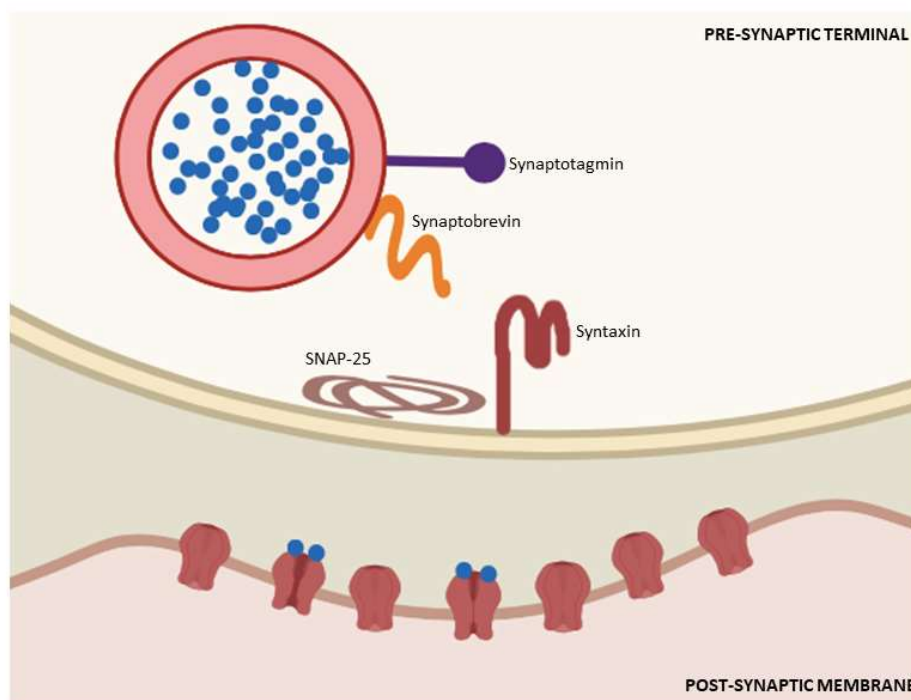


**Figure 1.3.1.1 SNARE proteins are involved in the trafficking, docking, fusion and exocytosis of synaptic vesicles at the NMJ.** A SNARE protein complex exists pivotal to the release of acetylcholine into the synaptic cleft. Synaptobrevin, Synaptotagmin, SNAP-25, and Syntaxin are some of the key snares involved in the docking and fusion of the synaptic vesicle to the presynaptic membrane.

to the presynaptic active zone is required for neurotransmitter release.<sup>120</sup>

SNARE proteins were originally divided into V-SNARE (vesicle) or T-SNARE (target) proteins where V-SNARE proteins were found incorporated into target vesicles and T-SNAREs found at the nerve terminal membrane. It was postulated that T-SNAREs form sub-complexes that act as a guidance cue for V-SNAREs, resulting in a *trans*-SNARE complex/SNAREpin.<sup>254</sup> During formation of a *trans*-SNARE complex, a four-helix bundle consisting of four SNARE motifs is formed, bringing together opposing membranes, catalysing fusion. Post-fusion, the complex is denoted as *cis*-SNARE complex and is disassembled by catalyst proteins including SNAP, resulting in recycled components that can form a new SNARE complex. It was also hypothesised that a SNARE protein possesses the capacity to participate in several SNARE complexes simultaneously, thus gaining the ability to control numerous membrane fusion events.<sup>254</sup> Furthermore, tethering factors influence formation of the SNARE complex.

More recently, SNARE's were classified as R- and Q- SNAREs, with R- being similar to V-SNAREs and Q- as T-SNAREs but are not confined to specific locations like previously thought. Instead, it was found that R-SNAREs and Q-SNAREs contribute arginine (R) residues and glutamine (Q) residues to the SNARE complex respectively and are therefore characterised accordingly. A SNARE complex consists of one R-SNARE motif along with three Q-SNARE motifs.<sup>254</sup> R-SNAREs include synaptotagmin and Q-SNARE's include syntaxin and SNAP25.

Three vital SNARE proteins in particular, neuronal Synaptobrevin-2 (VAMP-2), Syntaxin 1A and SNAP-25 protein sub-family, are involved in these docking events which ultimately result in the release of acetylcholine into the synaptic cleft.<sup>121</sup> Located in the plasma membrane, they are activated upon  $\text{Ca}^{2+}$  influx, forming a *trans*-SNARE complex prior to calcium activation. Furthermore, synaptotagmin-1 has also been shown to be involved in vesicle fusion with the membrane.<sup>122</sup> Certain  $\text{Ca}^{2+}$  receptor subtypes also

interact with SNARE proteins at the active zone.<sup>123</sup> Overall, they aid in ensuring synaptic transmission occurs in a matter of milliseconds.

### **1.3.2 The synaptic cleft**

The synaptic cleft at this neuromuscular junction approximates 50nm.<sup>124</sup> The cleft between the bouton and endplate is made up of a collagenous basement membrane.<sup>125</sup> The synaptic cleft contains basal lamina, a structure that provides structural support as well as binding sites for molecular binding, including agrin and AChE.<sup>126</sup> In *in vitro* co-culture models, the basal lamina can be observed to develop around the time of bouton maturation and AChR clustering in NMJ formation.<sup>127</sup> Thus, AChE positional identity is defined and controlled by the basal lamina.

### **1.2.3 Post-synaptic membrane specializations**

Early investigation of the developing post-synaptic terminal was often performed using lower order species, including amphibians such as *Xenopus* embryos. This was due to the difficulty of studying human junctions *in vivo*. These species provide systems with advantages such as quick formation and muscle cells that are singly innervated. However, they can lack the complex structure observed in the human NMJ, including active zones and presence of a basal lamina. Structure of the post-synaptic membrane varies significantly in all invertebrates.<sup>255</sup> For example, junction terminals in amphibians such as frogs are significantly larger than human, as the human NMJ was found to be amongst the smallest of all vertebrates studied. However, there is a huge increase in post-synaptic folding from frog to human. It is postulated that quantal content is inversely related to membrane folding, and that the increased folding in the human post-synaptic membrane amplifies quantal action, compensating for smaller terminals.<sup>255</sup>

At the post-synaptic membrane at the NMJ contains a large population of the neurotransmitter ACh receptors, associated with a plethora of extracellular proteins,

cytoplasmic proteins, as well as transmembrane proteins.<sup>128</sup> The post-synaptic membrane does not exist as an independent structure; instead, it receives signaling from both the synaptic cleft and the presynaptic membrane – signaling that modulates its morphology, size and composition. Before discussing structures and occurrences crucial for post-synaptic function, it is important to look at neuromuscular junction development.

## 1.4 Development of neuromuscular junctions

Formation of the neuromuscular junction is a complex process whereby coordinated interactions between a terminal nerve axon and muscle form specific subcellular specializations; a process that is also mediated by Schwann cells.<sup>129</sup> As muscle tissue develops in the embryo, as does the nervous system. Motor neuron axons extend and form a nerve-terminal at the muscle sarcolemma. This terminal initially branches and makes contact with the muscle fibre at several different locations. Thus, in early development, each muscle fibre is innervated by numerous neurons; however, upon maturation, elimination occurs for all but one nerve terminal axon, in a process referred to as axonal competition and synapse elimination.<sup>130</sup> The molecular pathways underpinning this process require further elucidation. Distal to proximal retraction of eliminated neurites can be observed *in vivo*, whereby a 'retraction bulb' is formed.<sup>130</sup> Axon retraction is not asynchronous for fibers of the same muscle, but occurs at different time-points during development. It is known to be an activity-dependent process, postulated to be modulated by acetylcholine.<sup>131</sup> Studies using nerve blockers have shown competition can be eliminated through blocking NMJ activity.<sup>132</sup> Molecular modulators of these events are thought to include thrombin, a serine protease, and serine-threonine protein-kinase-A (PKA).<sup>130</sup>

Synaptogenesis, the process by which a synapse develops between the two cell types, occurs. During this process, the presynaptic terminal is involved in the organization and distribution of post-synaptic constituents, which then interact with components of the

developing basal lamina. During the first stages of neuromuscular junction formation, specialized proteins present along the entire muscle before being redistributed and condensed at the contact site between the motor neuron and muscle fiber. This differential distribution of proteins is a result of selective expression of transcriptional genes from the nuclei located proximally to the developing synapse.<sup>133</sup> The synapses are then stabilized through recruitment of cytoskeletal elements.

Following maturation of the neuromuscular junction, the junctional length increases.<sup>134</sup> As the NMJ matures, morphology of the post-synaptic membrane is altered. First, an indentation can be observed, whereby a 'gutter' like shape appears in the muscle membrane, which is to be the synaptic cleft. Following this, the membrane invaginates, forming junctional folds around the nerve terminal, increasing the surface area of the post-synaptic end plate.<sup>134</sup> Post-natal maturations of the NMJ also serve to increase the efficiency of motor neurons, post-synaptic apparatus, and ultimately transmission at this junction. Unnecessary apparatus are eliminated from both pre- and post-synaptic terminals.<sup>135</sup> Remodeling of the adult NMJ also occurs as a result of altered activity. Extended periods of activity enables remodeling, resulting in size and morphology. Exercise for example, has been shown to modulate increases in junctional area, and increased dispersion of AchRs at the motor end-plate.<sup>136</sup>

#### **1.4.1 Acetylcholine receptor (AChR) accumulation**

A morphological characteristic of the NMJ is the clustering of acetylcholine receptors that can be found at the post-synaptic terminal, immediately beneath the motor nerve terminal. Electron microscopy revealed that AchR density at these post-junctional folds in excess of 200,000 per  $\mu\text{m}$ .<sup>137</sup> As previously discussed, some post-synaptic apparatus can be synthesized by myotubes aneurally, including acetylcholine receptors. However, positional identity and phenotypic characteristics of AChRs synthesized before NMJ formation are not the same as those found at the NMJ; for example, there is no clustering and studies suggest altered subunit composition.<sup>138</sup>

The acetylcholine clustering event itself requires elucidation, and was initially postulated to occur in one of two ways: either through motor induction, or aneurally and recognized by the ingrowing axon.<sup>138</sup> Evidence was put forward backing both ideas, and data suggests that the developmental biology of the NMJ may be subject to interspecies variation.<sup>139</sup> For example, clustering of acetylcholine receptors appears to occur aneurally in some mammals, but this is not the case in humans.<sup>140</sup> However, where aneural clustering does occur, they appear to differ in positional identity and morphology, often appearing less 'pretzel like' than NMJ clusters, thought to be a result of synapse shape due to the invaginated membrane.<sup>141</sup> Evidence for clustering at the human NMJ being a neural dependent process exists and includes the fact that AChR synthesis increases upon NMJ maturation.<sup>142</sup> The process of clustering and increased AChR synthesis appears to be contemptuous with the axonal competition phase of synapse elimination previously discussed.<sup>130</sup> Initially, micro-clusters of receptors form and aggregate, become more rigid and integrate into the myotube membrane, forming a plaque.<sup>134</sup> Other morphological and molecular events occur during maturation of the NMJ; these include: an increase in junctional length, and increased AChR plaque density.<sup>134</sup>

#### **1.4.1.1 The agrin-MuSk-raspyn-AchR pathway in AChR accumulation**

Denervation experiments suggest that the synaptic basal membrane may participate in an instructive role in synaptic generation.<sup>143</sup> In an attempt to identify molecules involved in AChR clustering, the argin-MuSK-raspyn pathway was sought out. Strong evidence exists both *in vivo* and *in vitro* for the involvement of the aforementioned molecules in AChR clustering and up-regulation of their synthesis.<sup>144</sup> Agrin, a heparin proteoglycan, it is not only thought to be a structural component of the basal membrane, but also an inducing factor of AchR clustering at the end-plate through tryrosine phosphorylation of the AChR beta-subunits.<sup>145</sup> As well as this, agrin promotes anchoring of the receptors to the post-synaptic cytoskeleton.<sup>146</sup> Agrin is a molecule



synthesized by motor neurons, which is capable of migrating down axons to a nerve terminal, where it is secreted into the synaptic cleft of the NMJ, where it binds to the basal lamina.<sup>147</sup> It has since been found that agrin is not only involved in the accumulation of AChRs at the NMJ, but is also involved in organization of other post-synaptic components, and *in vivo* mice studies show impaired post-synaptic differentiation in the absence of agrin.<sup>148</sup> Experiments using agrin-knockout mice have

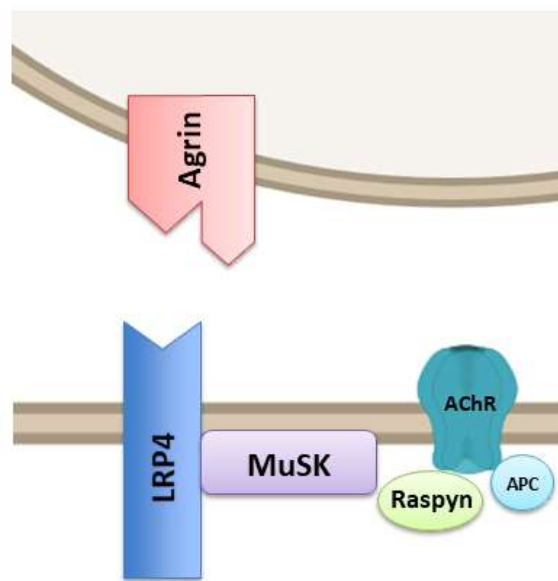


**Figure 1.4.1.1: Hypothesized organization of Agrin-Musk-Raspyn-AChR complex that forms at the developing neuromuscular junction.** AChRs are clustered at the NMJ, anchored through raspyn. Upstream of raspyn lies MuSk, part of the Agrin receptor complex, along with LRP4. APC is also thought to be involved, and is induced through Agrin.

shown that AChR clustering still occurs, however the clusters are distributed randomly on the muscle surface rather than at the active zones, suggesting agrin is pivotal to the specific clustering of AChRs during neuromuscular junction formation. Muscle fibers and Schwann cells have also been shown to possess the ability to produce agrin, although this is 1000-fold less effective at inducing AchR clustering than neuronal agrin alongside MusK.<sup>149, 121</sup>

Agrin, along with MuSK and Rapsyn are essential components necessary for the aggregation of AChRs. MuSK, a tyrosine kinase receptor, is thought to be part of the Agrin receptor complex.<sup>150</sup> Important evidence showing MuSK-deficient mice lacked post-synaptic differentiation, but maintained the ability to transcribe and form AChRs provided evidence for them being part of the agrin receptors.<sup>151</sup> Downstream of MuSK lies rapsyn, a pivotal, intracellular, membrane-associated-cytoplasmic protein involved in post-synaptic differentiation. Rapsyn can be found at the NMJ, appearing at approximately the same time as AChR clusters, as found in both *in vitro* and *in vivo* experimentation.<sup>152, 153</sup> Nevertheless, the mechanism underpinning rapsyn co-localisation with AChRs remains unclear.

Furthermore, agrin regulates the function of rapsyn. Rapsyn interacts directly with alpha-actinin and beta-catenin, which are involved in actin polymerisation. Actin regulates the function of rapsyn and is also hypothesised to stabilise this unstable protein by promoting its binding to Hsp90B, a heat shock protein, thus preventing it being degraded within the synapse.<sup>154</sup>

Recent investigation into the function of the well-known transcription factor Nuclear Factor  $\kappa$ B (NF- $\kappa$ B) has revealed its involvement in the regulation of rapsyn.<sup>138</sup> NF- $\kappa$ B is composed of homodimers or heterodimers of its constituent subunits, and is under tight regulation by inhibitor  $\kappa$ B (I $\kappa$ B), an inhibitor that prevents it from becoming active until phosphorylation by I $\kappa$ B kinase, ultimately leading to transcriptional regulation.<sup>138</sup> It was found that upregulation of Nf- $\kappa$ B promoted aggregation of AchR *in vitro* in C2C12 myotubes, whereas inhibition of Nf- $\kappa$ B attenuated this. Following on from this, it was then found that this transcription factor is an essential component in regulation of the NF- $\kappa$ B subunit RelA/P65, where elimination of this subunit results in decreased AChR clustering.<sup>138</sup>

Lrp4, a low-density lipoprotein receptor expressed specifically in myotubes at the site of

the neuromuscular junction, has also been hypothesised to be involved in formation of the neuromuscular junction as knockout studies in mice show that Lrp4 deficient mice lack the ability to form neuromuscular junctions.<sup>151</sup> Further studies into the role of Lrp4 in NMJ formation provide evidence for Lrp4 being an agrin-co-receptor, thus forming part of the AChR agrin-receptor complex. It is thought that Lrp4 binds to neural agrin and is required for induced Musk activation, and thus AChR clustering.<sup>151</sup> However, the mechanism by which Lrp4 aids in Musk activation remains uncertain. Another protein thought to be involved in AChR clustering is APC, which itself is also induced by agrin. APC is a key component in regulating cell migration and cell polarity and functions by binding to actin filaments/microtubules.<sup>156</sup> APC has been shown to be involved in the Wnt signalling pathway that regulates the cytoplasmic levels of beta-catenin<sup>156</sup>

In conclusion, neural-derived agrin is pivotal in triggering differentiation and function of the post-synaptic membrane during neuromuscular junction formation through activating MusK and inducing co-aggregation of rapsyn with AChRs on the post-synaptic end-plate. However, further research is required to elucidate the downstream signalling pathways of MusK and whether this signaling pathway cross-talks with the Wnt/beta-catenin signalling pathway during synapse formation.<sup>157</sup>

#### **1.4.1.2 ARIA in AChR accumulation**

As discussed, clustering of receptor proteins is involved in acetylcholine receptor accumulation. However, other factors are also involved, such as the selective transcription of AChR genes by nuclei specific to the synapse. ARIA is a secreted isoform of neuregulin-1 and is secreted by motor neurons into the synaptic cleft.<sup>159</sup> ARIA is a growth factor that binds ErbB tyrosine kinase receptors on the myotube surface, found to be concentrated at the active site of the NMJ.<sup>158</sup> This led to the hypothesis that ARIA and agrin work in a coordinated motor secreted fashion – agrin being involved in the physical accumulation of AChR's and ARIA activating the transcription of AChRs in the

local region.<sup>160,127</sup> *In vitro* findings show that ARIA increased mRNA for ACHR subunits, although subunit composition varies between species.<sup>161, 162</sup>

### **1.2.3.2 Nuclei accumulation**

The positional identity of nuclei within cells of the same type can usually be found to be the same or similar, strongly suggesting that signaling cues exist that direct the migration and 'homing' of these nuclei. However, little remains clear about the molecules responsible for anchoring nuclei in place in vertebrate skeletal muscle.

Nuclei can be found within a skeletal myotube at a relevantly even distribution; however, upon innervation and thus formation of the NMJ, clustering of nuclei at the myotube post-synaptic surface becomes apparent.<sup>163</sup> Specifically, these nuclei usually exist in clusters of between 2 and 6 nuclei anchored directly beneath the post-synaptic end plate membrane. These nuclei become functionally specialized, and *in vitro* studies have found them to be involved in transcriptional regulation of proteins required at the NMJ.<sup>134</sup> These nuclei, often termed 'fundamental nuclei' are characteristically found to contain hypertrophied nucleoli, and chromatin appears clear.<sup>164</sup> Fundamental nuclei are involved in active transcription of *AChR* genes. Neuromuscular junctions and myotubes devoid of this nuclei clustering have been found to be mature and viable, suggesting nuclear aggregation is not essential for myotube maintenance at the NMJ once mature.<sup>165</sup>

## **1.4 Investigating the neuromuscular junction.**

The neuromuscular junction, although a well-understood synapse compared to other synapses, still requires extensive analysis and elucidation. Knowledge of the NMJ has indeed significantly expanded over the past couple of decades, and it not only proves useful for morphological, physiological and pathophysiological studies of the NMJ, but the data obtained serves as a prototype for other synapses. However, much remains unknown with regards to molecular physiology and NMJ-specific diseases. As such,

modeling the NMJ is of significant importance to understanding the mechanisms underlying such pathologies.

### **1.4.1 Diseases involving neuromuscular junctions**

Diseases of the neuromuscular junction comprise a broad range of disorders that can be classified into antibody-mediated, toxic, metabolic or congenital categories.<sup>166, 167</sup> Much of the pathophysiology behind these diseases remains unknown, and therefore creating a model of the NMJ is paramount to finding treatments to the aforementioned diseases.

These diseases involving antibodies, genetic mutations or toxins interfere with the functional capacity of the neuromuscular junction, consequently affecting signal transmission to muscles. Disorders affecting these junctions result in varying degrees of muscle weakness due to reduced/inhibited end-plate potential as a result of structural changes, usually at the pre-synaptic terminal.<sup>168</sup>

One of the most common neuromuscular junction disorders is myasthenia gravis, a condition whereby an autoimmune attack of NMJ proteins leads to antagonistic effect the action of acetylcholine, by destruction of the receptor, or by completely removing the receptors from the postsynaptic membrane. These autoimmune antibodies have been found to target AchR, MusK as well as skeletal muscle proteins involved in neuromuscular transmission.<sup>169</sup>

Lambert-Eaton syndrome is another common autoimmune neuromuscular junction disorder. This disease is characterized by reduced acetylcholine release into the synaptic cleft from the presynaptic nerve terminal. This disease, which usually presents with proximal weakness of the lower limbs which then travels in a cranial-caudal direction is caused by autoimmune antibodies directed towards P/Q-type voltage-gated calcium ion channels.<sup>170</sup> These antibodies impede with the calcium-dependent process of acetylcholine release, and hence reduce contractile ability.

As well as autoimmune interference of the neuromuscular junction, some diseases are the result of neurotoxins. For example, botulism is a disease caused by one of seven bacterial toxins produced by *Clostridium botulinum*. This toxin enters cholinergic nerve terminals through binding to gangliosides, synaptotagmin or the synaptic vesicle protein SV2 (typically inside synaptic vesicles).<sup>171</sup> Following this, upon acetylcholine vesicle recycling, the toxin entraps itself inside the vesicle, before forming a pore that allows the toxin to bind to SNARE complex proteins, ultimately leading to insufficient acetylcholine release.<sup>171</sup>

On the other hand, some disorders result in excessive depolarisation and neurotransmission, causing muscle fasciculations, for example neuromyotonia (also known as Isaacs syndrome).<sup>172</sup> This condition, which often presents with involuntary muscle twitching and cramps, is of an autoimmune aetiology. The autoimmune antibodies leading to the pathophysiology of neuromyotonia target voltage-gated, their detailed, thorough elucidation and potential therapies are hindered by reproducibility of the true *in vivo* environment of such structures.<sup>172</sup> Therefore, a robust, functional model of neuromuscular junctions duplicating the neuromuscular junctions would be extremely valuable in furthering knowledge of these structures, and their related pathologies. This is especially the case in the aforementioned diseases, in which particular intracellular/extracellular proteins of the neuromuscular junction are targeted by toxins or autoantibodies.

#### **1.4.2 Modeling the NMJ: In vitro vs. in vivo.**

In order to study the physiology and pathologies of neuromuscular junctions, many *in vivo* systems have been developed, including mouse diaphragm or *Drosophila* abdomen.<sup>173, 174, 175</sup> However, these *in vivo* systems come with disadvantages including short-lived experimental time frames and difficulty in manipulation techniques. To overcome these complications, *in vitro* co-culture of motor neurons with myoblasts

model systems have been generated. Early studies involving these co-culture systems found the formation of immature, thin myofibers and as a result, do not provide a robust model for studying the structure in a physiological or functional capacity.<sup>176</sup> As well as this, many models, although they appear to be forming neuromuscular junctions that truly recapitulate features of their *in vivo* environment, have not been studied to the extent that may be required to prove this.<sup>121, 176, 177</sup> Moreover, model systems whereby specialized structures including pre-synaptic and post-synaptic elements of vertebrate neuromuscular junctions are analyzed rather than the basic components will prove advantageous in obtaining a purer sample of true neuromuscular junctions. It can be found that most of the current models are analyzed through exploitation of components such as AChRs, but these merely indicate the presence of a neuromuscular junction rather than providing concrete evidence.<sup>177</sup> Therefore, an *in vitro* co-culture system whereby components such as MusK, LRP4 and rapsyn are identified will be more standardized, reliable model that could also prove more appropriate for studying pathologies and potential treatments that target these specific proteins.

*In vitro* modeling of neuromuscular junctions provides a compelling model that can be used in a plethora of applications including studying signal computation, studying their structure, as well as modeling diseases. If an *in vitro* neuromuscular junction model that recapitulates those in the vertebrate central nervous system can be developed, then the aforementioned diseases can be studied in greater depth, which will allow for greater capacity to develop potential therapies. The development of new experimental models of functional neuromuscular junctions that recapitulate the *in vivo* environment during embryogenesis will provide a useful tool for pharmacological analysis. This will allow a platform for studying neuromuscular junction disorders, as well as regenerative medicines/therapies to be tested.

There exist many other advantages of *in vitro* models compared to *in vivo*. For example, by replicating the NMJ in an *in vitro* model, one is able to contribute to the reduction of

animals used in scientific research, which not only proves more ethical, but eliminates sample to sample variation. As well as this, *in vitro* models can often be used for larger scale experiments as they tend to be easily reproducible, with less regulation surrounding them and less limited by restrictions as they are more ethical. Results obtained from animal studies are often extrapolated and applied to human neuromuscular junctions, and this is a source of inaccuracy due to biological differences between animals and humans.

#### **1.4.2.1 *In vitro* co-culture modeling of the NMJ**

Synaptic transmission relies on communication between cellular constituents, thus a large scientific advance and effort on trying to mimic *in vivo* environment to elucidate mechanisms of transmission by creating an *in vitro* model of neuromuscular junctions. Currently, a plethora of models exist; none of these models are perfect however, all existing with their own advantages and limitations.

Most successful *in vitro* systems consist of a co-culture of a skeletal muscle cell line co-cultured with neural derivatives, whereby myotubes are formed and apparent interactions form between the two cell types.<sup>175</sup> This *In vitro* modeling has allowed for scientists to observe acetylcholine receptor clustering in greater detail, in the presence of laminin, and without.<sup>178, 179</sup> Elucidation of transmission at the NMJ has been made possible, as well as the biology underlying the formation of such a specialized synapse. For example, the idea that MuSK is required for NMJ formation and stability, as part of the agrin-MuSK-raspyn complex has only been allowed through *in vitro* verification.<sup>180</sup>

##### **1.4.2.1.1 Homologous vs. heterologous co-culture models**

The efficiency of the co-culture model often lies in the cell types used. Significant variation lies in the origin of the skeletal muscle and neurons and thus has an impact on not only NMJ formation, but also its similarity to the human NMJ. Homologous co-culture systems have been described, and although contain two human cell lines,



making them more 'applicable' to human biology, are often hindered by their own limitations, including requirement of a primary human tissue, lack of identifiable structures, and the requirement of difficult surface modificational procedures prior to co-culture.<sup>181</sup> Many heterologous co-culture systems have also been outlined whereby neural and muscle cells originate from different species – often containing one mouse or rat cell line.<sup>175</sup> These co-culture systems remain the most widely used systems. For example, the murine C2C12 myoblast cell line is used in a plethora of studies, including both myogenesis studies as well as NMJ and will be discussed below (section 1.4.2.1.2). Particular studies involving human skeletal muscles have found the presence of immature myotubes, often lacking mature myofiber structure, and thus a murine skeletal myofiber showing enhanced levels of differentiation and mature myofibers structure, can be more appropriate for comparison to the human *in vivo* NMJ.<sup>182</sup> Using a heterologous co-culture also allows the opportunity to differentiate between pre-synaptic structures and post-synaptic structures, which prove indispensable in developmental studies. This is because, when the motor neural component is derived, for example from human stem cells, and the muscle from mouse myoblasts, species-specific antibodies and protein analogues can be used to exploit proteins and antigens from different species.

As for the neural component of co-culture models, many approaches have been tried. These commonly include, embryonic mouse or rat spinal cords or spinal stem cells.<sup>193, 184</sup> Other methods of co-culture involve the use of neural derivatives differentiated embryonic stem cells.<sup>181</sup>

#### 1.4.2.1.2 C2C12 cell line in co-culture models

The C2C12 myoblast line is a cell line derived from murine skeletal muscle. This immortalized cell line is commonly used in myogenesis studies as well as co-culture systems as it readily differentiates into myotubes in low serum conditions.<sup>194, 187</sup> Upon differentiation, the mononucleate myoblasts form long, multinucleated myotubules

with relatively little spontaneous contraction; because the C2C12 derived myotubules tend to lack the ability to spontaneously contract, it is possible to predict the presence of a functional neuromuscular junction when contraction occurs in the presence of neurons, which can then be investigated further.<sup>188</sup>

This cell line has particular characteristics that make it different from human skeletal muscle, but many of these characteristics can be utilized opportunistically for specific areas of research.<sup>189</sup> For example, as previously mentioned, MuSK is a protein required for neuromuscular junction formation and stability, and is found in significantly higher levels in the C2C12 cell line than in human muscle.<sup>190</sup> However, this higher expression level has been utilized in studies looking at the function of MuSK in acetylcholine receptor clustering. *In vitro* co-culture studies were in fact used to isolate MuSK.<sup>191</sup> Another protein found to be markedly increased in co-cultures consisting of C2C12 myotubes as opposed to human skeletal muscle is acetylcholine esterase (AChE); again, this phenomenon has been utilized for neurotransmitter breakdown and recycling studies.<sup>208</sup> Moreover, in *in vitro* co-cultures involving C2C12 cells have been used to elucidate post-synaptic differentiation.<sup>193</sup>

#### 1.4.2.1.3 *In vitro* co-culture models involving derivatives of pluripotent stem cells

For the neural aspect of establishing a co-culture, embryonic stem cells are often used. Embryonic stem cells (ES) are cells obtained from the embryo during early embryogenesis capable of unlimited proliferation and differentiation.<sup>193</sup> These embryonic stem cells, due to their pluripotency, can be easily directed down a neural lineage before co-culturing with muscle.<sup>181</sup>

Scientists found that some cancers often contain the same broad range of differentiated cell types as the tissue they arise in, which led to the idea that this aberrant proliferation

and differentiation during oncogenesis is similar to that of stem cell proliferation and differentiation.<sup>196</sup> Teratocarcinomas are a subset of germ cell tumours that are highly malignant and contain a disorganized array of somatic and extraembryonic cells within bundles of embryonal carcinoma cells. The embryonal cells are the pluripotent cells of the tumour that propel proliferation and differentiation. Once extracted, it was found that these EC cells express characteristic surface antigens such as SSEA3, SSEA4, TRA-1-60, TRA-1-81 and GCTM2.<sup>194</sup> Furthermore, similar to ES, EC cells express OCT4, which can be found to be down-regulation upon differentiation, thus providing a caricature of ES cells.<sup>203</sup>

These embryonal carcinoma cells provide an experimental system to study the molecular mechanisms surrounding human embryonic development. Moreover, they are considered to be the neoplastic counterpart of embryonic stem cells.<sup>194</sup> EC cells are adaptable, easier to maintain and proliferate faster, making them easier to culture in the long-run. Embryonic stem cells require culturing in the presence of embryonic feeder cells in order to maintain their pluripotency whereas many EC cell lines can be cultured without feeders.<sup>194</sup> Furthermore, suboptimal culture conditions can result in spontaneous differentiation of embryonic stem cells, which leads to an impure population of cells containing unwanted cell types. As a result, a cell population, which is more restricted and easier to maintain in culture, is advantageous.

Considerable variation exists among the EC cell lines available, each with differing strengths and weaknesses depending on the lineage of interest in a particular area of research.<sup>196</sup> The differential capacity of EC cells compared to ES cells tends to be more restricted. This however, can be beneficial for certain experiments as it provides an easier, more manageable experimental alternative to embryonic stem cells. They are therefore cheaper and more robust as there is less spontaneous differentiation.<sup>169</sup> Thus, EC cells make an ideal candidate for the neural component of co-culture, as they are easily differentiated into motor neurons and easy to maintain.<sup>198</sup>

#### 1.2.3.1.3.1 NTERA2.cl.SP12 cell line

The isolation of particular EC clonal cell lines has provided a useful model for studying neurogenesis and neuromuscular junction formation. Neural differentiation studies often involve the use of the cell line N-TERA2 to study the mechanisms of neuronal development.<sup>198, 199, 200, 201, 202, 206</sup> This is advantageous to studying neurogenesis during embryonal development, as it is a human-derived cell line, and is thus more useful in elucidating mechanisms pertinent to that of human embryogenesis as well as being more applicable to medicinal investigation.

Through immunomagnetic sorting and single cell isolation techniques of SSEA-3 expressing cells within TERA-2 cultures, a cell line expressing high pluripotency markers which, upon differentiation with retinoic acid, undergo down-regulation of these markers to become mature, electrophysiologically active neurons.<sup>203, 242</sup> This cell line appears to show greater efficiency in differentiating in comparison to other TERA-2 cell lines such as TERA2.cl.D1.<sup>200</sup> Therefore, this cell line is a more robust, reliable model for neural differentiation studies.

The TERA2.cl.SP12 cell line can be manipulated, through exposure to retinoic acid, down a neural differentiation route to form spheroid cultures, or neurospheres.<sup>192, 201</sup> This neurosphere culture method overcomes many of the limitations of neuritogenesis in standard monolayer culture systems, including difficulty in visualization and quantification.<sup>204</sup> This is because the neurites that radiate from the central aggregate core, with no apparent overlapping, which can be problematic in monolayer cultures.<sup>204</sup>

## 1.5 Conclusions

In conclusion, neuromuscular junction development is an important process and primarily involves the development of two different cellular systems, which interact to form chemical synapses. Over the past decade, considerable attention has been focused

on developing *in vivo* and *in vitro* models of forming motor neurons as well as neuromuscular junctions.<sup>181, 205</sup> However, much of this research has focused on ES-derived neurons in the co-culture models. Here, we aim to further previous research and develop a robust, well-defined, co-culture model using the EC cell line TERA2.cl.SP12 to derive neurospheres that can then be co-cultured with C2C12 myotubes. Previous work at Durham University involved the co-culturing of C2C12 myoblasts with TERA2.cl.SP12 neurons in monolayers.<sup>206</sup> Although functional neuromuscular junctions formed, we believe that a co-culture involving neurospheres will allow a less complicated and more quantifiable, novel model system. This should allow for more reliable analysis of the neuromuscular junctions, including more reliable quantification of potential contractile events.

After development of neuromuscular junctions through employment of this co-culture system, we then look to develop methods of enrichment, identification, and/or purification of neurons and neuromuscular junctions when co-cultured with TERA2.cl.SP12 derived neurospheres. Once a robust experimental design has been established, it should be possible to carry out pharmacological manipulation of cholinergic NMJs to test their functional capacity.

### **1.5.1 Cell lines used**

The TERA2.cl.SP12 cell line will be used to provide a robust model of neurite outgrowth that can be co-cultured with C2C12 myoblasts. As previously mentioned, the TERA2.cl.SP12 line can be manipulated to commit to neural differentiation through formation of neurospheres.<sup>201, 204</sup> The C2C12 myoblast line is a cell line derived from murine skeletal muscle. This immortalized cell line is commonly used in myogenesis studies as well as co-culture systems as it readily differentiates into myotubules in low serum conditions.<sup>77, 184</sup> Upon differentiation, the myoblasts form long, multinucleated myotubules with relatively little spontaneous contraction; because the C2C12 derived

myotubules tend to lack the ability to spontaneously contract, it is possible to predict the presence of a functional neuromuscular junction when contraction occurs in the presence of neurons, which can then be investigated further.

## 1.6 Hypothesis, aims and objectives

### 1.6.1 Project hypothesis

We hypothesised that co-culturing neurons derived from TERA2.cl.SP12 pluripotent stem cells with a proven C2C12 myoblast lineage, neuromuscular junctions will form *in vitro*. This will allow anatomical and functional characterisation to be carried out. In addition, we hypothesised that co-culture conditions can be enhanced through manipulation of a signalling pathway common to both cell types.

### 1.6.2 Project aims

- To investigate the development of neuromuscular junctions *in vitro* after designing a novel, quantifiable co-culture system.
- To investigate the functionality of the co-culture system using a pharmacological approach.

### 1.6.3 Objectives

- Develop human neurons from TERA2.cl.SP12 stem cells through exposure to retinoids.
- Develop mammalian skeletal muscle from C2C12 myoblasts and characterize the differentiation process.
- Co-culture human neurons and mammalian skeletal muscle and characterize findings.
- Develop and characterize a novel, robust and reproducible, *in vitro* model of neuromuscular junction formation.

- Investigate the effects of ROCK-signaling on the co-culture system developed
- Manipulate the co-culture system pharmacologically to test functionality of neuromuscular junctions.

## 2.0 Materials and methods

Scientific techniques and experiments used throughout the project allowed the development and investigation of neuromuscular junction formation, ranging from advanced cell culture techniques to advanced microscopy. This chapter describes experimental procedures as well as equipment used in obtaining the results discussed.

### 2.1 Cell culture

#### 2.1.1 Cell line maintenance

##### 2.1.1.1 TERA2.cl.SP12

Embryonal carcinoma cells are derived from teratocarcinomas, germ-line tumours. These cells closely resemble embryonic stem cells and can therefore be used as models for stem cell differentiation. The embryonic carcinoma cell line TERA2.cl.SP12 is an early passage sub-cell line of the TERA2 line that was isolated through immunomagnetic sorting and single cell isolation techniques based on expression of pluripotency marker SSEA-3.<sup>203</sup> This TERA2.cl.SP12 cell line in particular, displays high levels of ES cell marker expression in undifferentiated state, followed by reduced levels of pluripotency markers and an increase in differentiation markers upon exposure to differential factors.<sup>194, 203</sup> The cell line is particularly useful for neural differentiation studies as it exhibits a propensity to produce neural derivatives when exposed to retinoic acid.<sup>198, 202, 211</sup> As an embryonal carcinoma cell line, TERA2.cl.SP12 does not require feeder cells, but instead culturing at high confluence maintains pluripotency potential.<sup>203</sup>

##### 2.1.1.1.1 Revival and Cryopreservation

Upon revival, the cells were rapidly transferred from -140 °C storage into a 37 °C water-bath to permit thawing. Immediately after thawing, the cells were then added to 9 mL maintenance media consisting of 10% foetal bovine serum (Thermofisher Scientific,



Massachusetts, USA) supplemented DMEM (ThermoFisher Scientific), 2mM L-glutamine (ThermoFisher Scientific) and 20 active units of penicillin and streptomycin (ThermoFisher Scientific), which was then centrifuged to obtain a cell pellet at 1000rpm for 3 minutes. The supernatant was then aspirated away allowing the cell pellet to be re-suspended in 10 mL maintenance medium before being transferred into a 25cm<sup>2</sup> BD Falcon culture flask (BD Falcon, Erembodegem, Belgium). This flask was incubated at 37 °C, 5% CO<sub>2</sub> in a humidified environment until fully confluent, at which point the cells were passaged into a 75cm<sup>2</sup> culture flask (BD Falcon) at a 1:1 ratio. Subsequent cells were maintained at high confluence to avoid loss of pluripotency.

For cryopreservation, confluent T75cm<sup>2</sup> flasks were trypsinised using 0.25% Trypsin EDTA (ThermoFisher Scientific) before centrifugation at 1000rpm for 3 minutes. Subsequent aspiration of the supernatant allowed for cells to be re-suspended in 10 mL heat treated FBS (ThermoFisher Scientific) supplemented with 10% dimethyl sulfoxide (DMSO, Sigma-Aldrich, Dorset, UK). This cell suspension was further aliquoted into 10 cryovials (ThermoFisher Scientific), each to contain a final volume of 1 mL of the cell suspension. Cryovials were then frozen down at a rate of -1 °C per minute at -80 °C; following which, cell stocks were transferred for storage at -150 °C.

#### 2.1.1.1.2 Maintenance

The pluripotent stem cell TERA2.cl.SP12 line was maintained in Dulbecco's modified Eagle's medium supplemented with 10% heat-treated FBS, 2mM L-glutamine and 20 active units of Penicillin and Streptomycin. The cells were maintained at 37 degrees Celsius at a carbon dioxide concentration of 5%. In order to retain the pluripotent potential of the stem cells, they were kept at high confluence (above 70%) in 75cm<sup>2</sup> BD falcon flasks and passaged whenever they reached 100% confluence, approximately every 3-4 days (see Figure 2.1.1.1.2).

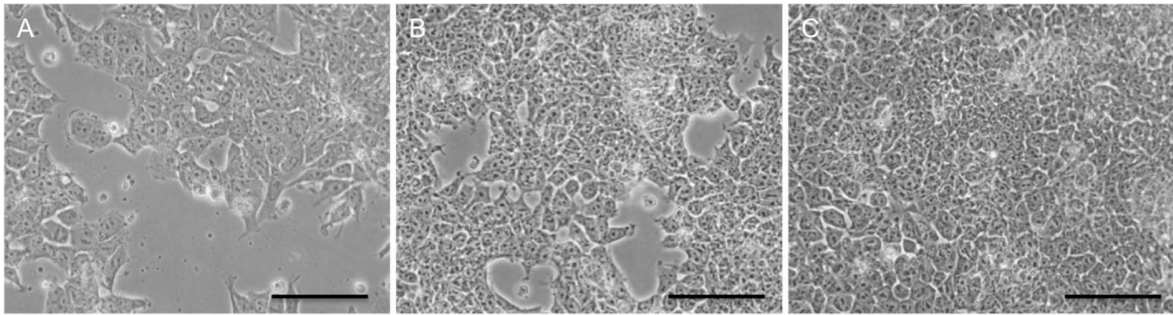


**Figure 2.1.1.1.2: TERA2.cl.SP12 cell population at low (A), medium (B) and high (C) confluence.** Phase contrast micrographs show the embryonal carcinoma line at different stages during the cell maintenance process. Cells should be maintained at high confluence to maintain pluripotency. Scale bars = 100  $\mu\text{m}$

Upon reaching full confluence in the 75cm<sup>2</sup> flasks (Panel C -Figure 2.1.1.1.2), cells were passaged to ensure pluripotency by splitting them in a 1:3 ratio. Media was aspirated from the flask before washing in 3ml sterile PBS. Following this, cells were mechanically dislodged from the flask using sterile acid-washed glass beads (ThermoFisher Scientific). The dislodged cells were then divided three-way and seeded into a further three 75cm<sup>2</sup> culture flasks and maintenance media was topped up to 20ml.

### 2.1.1.2 C2C12 myoblasts

The C2C12 myoblast line (ATCC, Middlesex, UK) is a cell line derived from murine skeletal muscle. This immortalized cell line provides a robust, reliable model of *in vitro* skeletal muscle differentiation and is thus readily used in proliferation and differentiation studies as well as co-culture systems.<sup>175, 200, 207</sup> C2C12 myoblasts readily proliferate in high-serum conditions. Upon differentiation however, the myoblasts undergo G2 phase cell cycle withdrawal, activation of muscle specific genes, before fusing to form long, multinucleated myotubules with relatively little spontaneous contraction.<sup>69</sup> Because the C2C12 derived myotubules tend to lack the ability to spontaneously contract, it is possible to predict the presence of a functional neuromuscular junction when contraction occurs in the presence of neurons, which can then be investigated further.

#### 2.1.1.2.1 Revival and Cryopreservation

C2C12 myoblasts were revived following the same method outlined for TERA2.cl.SP12 cells (refer to section 2.1.2.1.1), although they were revived directly into a T175cm<sup>2</sup> culture flask (Greiner Bio-One, Gloucestershire, UK).

For cryopreservation, approximately 60% confluent T175cm<sup>2</sup> flasks were trypsinised and the resultant cell suspension was centrifuged and then resuspended in 6 mL freezing media. Freezing media consisted of maintenance media supplemented with 5% DMSO. 1 cell suspension was added to a cryovial and frozen down.

#### 2.1.1.2.2 Maintenance

Mouse C2C12 myoblasts were maintained in DMEM supplemented with 10% fetal bovine serum, as well as 2mM L-glutamine and 20 active units of Penicillin and Streptomycin at 37 °C, 5% CO<sub>2</sub> in a humidified environment. Myoblasts were maintained around 40-50% confluent to avoid spontaneous differentiation, and thus maintenance of the myoblast population. To passage the cells, maintenance media was aspirated from the flasks before washing in approximately 4 mL PBS. 3mL of 0.25% Trypsin EDTA was then added to the flask and incubated for 3-4 minutes at 37 °C.

Trypsin was then neutralised through addition of 7 mL maintenance media before transferring the cell suspension into a 15 mL Falcon tube (Greiner Bio-One) for centrifugation at 1000rpm for 3 minutes. A viable cell count was then performed using a trypan blue (Sigma-Aldrich) exclusion assay using a haemocytometer and then the cells were seeded into T175cm<sup>2</sup>'s at a density of 0.5million per T175cm<sup>2</sup>. Maintenance media was then topped up to achieve a total volume of 25 mL.

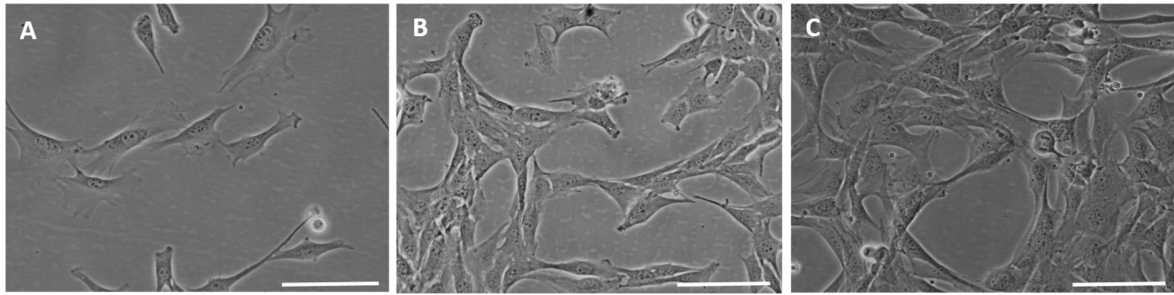


**Figure 2.1.2.2.2: C2C12 myoblasts at low (A), medium (B), and high (C) confluence.** Phase contrast images show the myoblasts at different stages in the maintenance process. Cells are to be maintained around 40-50% confluent, as shown in B to maintain myoblastic population. Scale bars = 25  $\mu\text{m}$

## 2.1.2 Neuron production from stem cells

TERA2.cl.SP12 stem cells were maintained as outlined in section 2.1.2.1.2. In preparation for neural differentiation, confluent T75 culture flasks were trypsinised with 0.25% trypsin/2mM EDTA for 3 minutes before addition of 7 mL fresh maintenance media to the flask in order to neutralise the trypsin. This resulting cell suspension was then pipetted into a 15 mL Falcon tube and centrifuged before removal of the supernatant and resuspension in 5mL maintenance media. Using a trypan blue exclusion assay, cell number was counted and  $0.5 \times 10^6$  cells were seeded into a fresh T75 culture flask. Maintenance media was then topped up to achieve a total volume of 20 mL.

### 2.1.2.1 Neuron production through natural retinoid and dissociation culture

For induction of differentiation from TERA2.cl.SP12 stem cells using natural retinoid compound all-trans-retinoid-acid (ATRA; Sigma-Aldrich). 20  $\mu\text{L}$  of 20 mM ATRA was added to the induction media to achieve a final concentration of 20  $\mu\text{M}$ . Differentiation media was changed every 3-4 days for 21 days.

### **2.1.2.2 Neuron production through synthetic retinoid and dissociation culture**

For neural differentiation of stem cells using synthetic retinoid EC23 (Reprocell Europe), 20 µL of 0.01 mM of EC23 was added to the induction media to achieve a final concentration of 0.01 µM. Differentiation media was changed every 3-4 days for 21 days.

Following 21 days differentiation through exposure to retinoic acid, all cultures were dissociated using 3 mL 0.25% trypsin/2 mM EDTA for 10 minutes at room temperature (RT). Subsequent neutralisation was carried out through addition of 7 mL maintenance media and then centrifugation to obtain a cell pellet that was then resuspended in 4 mL maintenance media. Cell suspensions were then split 1:4 and seeded into fresh T75 tissue culture dishes containing 20 mL maintenance media, without retinoids for 3-4 days. To enhance neural derivatives within culture, mitotic inhibitors were included in maintenance media: 1 µM cytosine arabioside (Sigma-Aldrich), 10 µM uridine (Sigma-Aldrich), and 10 µM 5'fluoro 2'deoxyuridine (Sigma-Aldrich).

Following this, the culture flasks were exposed to a light trypsinisation using 0.1% trypsin/EDTA for 2 minutes; for this, a 2.5X dilution of 0.25% trypsin/2 mM EDTA was carried out in versene (ThermoFisher Scientific). This trypsinisation allows cells that are loosely attached to the surface (predominantly neurons) to be mechanically dislodged through three-five lateral, sharp blows to the side of the culture flask, whilst other more adherent cells remain attached. These displaced cells are immediately neutralised using maintenance media and collected in a 15 mL Falcon, centrifuged, and counted using a trypan blue exclusion assay. Cells are then seeded at a density of  $2 \times 10^5$  /cm in 12-well or 48-well plates (Greiner Bio-One) for monoculture or co-culture studies.

More purified cultures of neurons were obtained through addition of resulting cell suspension back into a fresh T75 culture flask containing 20 mL maintenance media and

mitotic inhibitors, repeating the 3-4 day culture period before a further light trypsinisation.

### 2.1.3 Neurosphere formation

Maintenance media was removed from confluent T75 tissue culture flasks of TERA2.cl.SP12 stem cells and then they were washed in 3 mL sterile PBS. They were then trypsinised using 3 mL 0.25% trypsin/EDTA and counted using a haemocytometer to count viable cells after a trypan blue exclusion assay in which 10  $\mu$ L of cell suspension was diluted with 10  $\mu$ l of trypan blue. Following this, the cells were seeded into 90mm, sterile, untreated biological Petri dishes (ThermoFisher Scientific) at a density of  $1.5 \times 10^6$  per Petri dish. Maintenance media was topped up to 20 mL and incubated at 37  $^{\circ}$ C, 5% CO<sub>2</sub> in a humidified environment for 24 hours to promote aggregation of cells.

Following this 24-hour incubation period to allow the cells to aggregate, the synthetic retinoid compound, EC23 was added to the Petri dishes at a final concentration of 0.01  $\mu$ M. To achieve this, 20  $\mu$ L of a 0.01 mM EC23 stock was added to the existing 20 mL maintenance medium in the Petri dish, thus constituting the differentiation medium for neurosphere formation. These Petri dishes were cultured for 21 days at 37  $^{\circ}$ C, 5% CO<sub>2</sub> in a humidified environment, with a media change every 3-4 days. To change the

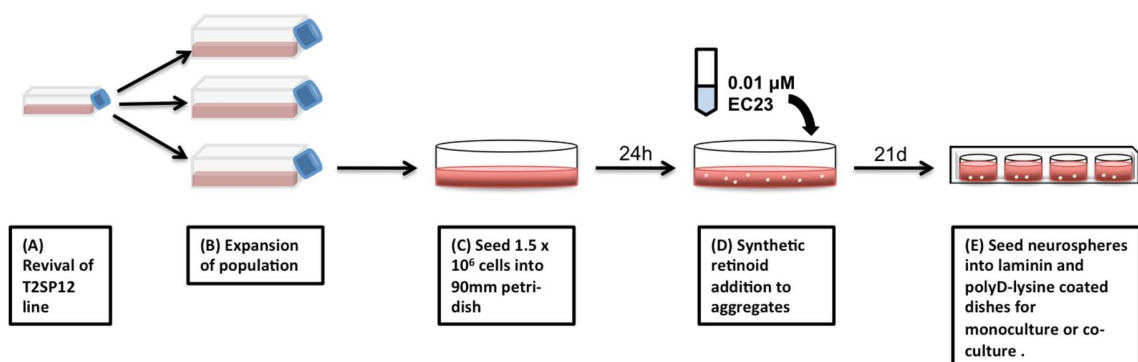


**Figure 2.1.4: The Key stages involved in neurite outgrowth for both 2D monoculture and co-culture studies.** After revival of the TERA2.cl.SP12 cell line (A), cell population is expanded and passaged where necessary (B), maintaining populations at high confluence. Cells are then seeded into Petri dishes, where they are allowed to aggregate for 24 hours (C) prior to addition of synthetic retinoid EC23 to direct aggregates down a neural lineage (D). After 21 days, mature neurospheres can be extracted from the media and added into plates for neurite outgrowth/co-culture studies (E).

differentiation medium, the cell suspension was transferred into a 50 mL Falcon tube and then left for 5 minutes, allowing the cells to settle to the bottom. Once settled at the bottom of the tube, the old differentiation medium was aspirated off before addition of 20mL of fresh differentiation medium to re-suspend the cell sediment. This new cell suspension was then directly seeded into a new 90mm untreated, biological Petri dish. After 21 days, the aggregates had formed mature neurospheres. See Figure 2.1.4.

## **2.1.4 Induction of neurite outgrowth from neurospheres**

### **2.1.4.1 Coating of culture plates for neurite outgrowth**

500  $\mu\text{L}$  coating solution consisting of 1  $\text{mgmL}^{-1}$  Laminin from Engelberth-Holm-Swarm murine sarcoma membrane (Sigma-Aldrich) as well as 500  $\mu\text{L}$  of 1  $\text{mgmL}^{-1}$  poly-D-lysine (Sigma-Aldrich) (produced through addition of poly-D-lysine powder to 49mL  $\text{Ca}^{2+}$  and  $\text{Mg}^{2+}$  free PBS and 1mL phosphate buffered saline was added to each well of a 12-well tissue culture plate or 150 $\mu\text{L}$  to each well of a 48-well plate. These plates were sealed using parafilm (ThermoFisher Scientific) and incubated overnight at room temperature. Following overnight incubation, the coating solution was aspirated off and each well was washed 3 times with sterile PBS ready for seeding of neurospheres.

### **2.1.4.2 Induction of neurite outgrowth**

Once mature neurospheres had been obtained after 21 days of TERA2.cl.SP12 culture in differentiation medium, individual neurospheres were seeded onto pre-coated 12-well and 48-well plates for 2D neurite outgrowth studies. To do this, neurospheres and differentiation medium were removed from the Petri dish with a 25mL pipette (Greiner Bio One, Gloucester, UK) before being passed through a 100 $\mu\text{m}$  cell strainer (BD Falcon), allowing the neurospheres to be separated from the differentiation medium as well as removing any single cells and cellular debris. The cell strainer was then backwashed

using fresh maintenance media into a new 90mm untreated, biological Petri dish. 300  $\mu\text{L}$  maintenance media as added to each well per 12-well plates and 150 $\mu\text{L}$  to each well in the 48-well culture plates. This maintenance media consisted DMEM, 10% FBS, 2 mM L-glutamine, 20 active units of penicillin and streptomycin supplemented with the following mitotic inhibitors: 1  $\mu\text{M}$  cytosine arabinose (Sigma-Aldrich), 10  $\mu\text{M}$  5-fluoro 2'-deoxyuridine (Sigma-Aldrich) and 10  $\mu\text{M}$  uridine (Sigma-Aldrich). A 200  $\mu\text{L}$  pipette was then used to extract 20  $\mu\text{L}$  of the media containing 1-2 neurospheres and adding them to each well. These plates were then incubated at 37 °C, 5% CO<sub>2</sub> in a humidified environment for 10 days.

#### **2.1.4.3 The effect of ROCK signaling on neurite outgrowth**

In order to investigate and enhance neurite outgrowth from neurospheres, a selective ROCK inhibitor, Y-27632 (TOCRIS Bioscience, Abingdon, UK) was added to the culture medium. For this, Y-27632 was added to the culture medium at the 10-day neurite outgrowth stage at a final concentration of 10  $\mu\text{M}$ .

#### **2.1.5 Myotube formation**

C2C12 myoblasts were seeded into 12-well plates for differentiation studies prior to immunofluorescence analysis and co-culture. Cells were seeded at a density of  $8 \times 10^3$  cells per well of a 12 well plate containing 3 mL maintenance media. This maintenance media was changed every 2 days until the cells reached approximately 90% confluent, at which point maintenance media was changed to differentiation media to induce differentiation of myoblasts into myotubes. Differentiation media consisted of DMEM supplemented with 2% horse serum (Sigma-Aldrich), 2mM L-glutamine and 100mg/ml Penicillin and Streptomycin. Mitotic inhibitors, 1  $\mu\text{M}$  cytosine arabinose, 10  $\mu\text{M}$  5-fluor 2'-deoxyuridine and 10  $\mu\text{M}$  uridine, can also be included in the differentiation media to prevent the cell population becoming over-confluent in culture.



### 2.1.5.1 The effect of ROCK signaling on myotube formation

To investigate the effect of ROCK signaling on myotube formation, ROCK inhibitor Y-27632 was added to differentiation media at a final concentration of 10  $\mu\text{M}$ . This differentiation media was changed every 2 days until mature myotubes were formed around day 5.

### 2.1.6 Neuron-myotube co-culture

For co-culture, 12-well plates were coated with substrate growth coating as outlined in section 2.1.5.1 24 hours prior to addition of C2C12 myoblasts. Mature myotubes were formed from C2C12 myoblasts as described in 2.1.6. Neurons produced from TERA2.cl.SP12 stem cells (as described in section 2.1.3) were seeded on top of mature myotubes in 12 well plates at a density of approximately  $2.0 \times 10^5$  cells/cm<sup>2</sup> per well. 3 mL of culture media was added to each well and a half-media change was carefully performed daily, making sure the base of the well was not disturbed. Culture media consisted of 10% FBS supplemented DMEM, 2mM L-glutamine and Penicillin/Streptomycin along with mitotic inhibitors: 1  $\mu\text{M}$  cytosine arabinose, 10  $\mu\text{M}$  5-fluor 2'-deoxyuridine and 10  $\mu\text{M}$  uridine. After 10 days, cultures were fixed using 4% paraformaldehyde for later analysis.

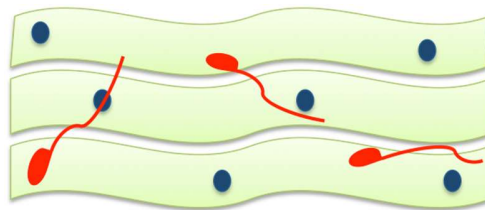


**Figure 2.1.7: Schematic showing the neuron-myotube co-culture set up.** Neurons (red) can be seeded in monolayers on top of mature myotubes (green) and co-cultured to allow potential interactions to form between the cell types.

### 2.1.7 Neurosphere-myotube co-culture

Glass coverslips (ThermoFisher Scientific) were added to 12 well plates before coating as outlined in section 2.1.5.1.

Mammalian myotubes were again produced from C2C12 myoblasts as outlined in section 2.1.6. After neurospheres were cultured (refer to section 2.1.4), neurospheres were washed with maintenance media by pipetting neurosphere cell suspension through a 100  $\mu\text{m}$  cell strainer (Sigma-Aldrich) into a 50 mL falcon tube. The cell strainer was then backwashed using maintenance media into a fresh sterile, biological 90mm Petri dish. Differentiation media was removed from the 12-well plate containing mature myotubes and replaced with 3 mL co-culture media, consisting of DMEM, 2mM L-glutamine, Penicillin/Streptomycin, and mitotic inhibitors 1  $\mu\text{M}$  cytosine arabinose, 10  $\mu\text{M}$  5-fluor 2'-deoxyuridine and 10  $\mu\text{M}$  uridine. Subsequent addition of neurospheres on top of the mature myotubes was performed by pipetting 20  $\mu\text{L}$  of the freshly washed neurosphere media containing approximately 3 neurospheres from the Petri dish into each well of the 12 well plate. A half media change was carried out every other day for 10 days until the co-culture was ready for fixation and/or analysis. This co-culture setup is illustrated in Figure 2.1.8.

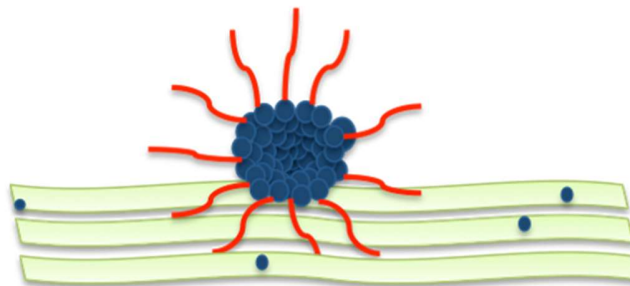


**Figure 2.1.8: Schematic showing the neurosphere-myotube co-culture set up.** Neurites radiate from the neurosphere (red) seeded on top of mature myotubes (green), allowing potential interactions to form between the two cell types.

### 2.1.7.1 Introduction of ROCK inhibitor Y-27632 into co-culture system

In order to investigate the effects of ROCK signalling on the co-culture system, the ROCK inhibitor Y-27632 was incorporated into the co-culture media (outlined in the previous section) at a final concentration of 10  $\mu\text{M}$ . This co-culture system required a half-media

change daily whereby 1.5 mL of media from each well of the 12 well plate was removed and discarded using a P1000 pipette, followed by addition of 1.5 mL fresh co-culture media.

#### **2.1.7.2 Addition of Acetylcholine to the co-culture system**

To investigate the functional capacity of the neurosphere co-culture system, non-selective AChR agonist acetylcholine chloride (Sigma-Aldrich) was introduced into the co-culture system after 10 days of co-culture, at a final concentration of 0.01  $\mu\text{M}$ . Cultures were immediately visualized using phase-contrast microscopy and any movement imaged/videoed. As a negative control, acetylcholine was added to 10-day old mature myotube monocultures at a final concentration of 0.01  $\mu\text{M}$ .

## **2.2 Analytical techniques**

### **2.2.1 Fixation of samples**

For fixation of samples in the 12 and 48 well plates, remaining media from each well was aspirated before washing in 1 mL PBS. Fixing solution – 4% PFA was then added to each well (2 mL to 12-well and 500  $\mu\text{L}$  to 48-well plates). For studies involving neurospheres, fixing solution was left for one hour to allow penetration of the neurosphere mass. For studies on C2C12 derived cells or monolayers of neurons, the fixing solution was left for 20 minutes. This fixing solution was then aspirated off before washing 3 times in 1 mL PBS. Plates were then stored in PBS prior to immunofluorescence analysis.

### **2.2.2 Immunofluorescence staining**

Subsequent to fixation, coverslips/wells were exposed to 0.1% Triton-X100 (ThermoFisher Scientific) in PBS for 10 minutes in order to permeabilise cells. After removal of permeabilisation solution, blocking buffer consisting of 0.01 % Tween

(Sigma-Aldrich), 1% neonatal goat serum (NGS, Sigma-Aldrich) in PBS for 1 hour, on ice. Primary antibody was then added and allowed to incubate for 1 hour whilst slowly rocking. Following its removal, primary antibody was washed off by performing 3 consecutive 10-minute washes in blocking buffer, directly followed by the addition of fluorescent secondary antibodies along with Hoerchst 33342 (Thermofisher) to counterstain nuclei. After 1-hour incubation with secondary antibodies, samples were subjected to 3 further 10-minute washes in blocking buffer and stored in PBS before analysis or mounting of coverslips.

All antibodies were diluted in blocking buffer, a summary of which can be found in section 2.2.5

### **2.2.3 Phalloidin staining of F-actin**

F-actin filaments were stained using phalloidin-FITC stain (Cytoskeleton Inc., DENVER, USA). The protocol for actin staining varied depending on the type of culture being stained, as outlined below.

#### **2.2.3.1 Phalloidin staining of F-actin in monoculture**

For phalloidin-FITC staining of F-actin in monocultures of C2C12 cells, cell cultures were fixed (see section 2.2.1) and stored in PBS. PBS was then removed and cultures were permeabilized for 5 minutes using 0.1% Triton-X100. Following this, permeabilisation buffer was pipetted off and cultures were washed in PBS for 30 seconds. A phalloidin-FITC stock solution was prepared consisting of 3.5  $\mu\text{L}$  per 500  $\mu\text{L}$  PBS and 300  $\mu\text{L}$  of this solution was added to each well of a 12-well plate. Once added, the plate was incubated at room temperature, in darkness for 30 minutes. Cultures then underwent three consecutive 30-second washes in PBS. To counterstain nuclei in the monoculture, Hoescht 33342 was added for 5 minutes (1:1000 dilution). Cultures were then rinsed and washed in PBS before storing in PBS or mounting.

### **2.2.3.2 Phalloidin staining of F-actin in co-culture**

In co-culture involving two cell types, for example neurons and C2C12 cells, immunocytochemistry was carried out and therefore the phalloidin-FITC stain was integrated into the protocol outlined in section 2.2.2. phalloidin-FITC was integrated into the secondary antibody solution with blocking buffer and incubated for 1 hour alongside the Hoescht 33342 stain to counterstain nuclei.

### **2.2.4 alpha-bungarotoxin staining**

To visualise acetylcholine receptors, alpha-bungarotoxin (Invitrogen, California, USA) stain was used. Alpha bungarotoxin is a 74-amino acid peptide that is extracted from the venom of *Bungarus multicinctu*. It binds to the alpha-subunit of acetylcholine receptors with high affinity, and thus, when conjugated to an Alexafluor molecule, is of extreme use in the identification and visualisation of nicotinic acetylcholine receptors in muscle and at neuromuscular junctions.

#### **2.2.4.1 Staining in monoculture**

In monoculture studies, cultures were permeabilized using 0.1% Triton-X100 for 10 minutes, followed by a 30 second wash in PBS. Alpha-bungarotoxin was diluted in PBS (1:400), and 300 µL of this solution was added to each well of a 12 well plate. Following removal of the alpha-bungarotoxin stain, cultures were washed for 30 seconds in PBS three times. Hoescht 3342 was then added to counterstain nuclei for 5 minutes, followed by a final PBS wash.

#### **2.2.4.2 Staining in co-culture**

For co-culture staining, alpha-bungarotoxin staining was incorporated into the secondary antibody solution involved in immunofluorescent staining and staining occurred as outlined in section 2.2.2. Thus, cultures were incubated for 1 hour with the stain alongside the hoescht 33342 nuclei stain.

## 2.2.5 Summary of antibodies and stained used in analysis

**Table 2.2.5-1 – Summary of primary antibodies used in immunofluorescence.** All of the primary antibodies used in immunofluorescence analysis of 2D samples; their respective supplier, product code and species in which they were obtained from are also listed. All of the antibodies were diluted in blocking buffer.

Target	Supplier	Product code	Host species	Dilution
B-III-tubulin	Cambridge bioscience	3525-100	Rabbit	1:600
Myosin heavy chain	R&D system	MAB4470	Mouse	1:500

**Table 2.2.5-2 – Summary of secondary antibodies used in immunofluorescence.** All of the secondary antibodies used in immunofluorescence analysis of 2D samples; their respective supplier, product code and species in which they were obtained from are also listed. All of the antibodies were diluted in blocking buffer at the dilutions listed above.

Antibody	Supplier	Dilution	Host	Product code
Alexafluor anti-rabbit 488	Thermofisher	1:600	Goat	A-11034
Alexafluor anti-rabbit 594	Thermofisher	1:600	Goat	AB-2556547
Alexafluor anti-mouse 594	Thermofisher	1:600	Goat	A-21203

**Table 2.2.5-3 – Summary of stains used in fluorescence analysis of cultures.** All stains have listed suppliers, product codes, the dilution used, and their emission wavelength.

Name	Target	Supplier	Product code	Dilution	Emission Wavelength
Acti-stain phalloidin-FITC	Actin	Cytoskeleton	PHDG1	3.5 $\mu$ L / 1mL solution	488
Hoechst 33342	Nuclei	Thermofisher	H3570	1:1000	
Alpha-bungarotoxin Alexafluor	Aceylcholine receptor	Thermofisher	B13423	1:400	594

## 2.2.6 ImageJ analysis of neurite outgrowth

In order to quantify neurite outgrowth, neurosphere cultures were stained as previously outlined, using the pan-neuronal marker TUJ1, which immunofluorescently stains neurites, whether they are in monolayer culture or in neurosphere culture. Digital images of the staining were obtained using the confocal microscope, then opened in Software package designed for image analysis – ImageJ (imagej.nih.gov). A scale was then set in the software, representative to the size of the image loaded. To do this, using the line tool, a line was traced over the existing scale bar on the image, followed by Analyse > Set Scale. A scale box then appeared, allowing the size of the scale bar to be inputted in  $\mu\text{m}$ .

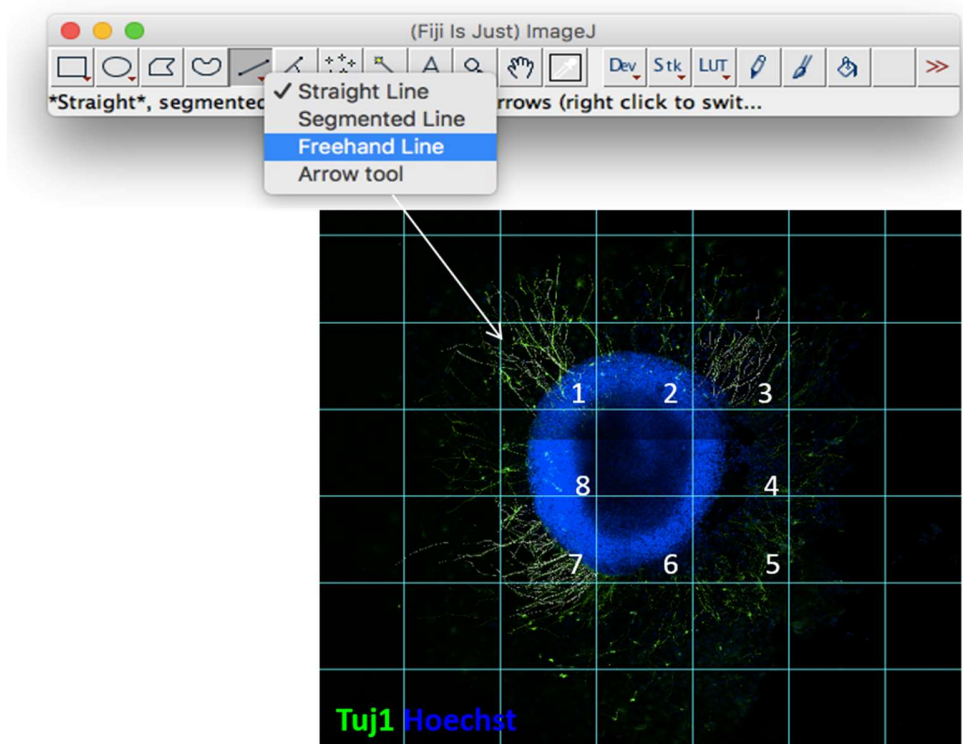


**Figure 2.2.6: Neurite quantification was performed using ImageJ.** To quantify neurite length and neurite density, a grid was overlaid over neurosphere images. Boxes containing edges of the neurosphere where neurites protrude were numbered accordingly. Then, using a random number generator, 3 numbers were obtained and the neurites within the boxes were traced using the freehand line tool (shown here) and measured.

To set up a random sampling method of neurite quantification, and to avoid bias of neurites quantified, a grid was over-laid on the image and boxes where neurites protruded were numbered appropriately. Then, using a random number generator (random.org), three random numbers were acquired, and the neurites within boxes with the corresponding number were measured (see Figure 2.2.6).

The 'Freehand Line' tool was then selected, and used to trace out neurites from central-most part, outwards. Following this, by clicking Analyze then measure, and Analyze then Draw, it was possible to measure the length of each neurite in  $\mu\text{m}$ , and to draw on the image which ones had been measured. Consequently, a table was produced containing a number assigned to each neurite measured, and its respective length. This raw data was then extracted and quantified to give neurite length, and neurite density per neurosphere. This method of neurite quantification was used throughout the project when neurites required quantification, and has previously been shown to be as efficient as quantifying all individual neurites.<sup>204</sup>

### **2.2.7 ImageJ analysis of myotube number**

To quantify myotube number in monoculture, myotubes were differentiated from C2C12 myoblasts as previously outlined, and images were taken daily following switching of media to differentiation media. Cultures were imaged using the 40X objective lens on the phase-contrast microscope. These images were then imported into Image J software for image analysis, where a scale bar of appropriate length was added. The line tool was used to draw on any myotubes measuring longer than 120  $\mu\text{m}$ , and the draw function (D) was used to keep track by permanently marking them. This quantification method was based on findings that mature C2C12 myotubes average a length between 130  $\mu\text{m}$  and 520  $\mu\text{m}$ .<sup>240</sup> Therefore, following this quantification method, myotube number herein refers to myotube number per 40X field of view (approximately 210  $\mu\text{m}$  x 170  $\mu\text{m}$ )



### **2.2.8 MHC quantification**

In order to quantify expression of MHC in mature myotubes using ImageJ, confocal microscope images obtained using the x20 lens were used. In these, F-actin of myotubes were stained green with phalloidin-FITC, nuclei counterstained blue with Hoechst, and MHC stained red with an anti-MHC antibody. Images were imported into the ImageJ software, and appropriate scale bars added. Myotubes measuring longer than 125  $\mu\text{m}$  were first counted and using the draw function (D), were marked for easy identification. Marked myotubes that expressed MHC (red) were then counted, and quantified as an expression of total myotubes present in each 20x image. For ease of identification of MHC expressing myotubes, Zen Blue software was used to split the colour channels, which allowed red only to be observed and compared to total myotubes.

## **2.3 Microscopy**

Different microscopy techniques were employed throughout this project.

### **2.3.1 Phase contrast microscopy**

Live cells were imaged/recorded using the Leica DFC 310FX with digital camera DMI 3000B. Objective lenses x10, x20, and x40 were used.

### **2.3.2 Confocal microscopy**

Confocal images were obtained on the Zeiss 880 confocal laser-scanning microscope with airyscan. The x10 EC Plan Neo DC I, x20 Plan Apochromat DIC II, x40 EC Plan Neo DIC II, and x63 Plan Apochromat DIC II lenses were used. Zeiss Zen software was used to capture images, tile-scans and Z-stacks.

## **2.4 Statistical analysis**

Graphpad Prism v6 was used for all statistical tests performed on data sets. Relevant statistical tests including Student's T-test and One-way ANOVA were performed.

Significance is represented in data shown using stars, where \* =  $p \leq 0.05$ ; \*\* =  $p \leq 0.01$ ;  
\*\*\* =  $p \leq 0.001$  and \*\*\*\* =  $p \leq 0.0001$ .

## 3.0 Results

### 3.1 Generation of human neurons from TERA2.cl.SP12 stem cells

Stem cells were cultured as outlined in section 2.1.1.1 and maintained at a high confluence to ensure pluripotent phenotype was maintained. This high confluence enables cell-cell contact between the stem cells is ensured, facilitating important crosstalk and signalling between cells, including Notch signalling. Human neurons were then generated from TERA2.cl.SP12 stem cells through various methods, using both natural and synthetic retinoids to direct the stem cells down a neural lineage.

#### 3.1.1 Differentiating human neurons from stem cells through exposure to retinoids

Monolayers of human neurons were produced through exposing TERA2.cl.SP12 to natural retinoid, 10 $\mu$ M ATRA or synthetic retinoid, 0.01  $\mu$ M EC23. The stem cells are extremely sensitive to retinoids, and form neurites in culture upon exposure. This method utilises the propensity of the embryonal carcinoma cell line to produce neural derivatives of a low-adhesive nature.<sup>200</sup> Any contaminating cells not of a neural lineage tend to be more adhesive, thus an increased purity of neurons can be obtained through repeated light trypsinisation to remove neural cells and transferring to a new culture flask.<sup>200</sup>

Upon treatment with either retinoid, stem cells lost their typical stem-cell morphological appearance, adopting a more neural-like phenotype. During this process the stem cells, which existed as rounded mononucleate clustered cells, lost their characteristic stem cell phenotype as they differentiated. Differentiating neural cells initially produced a protrusion at the leading edge of the cell, later elongating and maturing to become a neurite. Differentiated neurons were collected from the flasks in which they were

cultured with EC23 or ATRA, and seeded onto laminin and poly-D-lysine coated 12-well plates, and subsequently cultured for 5 days.

Immunofluorescence visualisation was achieved by staining cultures after fixation with pan-neuronal marker, TUJ-1, and nuclear counterstain, Hoechst. Neurons appeared larger than the cells from which they were differentiated, and more homogenous. Contaminating cells were observed in the background, shown by the positive nuclear staining (Figure 3.1.1). There were no apparent differences between the neurons produced through ATRA exposure, compared to EC23, although full neuron counts were not performed, and cells were seeded at the same density in both cases. Mitotic inhibitors were included in the culture medium to prevent further proliferation of any contaminating cells. Contaminating cells were obvious in culture (circled, Figure 3.1.1).

### **3.1.2 Formation of neurospheres from stem cells through synthetic retinoid exposure**

Another approach to neurite outgrowth can be performed through generation of spheroid cultures from TERA2.cl.SP12 stem cells. Confluent TERA2.cl.SP12 stem cell cultures (Figure 3.1.2, Panel A) are dissociated and seeded into Petri dishes, where they are allowed to adhere for 24 hours to form stem cell spheroids (Figure 3.1.2, Panel B). At which point, they are cultured in the presence of synthetic retinoid EC23 for 21 days, promoting acquisition of a neural lineage.

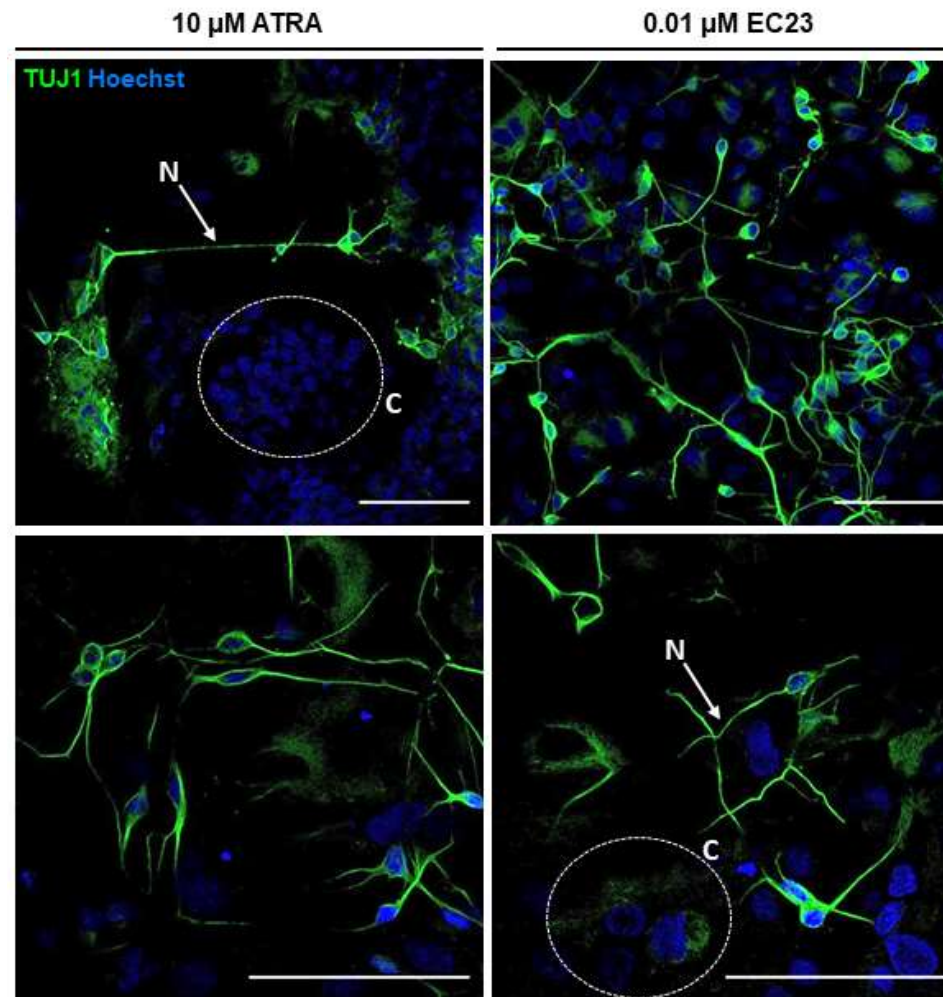


**Figure 3.1.1: TERA2.cl.SP12 stem cells can be differentiated into human neurons through exposure to retinoids using cell dissociative culture method.** Neurons differentiated from stem cells using natural retinoid ATRA (left) or synthetic retinoid EC23 (right) were seeded into laminin and poly-D-lysine coated 2D culture plates for 5 days before fixation and immunofluorescence analysis. Confocal images show Tuj1 (green) stained neurites (N) and Hoechst (blue) stained nuclei. Contaminating cells are also present (C). Bottom panel is higher magnification than upper panel. Negative control not shown. Scale bars = 100  $\mu$ m.

### **3.1.3 Neurite outgrowth from neurospheres**

Neurospheres appeared in suspension culture as masses of aggregated cells (Panel A, Figure 3.1.2). Once seeded onto laminin and Poly-D-Lysine coated plates, neurites began to protrude radially from the central mass of cell (Figure 3.1.2, C+D). Growth cones can be identified at the distal tip of axons (Figure 3.1.2, labelled GC).

Immunocytochemistry was performed on neurospheres after 10 days of neurite outgrowth cultures (Figure 3.1.3), whereby neurites were stained with pan-neuronal marker TUJ-1 (green) and nuclei were counterstained with Hoechst (blue). This staining approach allowed projecting neurites to be visualised clearly, but also highlighted cell migration from the central mass of perikarya (Figure 3.1.3, circled). Immunocytochemical analysis also allowed more accurate visualisation of neurites as thinner axons could be missed when using phase-contrast microscopy. Higher magnification images of growth cones were also obtained, showing the characteristic shape found at the distal tip (Figure 3.1.3, labelled GC)

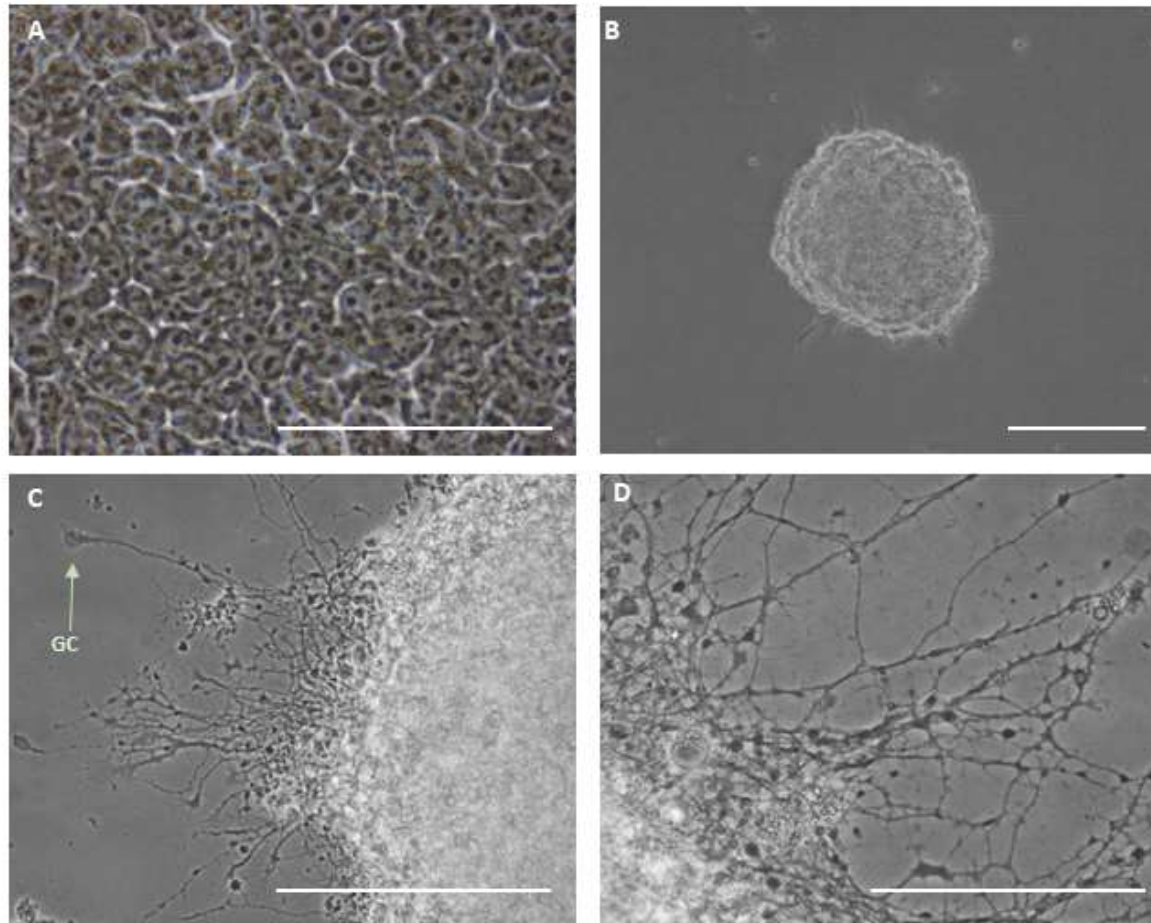


**Figure 3.1.2: TERA2.cl.SP12 stem cells can be cultured to form neurospheres capable of producing neurites through retinoic acid exposure.** Confluent stem cells (A) were dissociated from culture flasks, seeded into Petri dishes and allowed to adhere for 24 hours before addition of synthetic retinoid, EC23. They were then cultured for 21 days. Following this, neurospheres were seeded into laminin and poly-D-lysine coated plates along with maintenance media supplemented with mitotic inhibitors: 1  $\mu\text{M}$  cytosine arabinose, 10  $\mu\text{M}$  5-fluor 2'-deoxyuridine and 10  $\mu\text{M}$  uridine (B). Neurite outgrowth was allowed to occur for 10 days; during which, neurites project outwards from the central mass of nuclei (C+D). Growth cones can be observed at the leading tip of the axon (labelled, GC). Scale bars A and D = 100  $\mu\text{m}$ , B and C = 200  $\mu\text{m}$ .

### **3.1.4 Enhancing neurite outgrowth from neurospheres through ROCK inhibition by Y-27632**

Once reproducible neurite outgrowth from TERA2.cl.SP12 neurospheres was achieved, the involvement of Rho A signalling pathway in neurite outgrowth was investigated. Neurite extension is a process reliant on actin remodelling; a mechanism involving a culmination of Rac and Cdc42 activation and inhibition of RhoA and ROCK signalling. Previous models of neurite outgrowth have included inhibitors of ROCK when culturing to enhance the process of neurite outgrowth.<sup>198, 204</sup> Of particular interest is the action of ROCK inhibitor Y-27632, and was therefore included in the culture media to enhance outgrowth.

The ROCK inhibitor Y-27632 was added to the culture medium at a final concentration of 10  $\mu$ M for the 10 day neurite-outgrowth phase. This appeared to significantly increase neurite outgrowth from neurospheres compared to those cultured without ROCK inhibitor (see figure 3.1.4-1). Neurites (TUJ-1 positive - green) appeared to be significantly greater in number in cultures treated with Y-27632. As well as this, the ROCK inhibitor appeared to reduce the number of non-neuronal cells migrating from the central cellular mass. Migrating cells appeared to saturate areas surrounding neurites in the untreated control, but the Y-27632 treated cultures appeared to be free of these migrating cells and are subsequently much tidier than untreated cultures. The neurites in the Y-27632 treated cultures were very dense and formed a 'brush-like' border radiating outwards from the central mass of cells. Y-27632 treated neurites also appeared longer in comparison to untreated cultures.



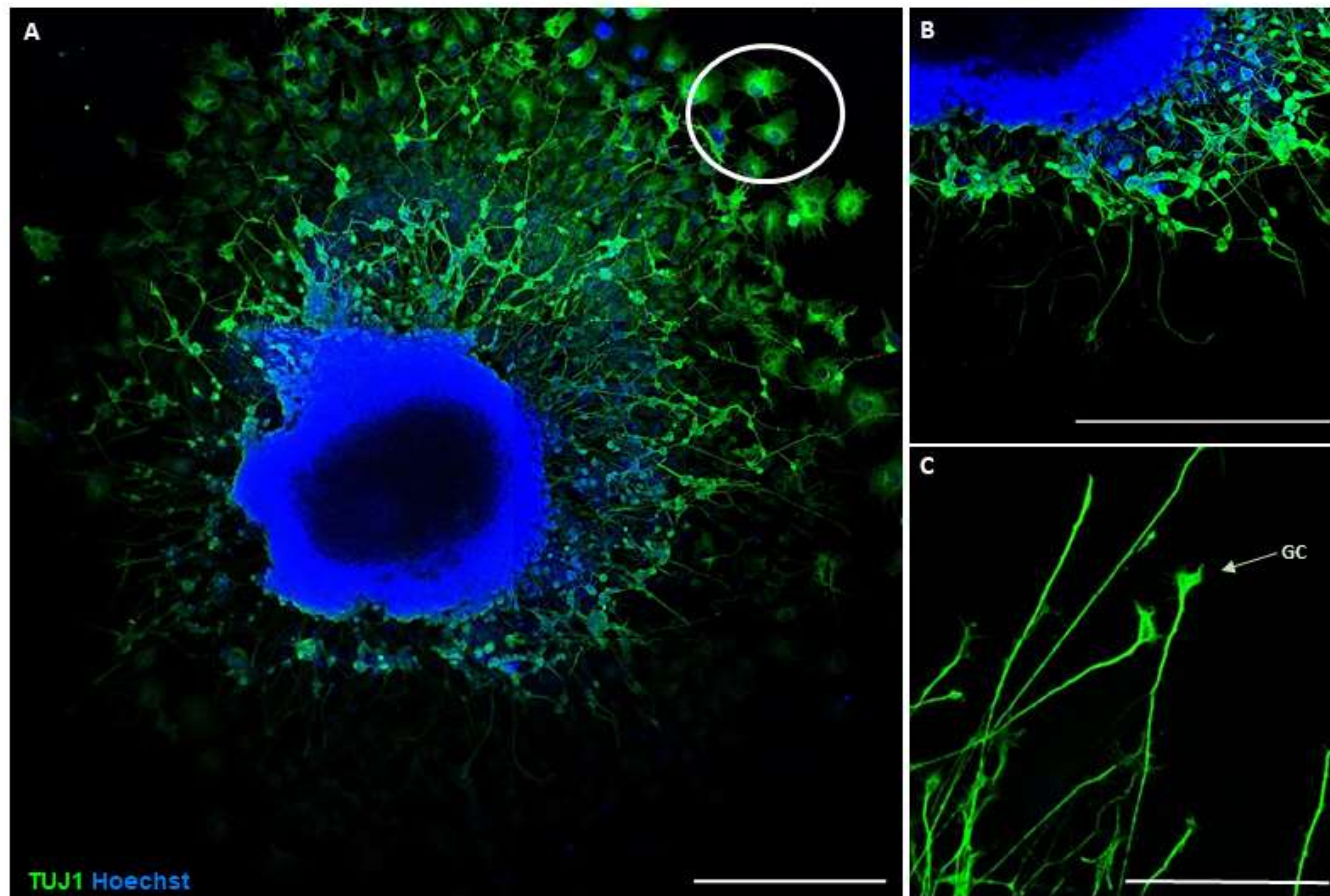


**Figure 3.1.3: Neurites radiate outwards from the central mass of cells of the neurosphere.** Immunofluorescence analysis of neurite outgrowth allows clear observation of neurites radiating outwards from the central, spherical mass of nuclei (A+B), with neurites stained green (TUJ1) and nuclei stained blue (Hoechst). Growth cones can be clearly identified at the leading edge of the neurites (C - labelled, GC). Contaminating cells can also be observed surrounding the neurosphere (circled in A). Scale bars A and B = 500  $\mu\text{m}$ , C = 100  $\mu\text{m}$ .

Analysis was performed to quantify the effect of Y-27632 treatment on neurite outgrowth (Figure 3.1.4-2). Both neurite length and neurite density were quantified using the method described in section 2.2.6. Quantification revealed that the aforementioned parameters, neurite length and neurite density, were increased by ROCK inhibitor Y-27632 (Panel B). Neurite length was significantly increased ( $p < 0.0001$ ). Neurites averaged a length of 350  $\mu\text{M}$  in Y-27632 treated cultures compared to the average of 290  $\mu\text{M}$  in the untreated control. Furthermore, neurite density was also significantly increased ( $p < 0.01$ ). Neurite density, on average, was more than doubled by treatment with the ROCK inhibitor.

## **3.2 Production of myotubes from mammalian C2C12 myoblasts**

C2C12 myoblasts were used to examine the developmental and functional biology of mammalian skeletal muscle *in vitro* as a target for neurite interaction.

### **3.2.1 Differentiating C2C12 myoblasts into myotubes**

C2C12 myotubes, a cell line derived from mice, were maintained as described in 2.1.1.2. To induce differentiation of C2C12 myoblasts into myotubes, a media switch involving the replacement of the culture medium to a differentiation media containing 2% horse serum was performed. This differentiation process was initiated upon withdrawal of the cells from the cell cycle at the G2 stage and proliferation ceases. Following this, a multistep process was observed, during which mononucleate myoblasts (Figure 3.2.1 - Panel 1 - A) migrated towards one another (B), aligned (C), fused (D), and elongated (E) to form multinucleate myotubes.

From the point of the aforementioned media switch, differentiation occurred over a period of 4-5 days to form mature myotubes, as shown in Panel 2, Figure 3.2.1. In this figure, myoblasts/myotubes were stained green with an actin stain, phalloidin, which specifically stains F-actin. Nuclei were stained

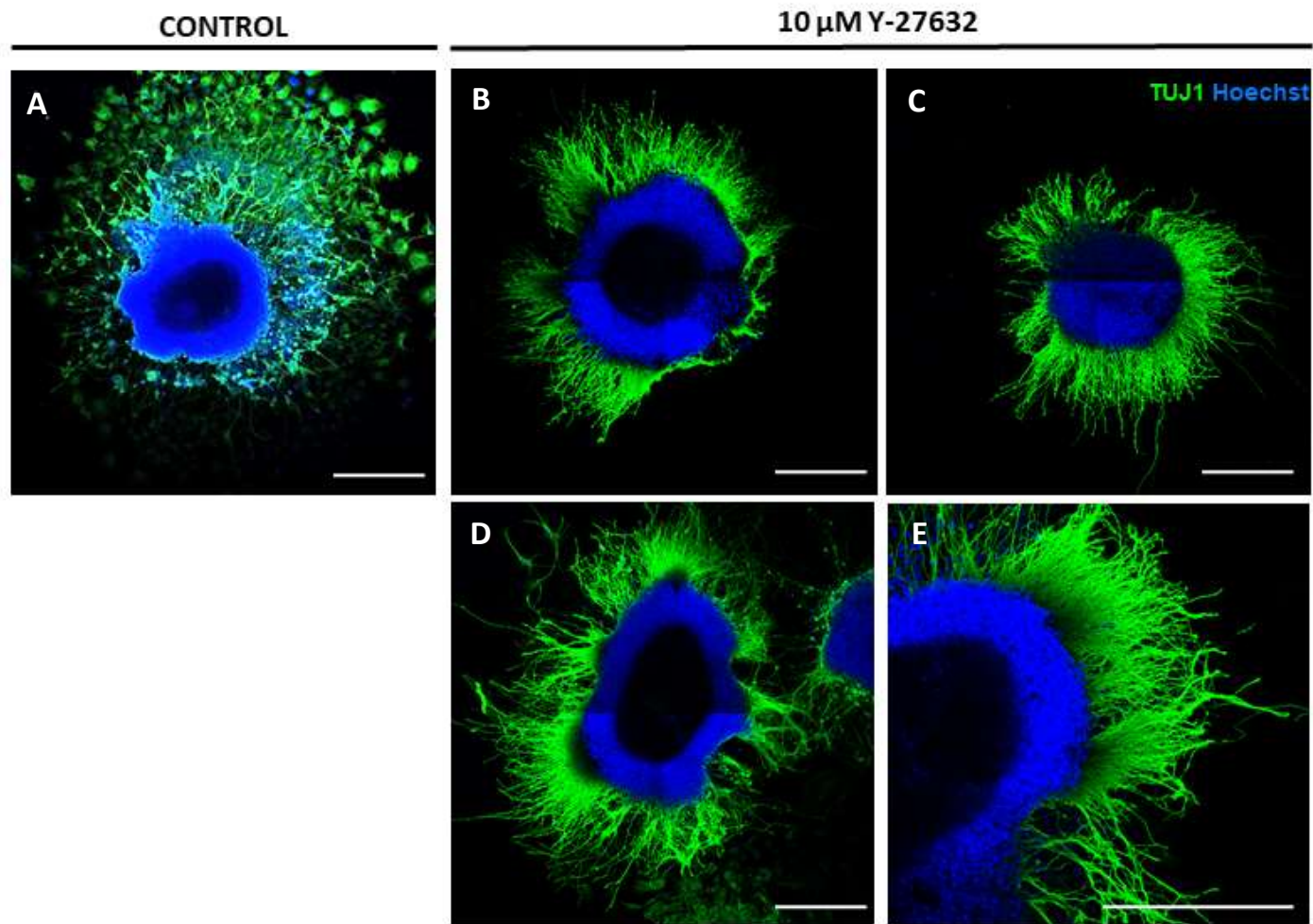


**Figure 3.1.4-1: The effect of RhoA/ROCK signalling on neurite outgrowth from TERA2.cl.SP12 neurospheres.** ROCK inhibitor Y-27632, when included in neurite outgrowth media at a final concentration of 10  $\mu\text{M}$ , appeared to enhance neurite length, neurite density, as well as decrease cellular migration from neurospheres after 10 days of neurite outgrowth (B-E). Neurites, stained green (TUJ1) appear to be significantly more densely populated than the control (A), radiating from the central aggregation of nuclei (blue). No contaminating cells were observed in ROCK treated cultures. Scale bars: 250  $\mu\text{m}$

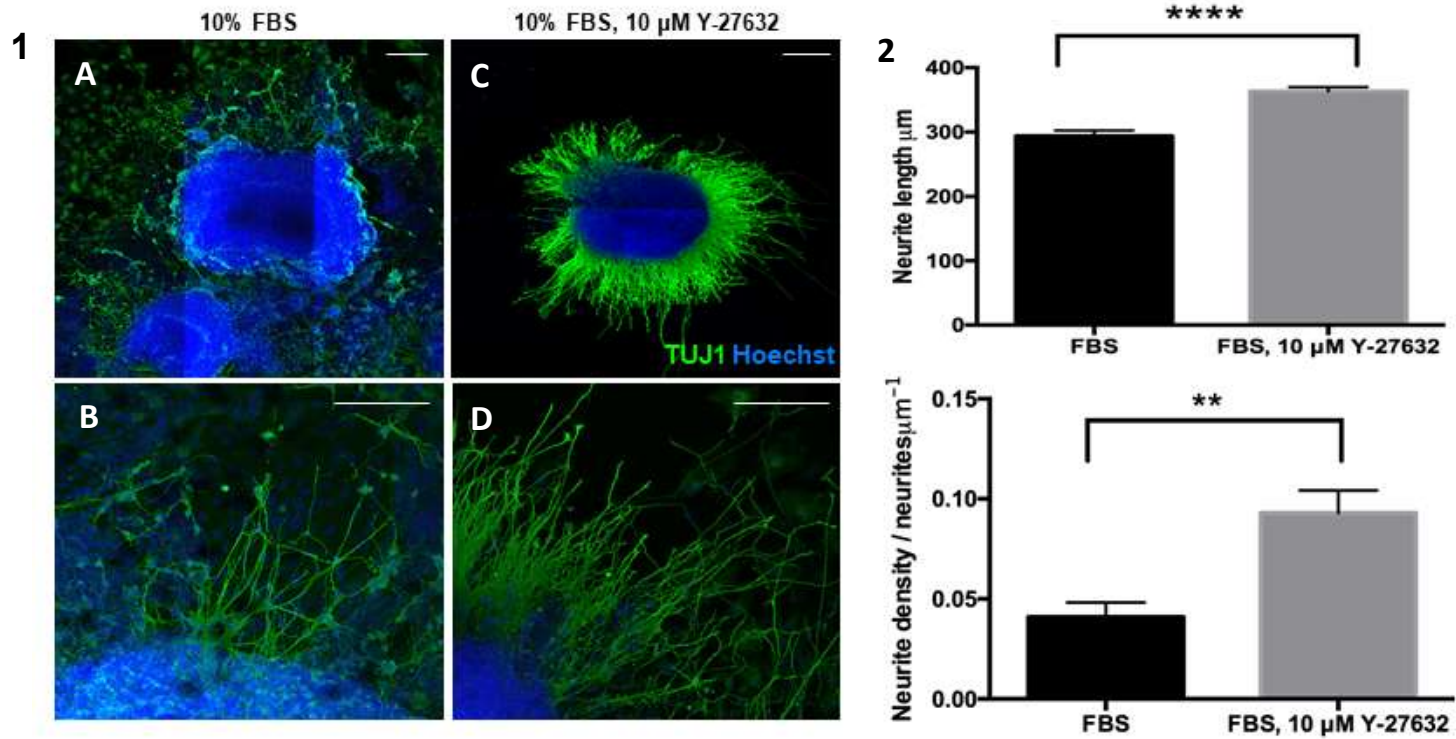


**Figure 3.1.4-2: Neurite outgrowth from TERA2.cl.SP12 neurospheres is enhanced in vitro through ROCK inhibitor Y-27632.** Quantification of neurite outgrowth in FBS and ROCK inhibitor Y-27632 shows that both neurite outgrowth, and neurite density are increased significantly through ROCK inhibition (panel 2). Control neurospheres (A+B) are shown in the left hand side of panel 1, and Y-27632 treated neurospheres (C+D) shown right. Nuclei are highlighted in blue (Hoechst), and neurites in green (TUJ1). Scale bars = 100  $\mu$ m. Graphs represent data  $\pm$  SEM. Negative control not shown. \*\* =  $p < 0.01$ , \*\*\*\* =  $p < 0.0001$ . N = 3.

blue with Hoechst. The media change was performed when myoblasts reached approximately 70-80% confluent, at which point the myotubes were randomly distributed in culture. The mononucleate myoblasts existed as structures of an overall similar average size to one another, but shape varied. During the first two days of differentiation (Figure 3.2.1, Panel 1) myoblasts migrated within the culture, migrating towards each other. Following this migration, myoblasts arranged themselves linearly, whereby the long axis of the cells lined up before fusion occurred. Some fusion became evident at day 2 of differentiation, once migration and alignment had occurred, although myotubes within culture could be seen to differentiate at slightly different rates.

At day 3 of differentiation, this fusion process was very apparent, and myotubes began to appear as linear, ordered structures rather than a disorganised array of cell bodies. By day 4, myotubes were easily identifiable in culture with few existing myoblasts. These remaining myoblasts fused to form mature myotubes by day 5, at which point, myotubes appeared as long, thin, structures containing multiple nuclei. Myotubes formed running near parallel to one another, emanating and terminating in roughly the same direction, however, overlapping of myotubes was evident.

### **3.2.2 Quantification of the differentiation process**

The differentiation and formation of C2C12 myotubes from myoblasts was quantified using methods outlined in Section 2.2.7. This method of quantification briefly comprised using the number of mature myotubes per area as an estimate of the differentiation status of the culture during each day of differentiation. Three random areas of culture were imaged using the 40X objective lens on the phase contrast microscope, an area spanning approximately 210 x 170  $\mu\text{m}$ . Following this, myotubes that appeared as continuous tubular structures measuring over 125  $\mu\text{m}$  were counted as mature myotubes (see Figure 3.2.2 - A). This method was found to be more appropriate than



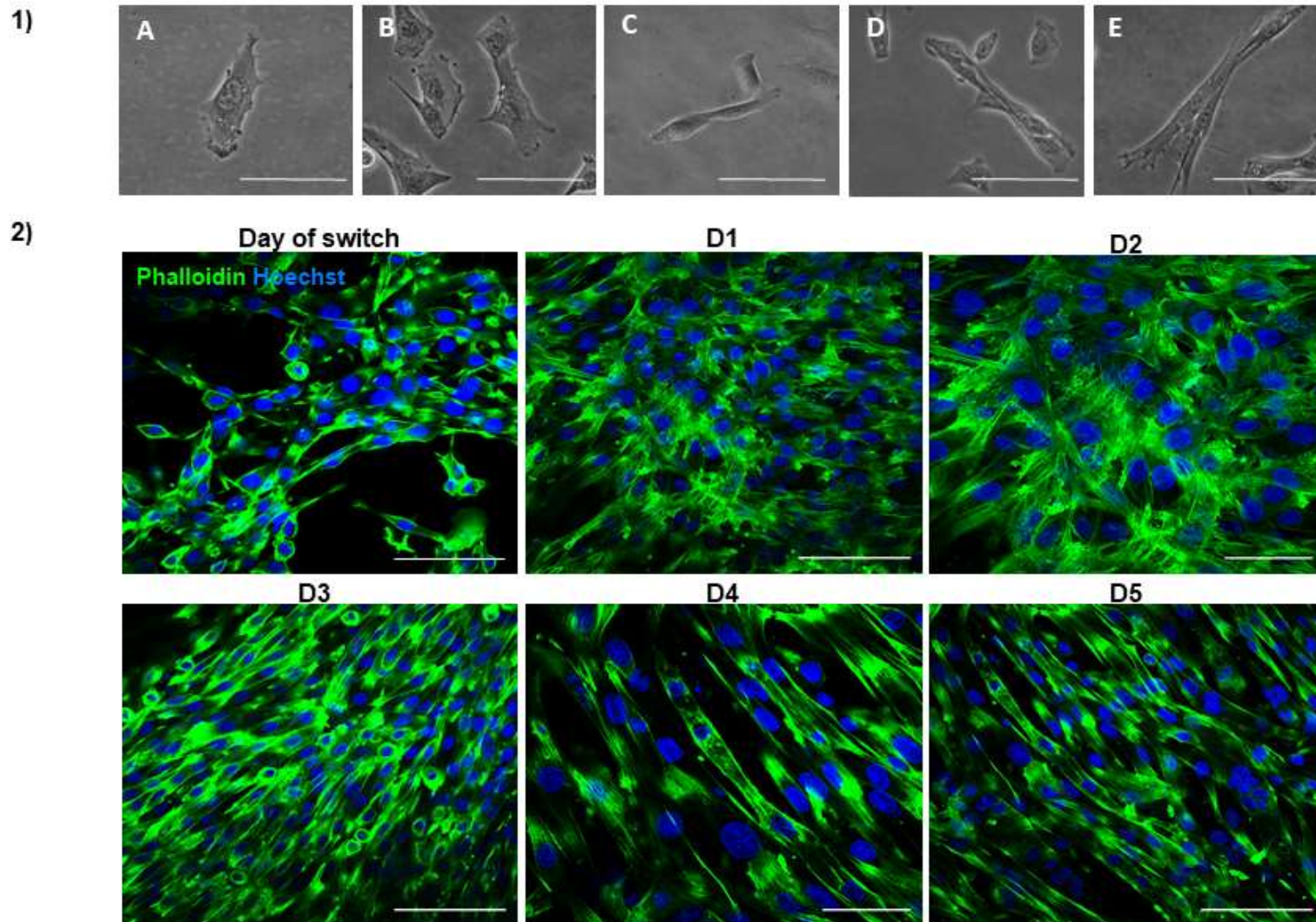


**Figure 3.2.1: C2C12 myoblasts fuse and elongate to form multinucleate myotubes upon serum withdrawal.** Panel 1 shows (A) a single myoblast prior to differentiation, which then migrates towards other myoblasts (B) upon entering differentiation process. These myoblasts align (C), and fuse (D) to form maturing myotubes (E). Immunofluorescence analysis in Panel 2 shows C2C12 myotube differentiation showing the process of myoblast alignment, fusion and elongation, resulting in the formation of multinucleate myotubes. The F-actin cytoskeleton is stained with phalloidin 78 (green), and nuclei are stained with Hoechst (blue). 2) shows quantification of myotube differentiation, through increasing mature myonumber per day. Scale bars = 50  $\mu\text{m}$ .

measuring other morphological components of the myotubes such as myotube diameter, as the diameter of each individual myotube varied significantly from one another, and within themselves at different points along their length (demonstrated in B, double ended arrows – Figure 3.2.2).

Using this method of quantification, the number of mature myotubes increased per day over the 5-day differentiation period. By day 5, nearly all structures appeared as long, thin, mature myotubes, with virtually no proliferating myoblast remaining. During the first two days of differentiation, no mature myotubes were present in culture (C – Figure 3.2.2). However, from days 3-5, the number of myotubes significantly increased from approximately 4 per area in day 3, to 14 at day 5 per area. As previously mentioned, the diameter of these mature myotubes varied significantly (Figure 3.2.2, arrows), as did the overall length of the myotubes. The number of mature myotubes present in culture roughly doubled per day after day 2 until nearly all remaining myoblasts were incorporated into an existing myotube.

### **3.2.3 Assessing contractile apparatus of myotubes**

Another approach to assess the formation and functionality of C2C12 myotubes was to examine their contractile apparatus. Myosin heavy chain (MHC) is a motor protein component of mammalian skeletal muscle thick filaments. These filaments propagate contraction through conformational changes and their resulting dynamics on actin filaments. Myosin heavy chain is expressed in mature myotubes and was used as a marker of the myotube.<sup>181</sup>

Figure 3.2.3, panel 1 shows immunofluorescent analysis of C2C12 myotubes during the differentiation period, from day one of differentiation (Figure 3.2.3, panel 1 - D1) up to day five (Figure 3.2.3, panel 1 - D5). Fixed cultures were stained red with an anti-MHC antibody, to stain for the contractile myosin heavy chain proteins within the myotubes present. MHC expression clearly increased

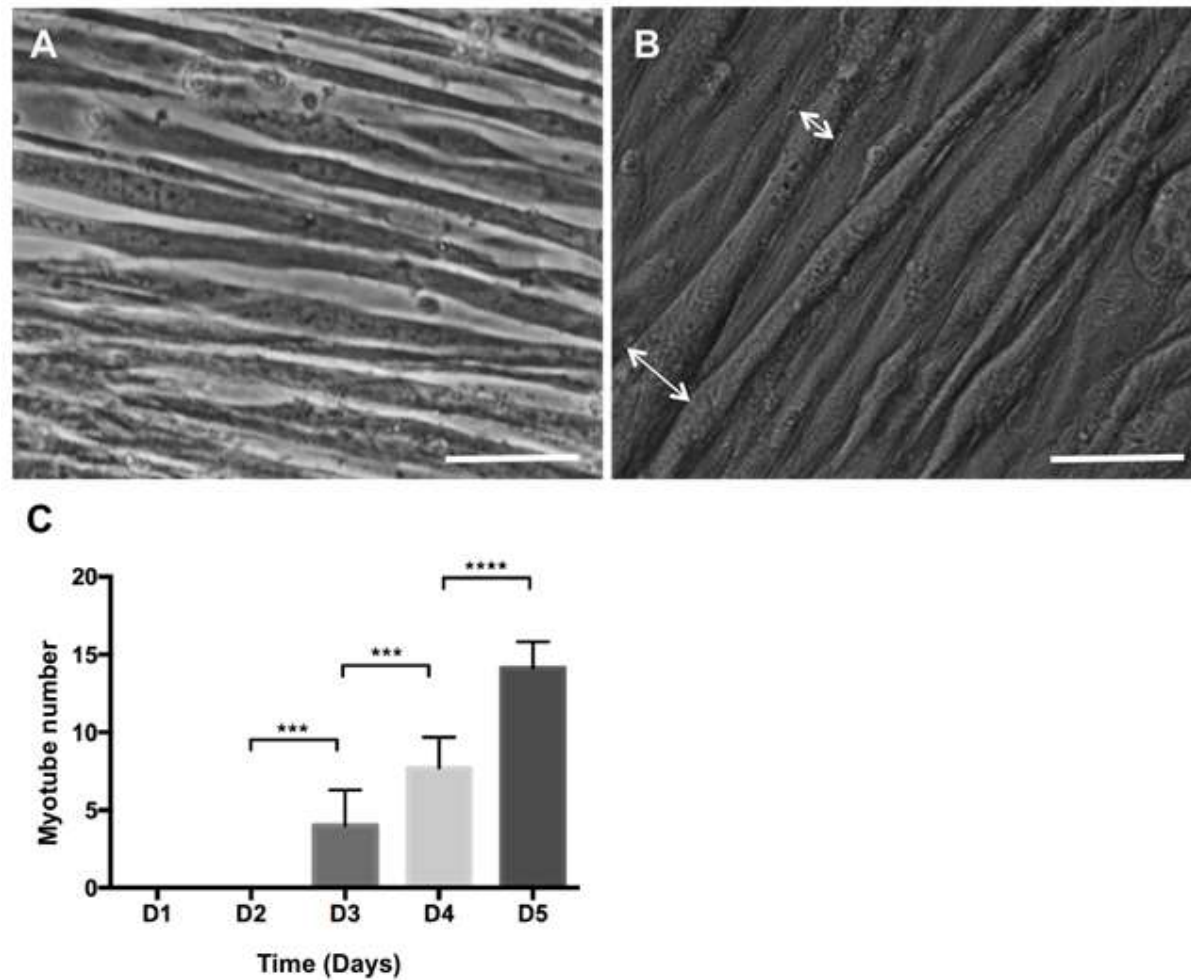


**Figure 3.2.2: Quantification of C2C12 myotubes per day during differentiation.** Phase contrast images were taken using the 40X optical lens (A and B) to allow observation and counting of myotube number per day in culture after switching from maintenance media to differentiation media. Myotube number increased per day (C) and is an efficient method of quantifying the differentiation process, as myotube length and diameter are subject to significant variation between cultures (see double ended arrows, B) Graphs represent data  $\pm$  SD. \*\* =  $p < 0.01$ , \*\*\* =  $p < 0.001$ , \*\*\*\* =  $p < 0.0001$ . Scale bars A and B = 50  $\mu$ M.



per day of differentiation, starting with no visible staining on the first day of differentiation, to abundant staining at day 5. This closely correlated with the number of mature myotubes present at each day of differentiation, as outlined in Section 3.2.2; as myoblasts fused to form myotubes from approximately day 3 onwards, the MHC expression became more evident. By day 5, most myotubes imaged stained positively for MHC, suggesting the presence of fully matured myotubes.

MHC was clearly expressed during the later stages of myotube differentiation rather than early stages. Panel 2, Figure 3.2.3 shows quantification of MHC expression during C2C12 differentiation, performed as outlined in Section 2.2.8. Here, MHC expression was shown as a percentage of tubular structures present per area. This shows that there was no myosin heavy chain, or undetectable levels during the first day of differentiation. Following this, percentage expression increased from day 2 through to day 5, with a significant MHC expression increase evident between day 3 and day 4, correlating with the fusion and maturation of myotubes. This expression then increased from approximately 50% at day 4 to above 90% after 5 days of differentiation, suggesting that nearly all structures present in culture were mature myotubes, consistent with previous results. The differences in expression between day 3 and 4, and day 4 and 5 were statistically significant ( $p < 0.0001$ ).

### **3.2.4 Enhancement of myogenic differentiation through ROCK inhibition by Y-27632**

To investigate the role of Rho A /ROCK signalling through ROCK inhibition on C2C12 differentiation and thus myogenesis, the selective ROCK inhibitor Y-27632 was included in the differentiation medium for C2C12 myoblasts at a final concentration of 10  $\mu$ M, and differentiation was allowed to proceed for 5 days as standard. Results were compared to control cultures, which contained normal differentiation media, with no ROCK inhibitor. The results in Figure 3.2.4 show C2C12 myoblasts differentiating into

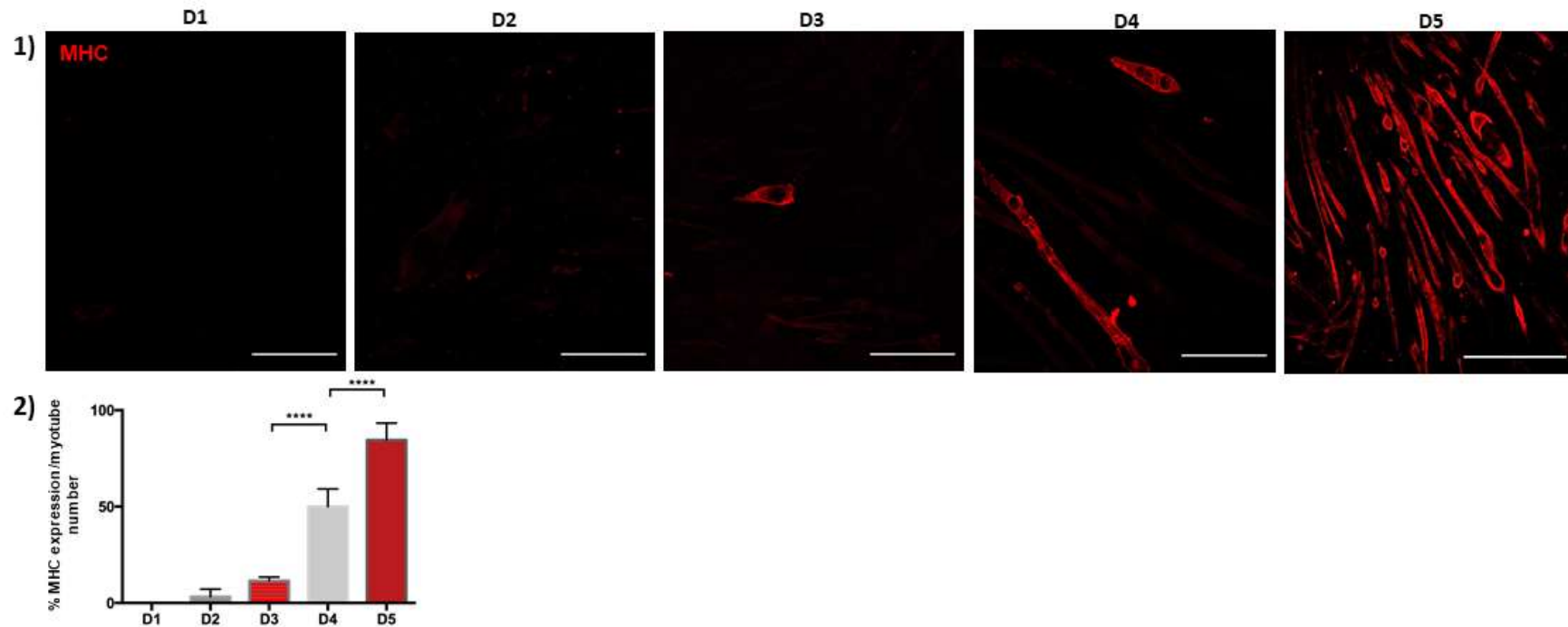


**Figure 3.2.3: Myosin heavy chain (MHC) expression increases during C2C12 differentiation.** Myosin heavy chain (MHC) expression increases as the myoblasts form mature myotubes. Myoblasts fuse and elongate to form multinucleate myotubes around day 5. During this differentiation process, MHC expression (red) increases as myotubes become equipped with contractile proteins. Scale bars: 100  $\mu$ m. Panel 2 shows quantitative analysis of MHC expression as a percentage of mature myotubes found on each day of the differentiation process. Graphs represent data  $\pm$  SD. \*\* =  $p < 0.01$ , \*\*\* =  $p < 0.001$ , \*\*\*\* =  $p < 0.0001$ . N=3.

myotubes during the 5-day differentiation period in the presence of Y-27632, the selective ROCK inhibitor. The data suggest that through inhibition of ROCK signaling, the differentiation of myotubes appears to be further enhanced. Although cultures appeared morphologically comparable after the first day of differentiation (Panel 1, Figure 3.4.4 – D1), myotubes were evident in the cultures treated with Y-27632 on day 2 (Panel 1, Figure 3.4.4 – D2), as identified by the white arrows. Compared to the visibly disordered myoblasts at D2 in the control, lacking any obvious arrangement, the treated cultures appeared more orderly. Where myoblasts remained between the forming myotubes, they appeared more orderly than the control counterpart, with myoblasts appearing to be more aligned than sporadically organized. By day 3, Y-27632 treated myotubes appeared as conspicuous, tubular structures, similar to the myotubes at days 4 or 5 of differentiation in untreated samples.

Quantification of the effect of ROCK inhibitor Y-27632 on C2C12 differentiation was performed as outlined in Section 2.2.7. This quantification revealed myogenic differentiation of the C2C12 cell line was increased through ROCK inhibition (panel 2, Figure 3.2.4). This increased differentiation was especially apparent at day 2, where approximately 7 myotubes were present per field of view in treated cultures, compared to almost none in untreated cultures. Myotube numbers increased per day after day 2, plateauing at day 4 as most myoblasts were incorporated into myotubes. Nonetheless, myotube number was significantly increased per day compared to the untreated controls. Final myotube number was also increased in treated cultures, suggesting an involvement of ROCK in stimulating myoblast fusion.

#### **3.2.4.1 Effect of ROCK inhibition on Myosin Heavy Chain expression**

In order to further quantify the effect of the selective ROCK inhibitor Y-27632 on C2C12 differentiation, a marker of terminal phenotypic differentiation was used to stain myotubes – myosin heavy chain (MHC). Although only a small quantity, myosin heavy chain was identified in cultures fixed and stained with red anti-MHC after one day of

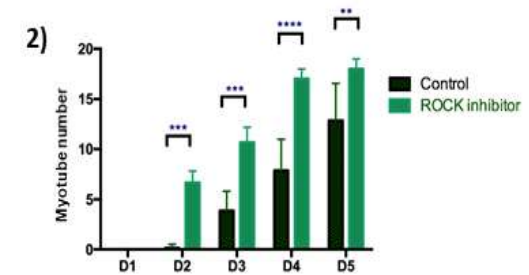
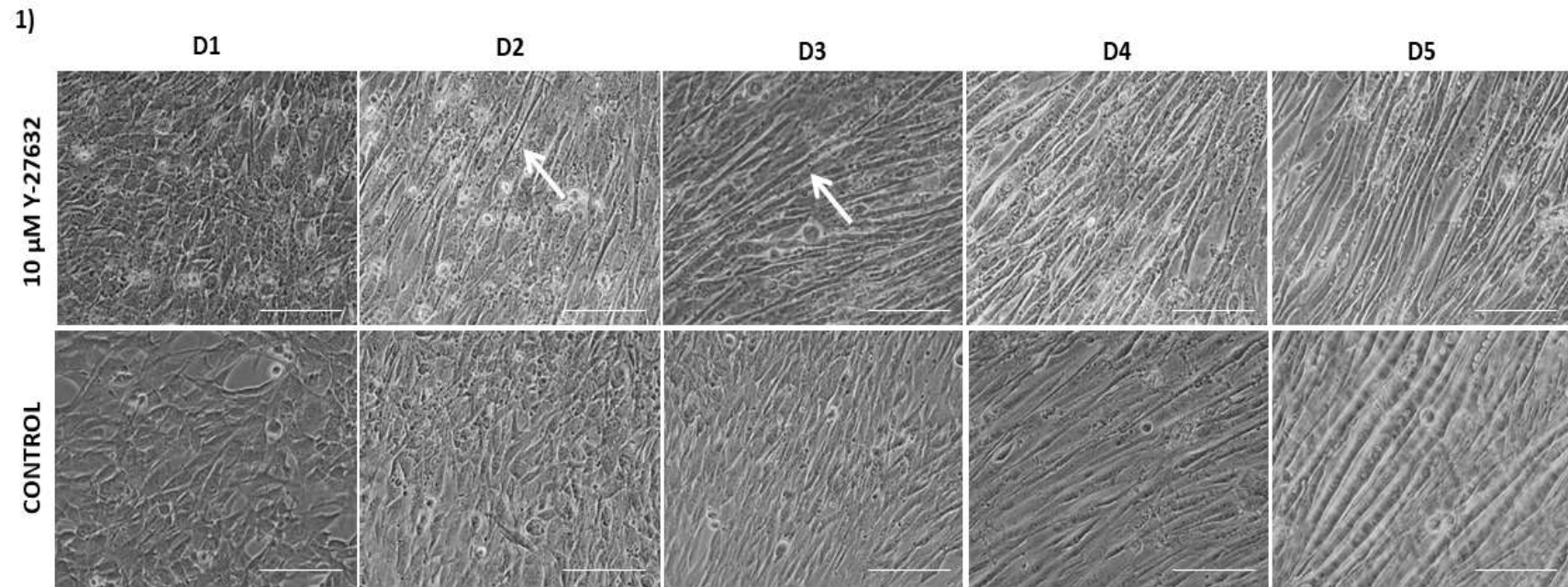


**Figure 3.2.4: ROCK inhibitor Y-27632 appears to enhance differentiation of C2C12 myoblasts.** ROCK inhibitor Y-27632, when included in differentiation media at a final concentration of 10  $\mu$ M, appears to enhance the differentiation of C2C12 mononucleate myoblasts into multinucleate myotubes. Phase contrast images show this differentiation, which occurs over 5 days. By day 5, mature myotubes can be observed. Morphological differences in differentiation appear around day 2 (D2), and day 3 (D3), where myotubes begin to appear (indicated by arrows) in the Y-27632 differentiated cultures, but cannot be observed under normal differential conditions. Scale bars = 100  $\mu$ m. Panel 2 shows quantification of mature myotubes per day between the two conditions. Graphs represent data  $\pm$  SD. \*\* =  $p < 0.01$ , \*\*\* =  $p < 0.001$ , \*\*\*\* =  $p < 0.0001$ . N=3.



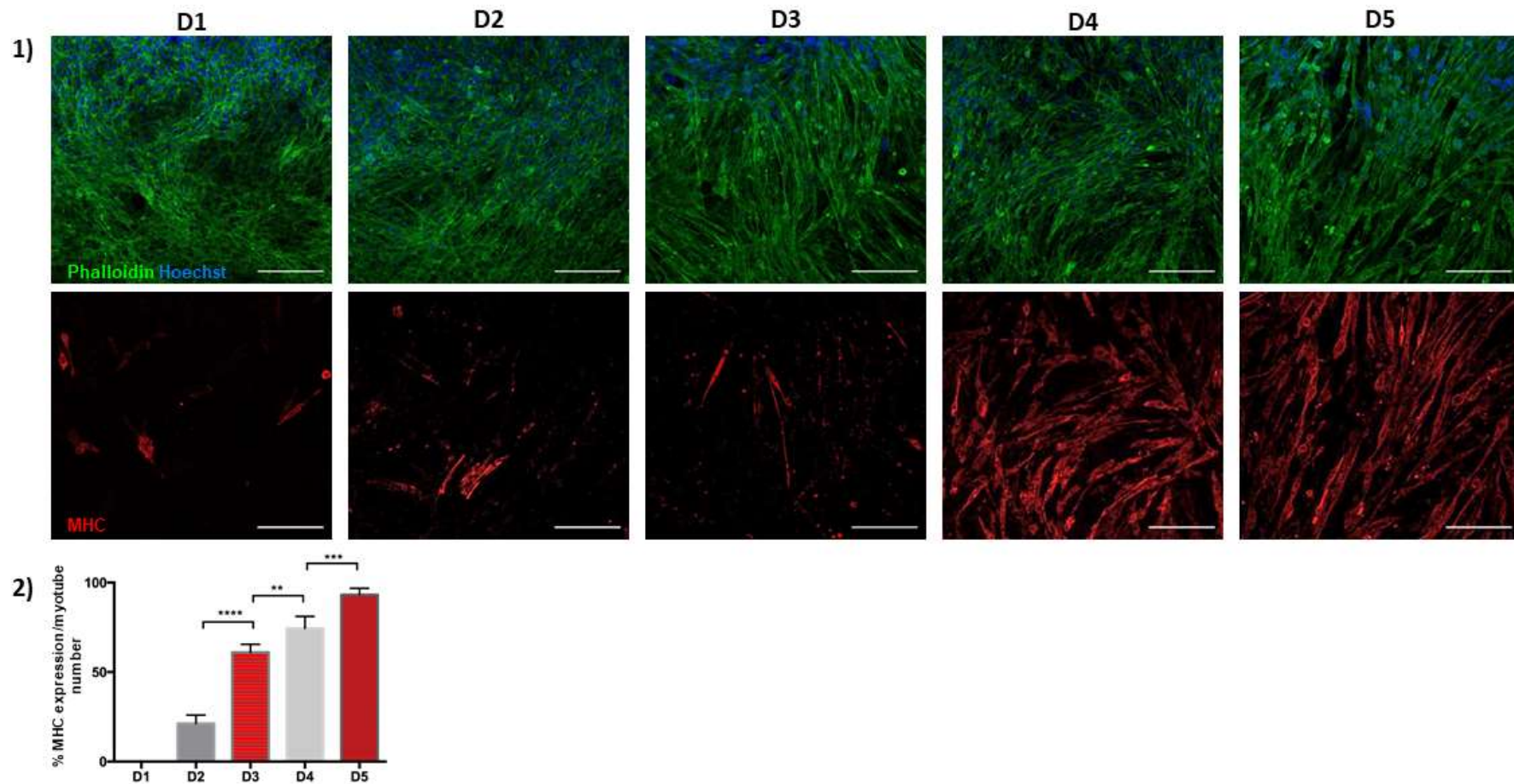


**Figure 3.2.4.1: ROCK inhibitor Y-27632 appears to enhance differentiation of C2C12 myoblasts.** ROCK inhibitor Y-27632, when included in differentiation media at a final concentration of 10  $\mu$ M, appears to enhance the differentiation of C2C12 mononucleate myoblasts into multinucleate myotubes. Phase contrast images show this differentiation, which occurs over 5 days. By day 5, mature myotubes can be observed. Morphological differences in differentiation appear around day 2 (D2), and day 3 (D3), where myotubes begin to appear (indicated by arrows) in the Y-27632 differentiated cultures, but cannot be observed under normal differential conditions. Scale bars = 200  $\mu$ m. Panel 2 shows quantification of mature myotubes per day between the two conditions. Graphs represent data  $\pm$  SD. \*\* =  $p < 0.01$ , \*\*\* =  $p < 0.001$ , \*\*\*\* =  $p < 0.0001$ . N=3.

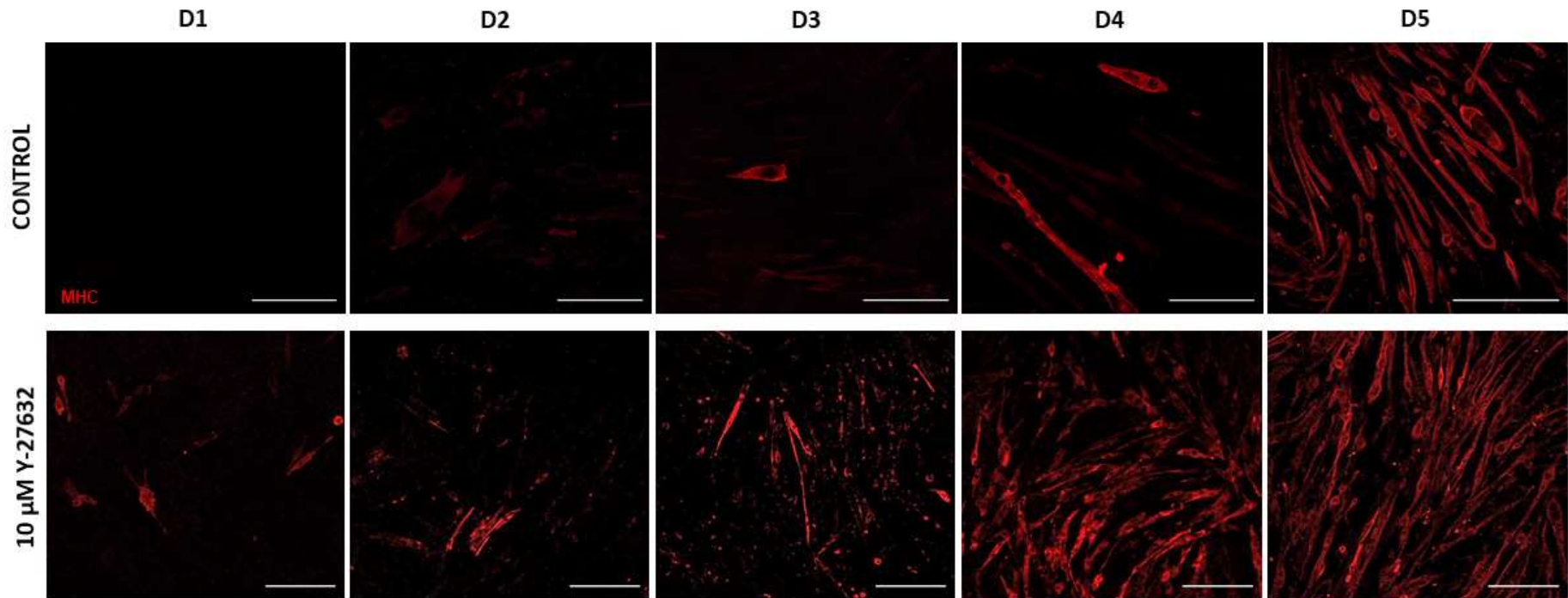


**Figure 3.2.4.1-2: MHC expression increased earlier in differentiation process when myoblasts are differentiated with ROCK inhibitor.** Myosin heavy chain (MHC) expression is enhanced earlier on in the differentiation process of C2C12 myotubes, as highlighted by the confocal images here in red. Scale bars = 200  $\mu$ m

differentiation (panel 1, Figure 3.2.4.1). Myosin heavy chain expression then increased at each day of differentiation, with abundant positive staining appearing at day 4 and day 5.

Quantitative analysis of MHC expression was then performed by assessing percentage of mature myotubular structures present in culture expressing MHC per area (panel 2, Figure 3.2.4.1). MHC expression, although partially expressed by approximately 20% of myotubes at day 2, notably increased between day 2 and day 3 of differentiation. Following this, expression increased to almost 100% of myotubes by day 5 in cultures treated with ROCK inhibitor Y-27632. This expression plateaued after day 3, although still increasing. Increasing expression is statistically significant throughout the full 5 day differentiation process.

When comparing myosin heavy chain expression between cultures treated with ROCK inhibitor Y-27632 to untreated controls, the effect of ROCK inhibition became truly apparent. In Figure 3.2.4.1-2, myotubes stained red with anti-MHC appeared earlier, and were more abundant in cultures treated with Y-27632. In the untreated control, next to no expression was observed in cultures differentiated for 1 and 2 days, but myosin heavy chain was detectable in the treated cultures of the same time periods. The largest difference in expression became apparent at day 3 and day 4 of differentiation, whereby expression was evident in many myotubes in treated cultures by day 3, but scarce in untreated.

### **3.2.5 The effect of mitotic inhibitors on myotubes**

Mitotic inhibitors are often used in cell culture during the differentiation period. Proliferation and differentiation are two independent processes of developmental biology. In order for C2C12 myoblasts to differentiate into myotubes, they must first exit the cell cycle and thus cease proliferation. Mitotic inhibitors can be used in monoculture or co-culture of certain cell types to aid this cell-cycle arrest to direct the cells down a

differentiation programme.<sup>185</sup> C2C12 cell culture however, involves the withdrawal of maintenance media with its immediate replacement by differentiation media consisting of low-serum conditions. These low-serum conditions aim to starve the cells of nutrients, ultimately forcing them to withdraw from the cell cycle.

The effect of three well-studied mitotic inhibitors on C2C12 differentiation was investigated. Common mitotic inhibitors used in cell culture include uridine, 5'fluoro 2'deoxyuridine and cytosine arabinose, exploiting their ability to interfere with DNA synthesis, thus facilitating cell cycle arrest. 5'fluoro 2'deoxyuridine for example, in its active cellular form, is a potent inhibitor of the enzyme thymidylate synthase, which ultimately decreases the availability for thymidylate required for DNA synthesis.<sup>249</sup> Cytosine arabinose is a mitotic inhibitor that interferes with DNA synthesis during S phase cell cycle in its intracellular active triphosphate form.<sup>250</sup>

Mitotic inhibitors uridine, 5'fluoro 2'deoxyuridine, and cytosine arabinose were included in the differentiation media each at final concentrations of 1  $\mu$ M cytosine arabinose, 10  $\mu$ M 5-fluor 2'deoxyuridine and 10  $\mu$ M uridine, respectively. They were not however, included in maintenance media either before or after the differentiation period for the C2C12 cells. As a result, their presence had no apparent effect on differentiation or the resulting viability of myotubes as the myoblasts have already withdrawn from the cell cycle upon initiation of differentiation – the point at which they were included in the media. They may however, stop any remaining undifferentiated myoblasts in culture from proliferating, resulting in the cultures becoming over-confluent. (Data not shown)

### **3.2.6 Maintaining mature myotubes *in vitro***

C2C12 myoblasts were maintained in maintenance media consisting of DMEM supplemented with 10% FBS, penicillin, streptomycin and L-glutamine as outlined in Section 2.1.1.2. To initiate differentiation of myoblasts into myotubes, maintenance



media was removed and replaced with differentiation media, consisting of DMEM supplemented with 2% horse serum in the place of FBS, along with aforementioned supplements. However, once differentiation has occurred during the 5-day differentiation period, it was found that mature myotubes could not be maintained in their differentiation media beyond the 5 day differentiation period for longer than a day or two. Instead, the cultures started to undergo cell death.

To overcome this, mature, fully differentiated cultures of myotubes (Figure 3.2.6 – D5) were then switched back to the maintenance media, in which they could be maintained longer term with regular media changes, approximately every 2-3 days. Phase contrast images 5 days after this switch back to maintenance media (Figure 3.2.6-M5) showed myotubes still appeared fully viable and morphologically identical to D5 cultures. After 10 days of maintaining myotubes in maintenance media post-differentiation (Figure 3.2.6 - M10), myotubes still remained viable in culture. Small circular, vacuole-like structures (Figure 3.2.6 - arrow) were observed in approximately 5% of myotubes within the cultures, but the myotubes did not undergo cell death, nor did the vacuoles appear to migrate. Myotubes were maintained as long as 20 days post-differentiation, concluding that myotubes containing the vacuoles remained viable.

The same method of maintaining mature myotubes was performed on myotubes differentiated with ROCK inhibitor Y-27632, where the differentiation media was replaced with ROCK inhibitor and horse serum free media post-differentiation. This enabled myotubes to be maintained long-term.

### **3.2.7 Acetylcholine receptor distribution in mature myotubes**

Acetylcholine receptors, AChRs, are ligand gated ion channels that comprise acetylcholine binding site receptors. They bind to the neurotransmitter acetylcholine in their junctional form, located at the neuromuscular junction. However, they can be

found outside of the area of the neuromuscular junction across myotubes, prior to innervation.<sup>209</sup>

To investigate acetylcholine receptor presence, distribution and localisation in the differentiating C2C12 myoblasts/myotubes, a marker of the receptors, alpha-bungarotoxin ( $\alpha$ -BTX) was used.  $\alpha$ -BTX is a component found in the snake venom of the *Bungaris multicinctus*.<sup>210</sup> A type of neurotoxin, it competitively, as well as irreversibly binds to acetylcholine receptors; ergo, in its fluorophore, antibody form, can be used to visualise acetylcholine presence and distribution in cells.

C2C12 myoblasts/myotubes were immunocytochemically stained using  $\alpha$ -BTX at different stages of differentiation (Figure 3.2.7). The F-actin of cells were stained green with phalloidin, staining their actin cytoskeleton, along with co-stain hoechst to stain their nuclei.  $\alpha$ -BTX was included to stain AChRs red. No positive  $\alpha$ -BTX stain was observed at day 1 of differentiation (Figure 3.2.7 – D1 lower panel). However at day 3, very minute positive staining emerged (Figure 3.2.7 – D3. See arrows). This positive staining manifests as red dots randomly distributed along the length of the myotubes. This became more apparent by day 5 (Figure 3.2.7 – D5, arrows), at which point myotubes exhibit slightly more positive staining, therefore indicating the presence of a higher quantity of AChRs along their length. These results show that acetylcholine receptors are present in C2C12 myotubes, although not expressed in earlier stages of their differentiation. These receptors however, are difficult to visualise due to their small size and unclustered nature.

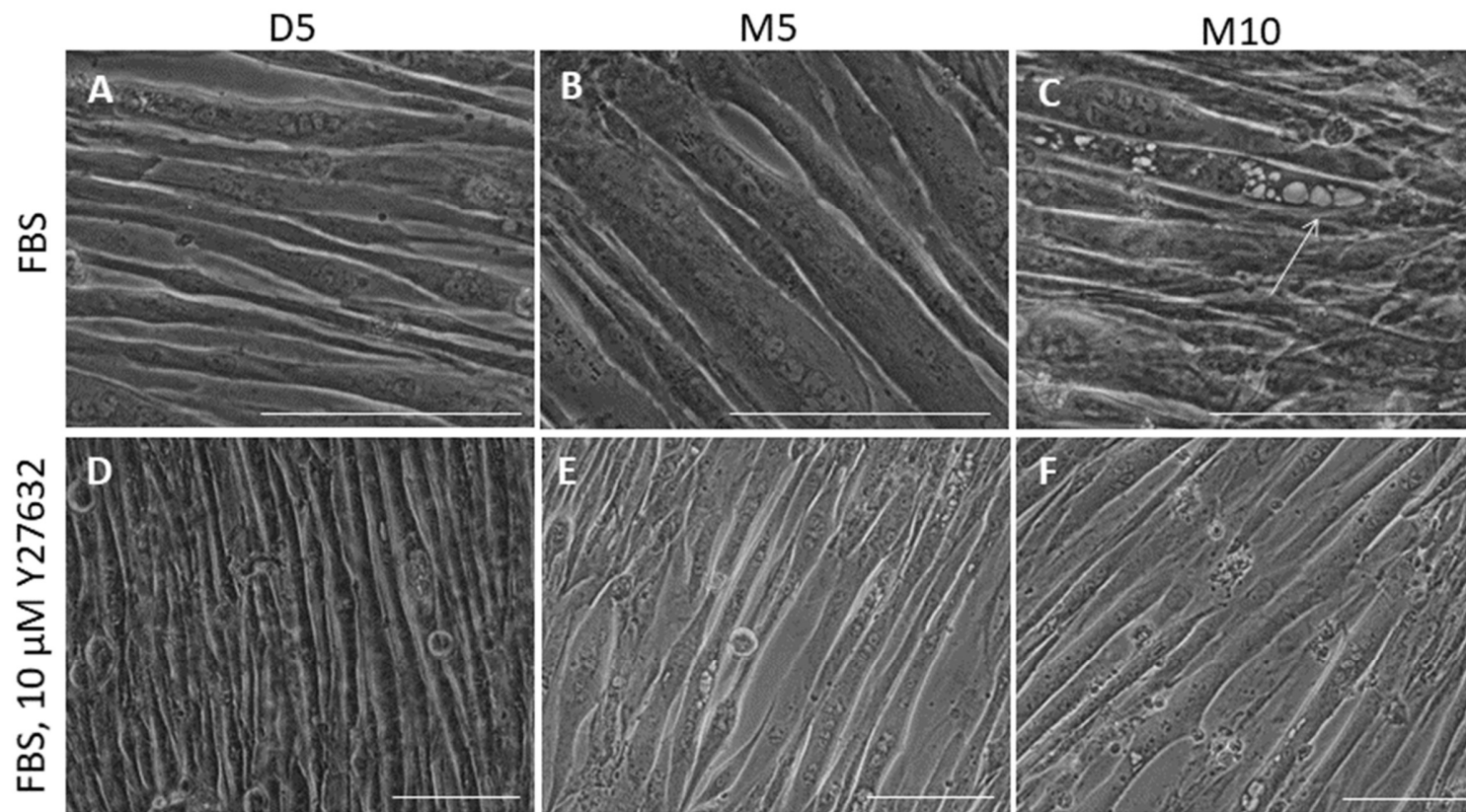


**Figure 3.2.6: C2C12 myotubes can be maintained in vitro following differentiation.** Phase contrast images show mature C2C12 myotubes at day 5 of differentiation (D5) in differentiation media, 5 days after switching the myotubes back to maintenance media (M5), and 10 days after the switch back (M5). Myotubes remain alive and viable, with no apparent cell death occurring. Circular vacuoles appear to accumulate in a couple of myotubes per 12 well plate (arrow), but did not appear to affect the viability of the myotubes. Scale bars = 100 μm.

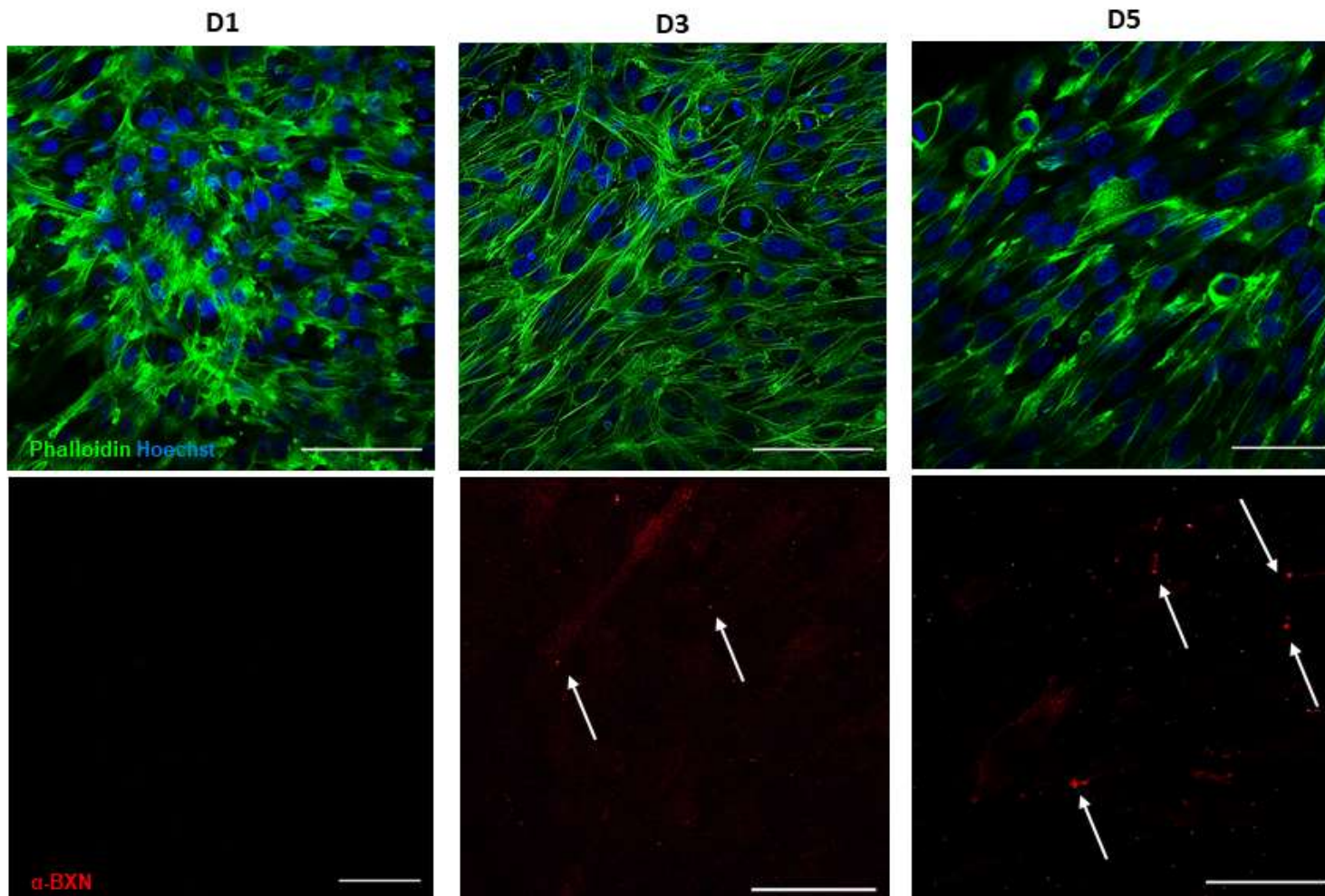


**Figure 3.2.7: Acetylcholine receptors are randomly distributed along C2C12 myotubes aneurally.** Myotubes at day 1 (D1), day 3 (D3), and day 5 (D5) of differentiation were analysed using immunocytochemistry to show the F-actin cytoskeleton (phalloidin: green), nuclei (Hoechst: blue), and acetylcholine receptors ( $\alpha$ -bungarotoxin: red) at each time point in the differentiation process of C2C12 myotubes. Arrows depict positive staining of acetylcholine receptors. Scale bars: 50  $\mu$ m.

### **3.3 Development of a novel co-culture system for the production of neuromuscular junctions**

To develop an *in vitro* co-culture system aimed at producing neuromuscular junctions, TERA2.cl.SP12 stem cells were used to generate human neurons and C2C12 myoblasts were used to form skeletal muscle.

#### **3.3.1 Co-culturing dissociated neurons in monolayers on mature myotubes**

A co-culture method initially developed within the Przyborski laboratory at Durham University was repeated with modifications, outlined in Section 2.1.6.<sup>206</sup> In brief, two separate neuronal cultures were generated from TERA2.cl.SP12 stem cells using the different retinoid compounds, ATRA (a natural retinoid) and EC23 (a synthetic retinoid). ATRA, a naturally occurring form of retinoic acid, was used to induce neural derivatives from the stem cells. EC23, a synthetic retinoid, was used separately to also induce the formation of neural derivatives. Following a 3-week exposure period, neuro-epithelial rosettes formed, with neurons filling gaps between epithelial-like non-neuronal 'contaminating' cells.

A light trypsinisation was then performed, as neural cells produced in culture are less adherent than the aforementioned contaminating cells. Resulting supernatant was then collected and seeded into a new flask for 5 days, before a second trypsinisation was performed to obtain neuron-pure populations of neurons (>95%). Dissociated neurons were then seeded on top of mature myotubes and cultured for 5 days – hereby termed the 'dissociation co-culture' method. This method of co-culture produces single neurons that are then seeded on top of pre-differentiated myotubes, allowing potential interactions to develop.

Subsequent to this 5-day co-culture period, samples were fixed and immunofluorescent analysis was performed. The co-cultures were used to identify any potential interactions formed between the two cell types, as well as structures expected to be present if neuromuscular junction formation occurred. To confirm the neural identity of cells produced through the dissociation culture method, a pan-neuronal marker – TUJ1, was used to stain neural cells red (Figure 3.3.1). Neurons derived from TERA2.cl.SP12 stem cells stain strongly for TUJ1 and can be easily identified against the myotubes, which were stained green with phalloidin, an F-actin stain. Nuclei were counterstained blue with nuclear stain Hoechst.

Differentiated neurons appear as long thin axonal extensions projecting away from the cell body. Growth cones can also be observed at the leading edge of the axon (Figure 3.3.1 – labelled GC). Myotubes appear tubular and of a linear orientation alongside one another. Neurites and myotubes remain viable in co-culture, with co-localisation and potential interactions appearing to form between the two cell types. Neurons grow and ‘interweave’ with myotubes, rather than existing as monolayers on top of the myotubes. Neuron terminals co-localise with myotubes, suggesting that myotubes may secrete chemotactic factors, influencing the growth and direction of axonal growth dynamics.

### **3.3.2 Co-culturing neurospheres with myotubes**

A novel co—culture method was developed utilising the ability of TERA2.cl.SP12 stem cells to form neurosphere structures when allowed to aggregate in culture.<sup>204</sup> This method (described in Section 2.1.7) briefly involved seeding stem cells into Petri dishes, allowing them to adhere for 24 hours before addition of synthetic retinoid EC23 to form neurospheres. After 21 days maturation in culture, neurospheres were seeded onto mature myotubes and co-cultured for 10 days (Figure 3.3.2-1).



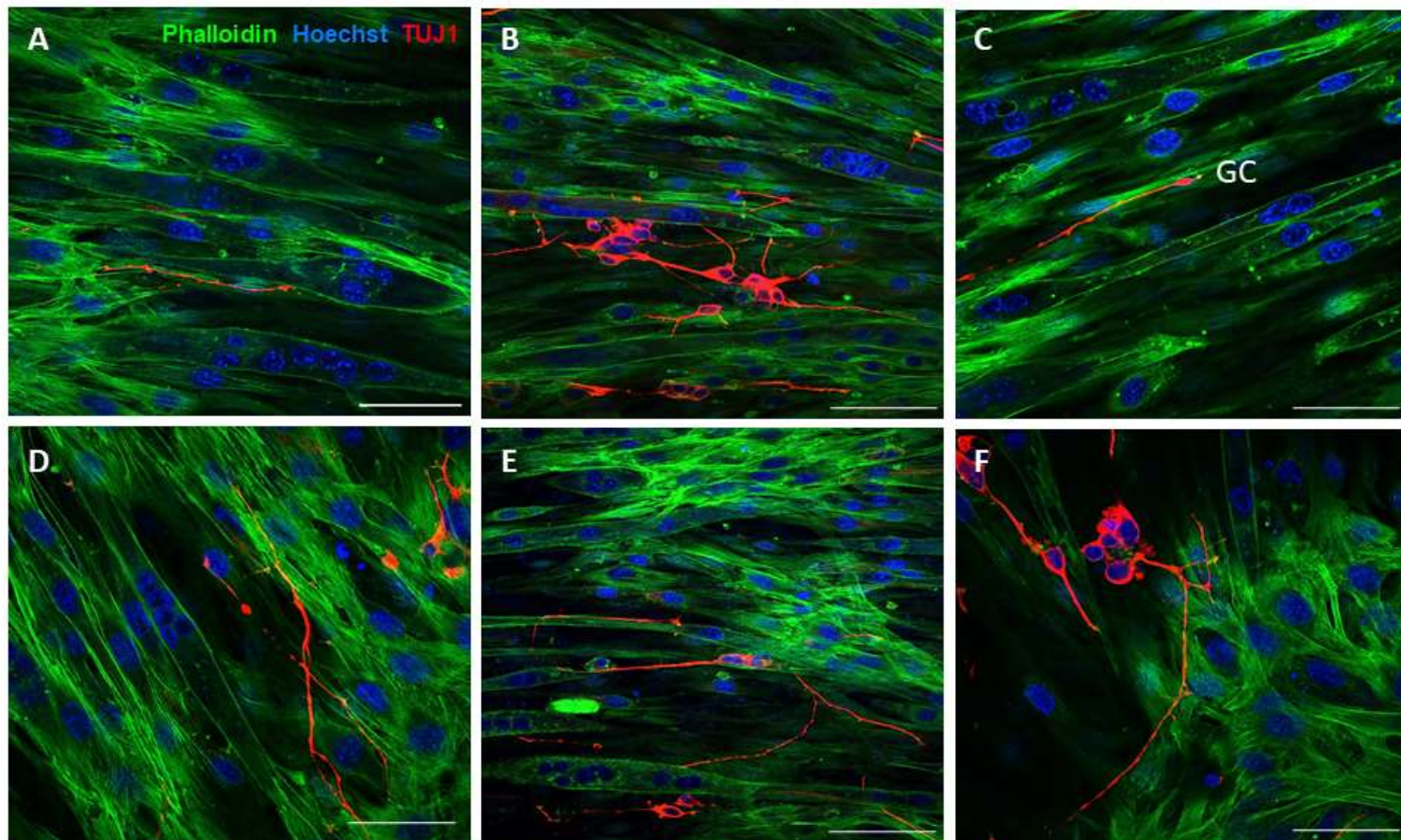


**Figure 3.3.1** Neuron endings co-localise with myotubes in co-culture when neurons differentiated from TERA2.cl.SP12 are co-cultured with mature C2C12 myotubes for 5 days. Neurons are seeded on top of myotubes at a density of 250,000 per well of a 12 well plate, and left to co-culture for 5 days. Immunocytochemical analysis shows neurons (TUJ1: red) co-localise with F-actin of myotubes (phalloidin: green). Nuclei are stained with Hoechst (blue). Scale bars: 100  $\mu$ m

This method of directing stem cells down a neural lineage resulted in the formation of cellular aggregates, from which neurites projected radially when seeded on top of myotubes in co-culture (Figure 3.3.2-1 - A). After 10 days of co-culture, cultures were fixed and analysed through immunocytochemistry to reveal cell-specific structures and areas of co-localisation. Myotubes were stained green with an F-actin stain phalloidin, whilst neurons stained red using pan-neuronal marker TUJ1, and nuclei stained blue with Hoechst. This co-culture model allowed an easily identifiable, plentiful supply of neurons, observed radiating outwards from the central neurosphere and terminating at the myotube surfaces. Neurites project from the neurosphere over the full circumference of the neurosphere, and the contrasting colours makes each cell type easily identifiable in the immunofluorescent analysis. This novel co-culture method provides a robust, reproducible method for observing areas of co-localisation between neurite and myotube. Small quantities of cellular migration away from the central mass of perikarya was occasionally observed in Figure 3.3.2-1 - C, but this is confined and rare.

Neurites within the co-culture appeared to extend along the mature myotubes. Most neurite endings were observed at a myotube surface (Figure 3.3.2-2). At higher magnifications of confocal microscopy, close interactions were noticeable between the two cell types. At higher magnifications, growth cones can were clearly identified at the leading edge of the neurite (Figure 3.3.2-2 - labelled GC). These neurites extended towards the myotubes shown centre in Figure 3.3.2-2 - B, where the growth cones appeared to make contact with the myotube above nuclei. The growth cone and myotube co-localisation suggest chemotactic factors are secreted by the myotube, involved in axonal growth and guidance. Another example of this co-localisation between neurite ending and myotube is shown clearly in Figure 3.3.2-2 - C, where the axonal terminal runs parallel and appears to be fusing with the side of the myotube, adjacent to the nucleus.



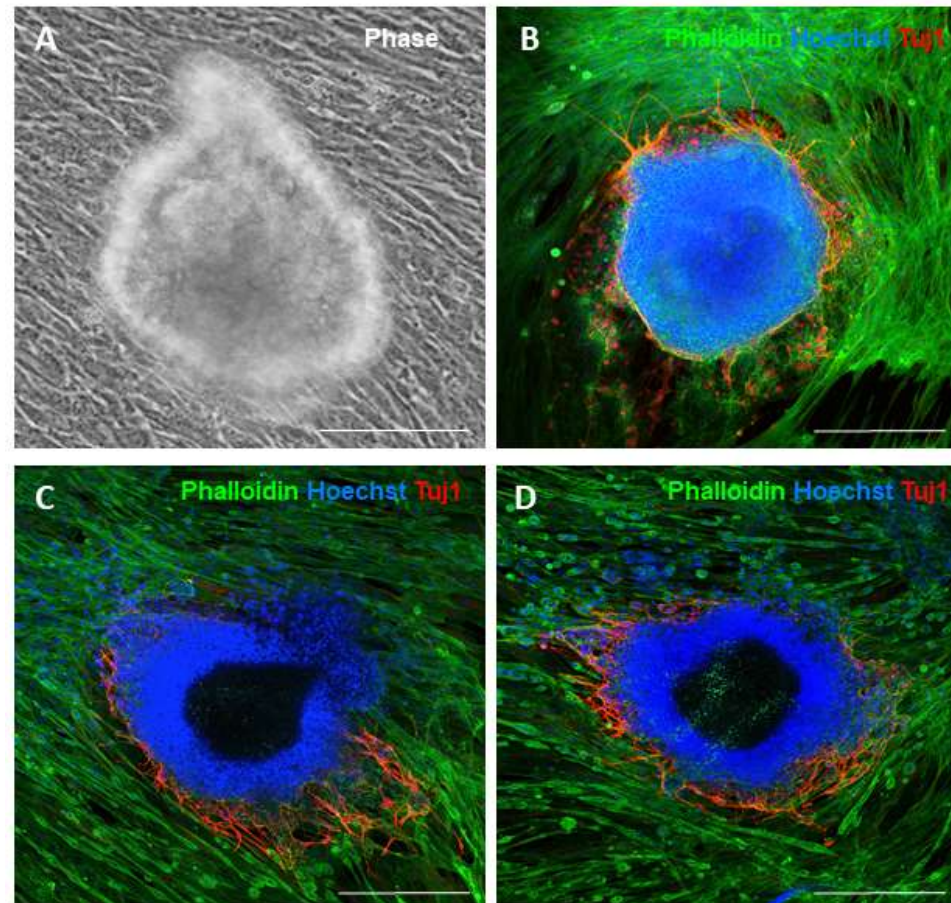


**Figure 3.3.2-1: TERA2.cl.SP12 derived neurospheres can be co-cultured with mature C2C12 myotubes for 10 days.** Phase-contrast image (A) shows the set up on day one of co-culture, whereby neurospheres are seeded on top of mature myotubes in 12-well plates. Immunocytochemistry shows that neurites, stained red (TUJ1), project outwards from central mass of cells, towards green stained F-actin of myotubes (phalloidin). Scale bars: 500  $\mu$ m

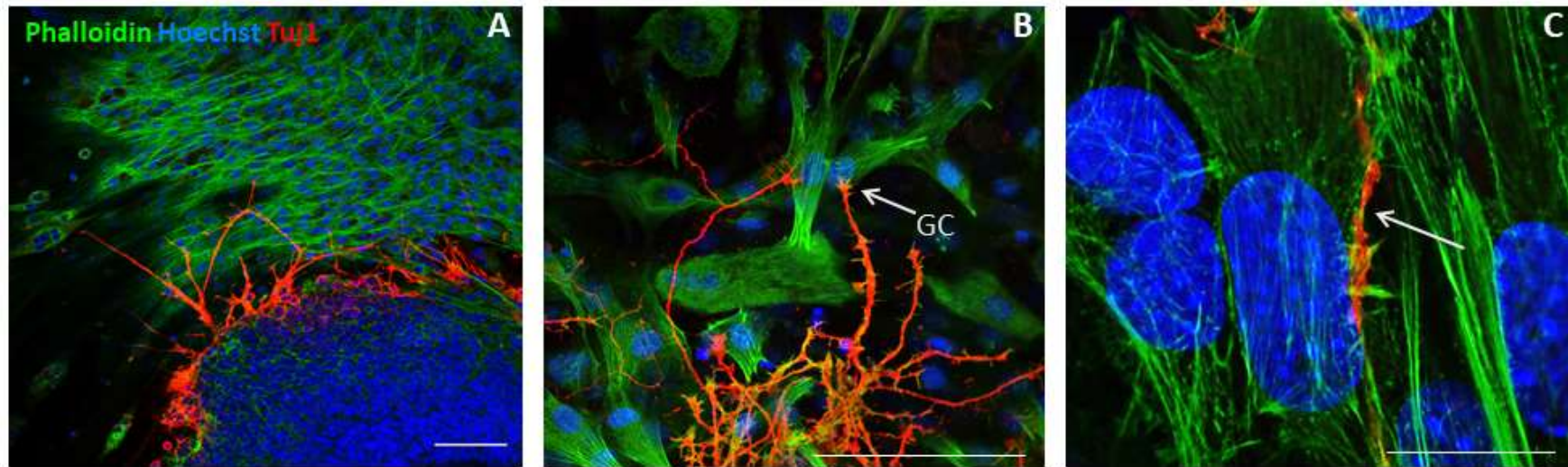


**Figure 3.3.2-2: Neuron terminals co-localise with myotubes showing evidence of sites of contact in neurosphere-myotube co-cultures.** After 10 days of co-culture between TERA2.cl.SP12 derived neurospheres and C2C12 myotubes, co-localisation and potential interactions between the two cell types can be observed. Here, using immunocytochemistry, neurites are stained red (TUJ1), F-actin of myotubes green (phalloidin), and nuclei blue (Hoechst). Scale bars: A = 100  $\mu\text{m}$ , B + C = 50  $\mu\text{m}$

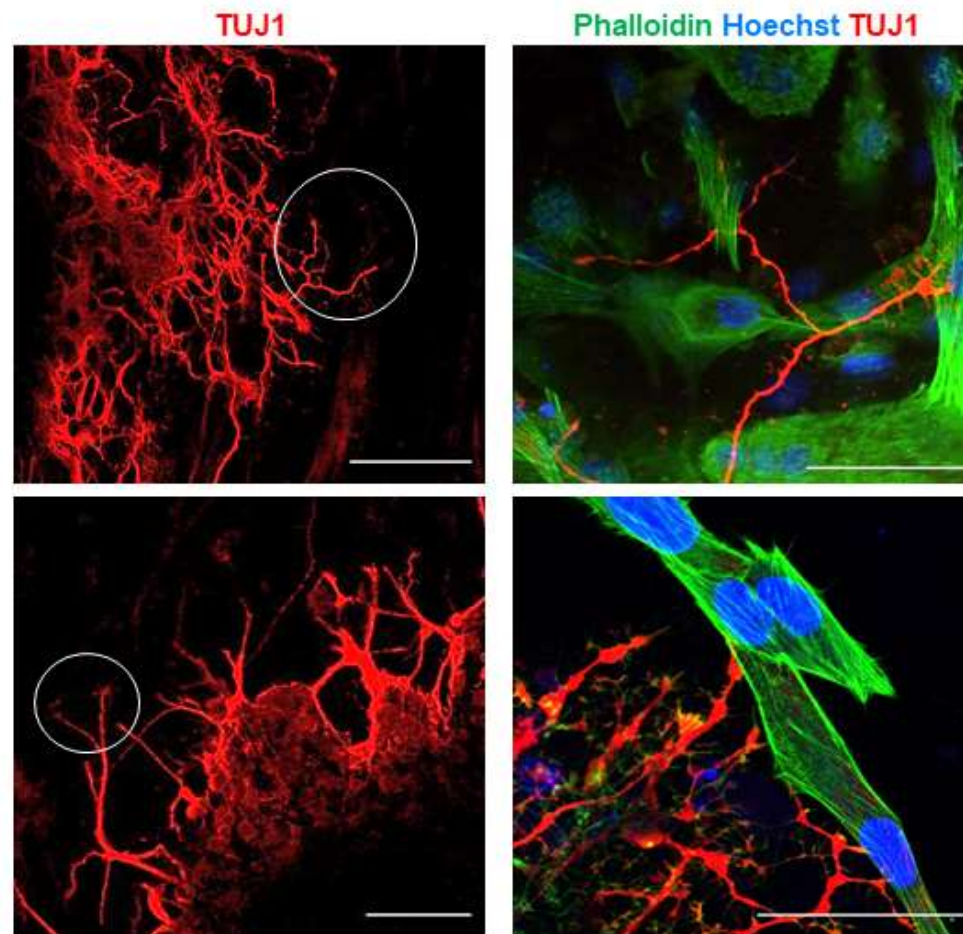


**Figure 3.3.2-3: Some neurite branching can be observed in co-culture as well as more than one neurite contacting particular myotubes.** After 10 days of co-culture between TERA2.cl.SP12 derived neurospheres and C2C12 myotubes, some neurites branch into two or three neurites (Circled. A, B and C. TUJ-1 – Red). As well as this, more than neurite appears to make contact with some myotubes (phalloidin stained F-actin – Green), suggesting neurite elimination/competition was occurring (D). Scale bars: A+B = 100  $\mu\text{m}$ , C+D = 50  $\mu\text{m}$

Unlike in monoculture, in which neurites project radially, in co-culture, growing neurites follow a more perturbed pathway, implicated by the morphological and chemotactic influences of the myotube. Nevertheless, the culture methods developed herein provide an opportunity whereby structures are easier to locate and analyse than previous approaches used.

Many neurites were observed to branch/fork, forming more than neurite terminal from one neurite stem (Figure 3.3.2-3 – circled). As well as this, some myotubes had more than one neurite terminal bouton appearing to make contact with their surface, suggesting more than one interaction and potential neuromuscular junction was forming.

### **3.3.3 Enhancement of neurite outgrowth in co-culture through ROCK inhibition by Y-27632**

As previously established, neuritogenesis as well as myogenesis can be enhanced through inhibiting Rho A/ROCK signalling through ROCK inhibitor Y-27632. Results showed that neurite outgrowth was increased from TERA2.cl.SP12 derived neurons in monoculture. As well as this, differentiation of C2C12 myoblasts is increased through ROCK inhibition in monoculture. Therefore, the effect of Y-27632 was investigated in the co-culture system as it has potential to increase neurite outgrowth within co-culture, creating a novel, reliable co-culture model system. To investigate this, Y-27632 was included in the differentiation medium at a final concentration of 10  $\mu$ M, in the 10-day co-culture period. Neurite outgrowth (TUJ1 - red) from neurospheres appeared to be enhanced compared to the untreated control (Figure 3.3.3-1). A greater number of TUJ1 positive neurites visibly radiated from the neurosphere towards the mature myotubes (F-actin – green). Neurites also appeared longer than those in monoculture, yet still extended to co-localise with myotubes at their leading edge (Figure 3.3.3-1 - C). Higher magnifications of neurite outgrowth in co-culture revealed neurite density would appear to be significantly increased in areas (Figure 3.3.3-1 - D). Another observation is



that there appears to be less cellular migration from the central neurosphere, a phenomenon found to be notably significant in monoculture, although not quantified here.<sup>28, 204</sup> Results suggest that inhibition of ROCK through Y-27632 does not interfere with growth cone formation or co-localization between the neurites and myotubes, as both are very much apparent in all cultures examined.

Quantification of neurite outgrowth in this novel co-culture set up involving neurospheres and C2C12 myotubes treated with Y-27632 revealed that neurite length as well as neurite density are significantly increased in co-culture (Figure 3.3.3-2). Quantification of neurites in co-culture were then compared to neurites in monoculture in both untreated (no ROCK inhibitor) and treated (ROCK inhibitor) conditions (Figure 3.3.3-3). This data suggests that ROCK inhibitor had a stronger effect in monoculture, although neurite outgrowth in co-culture was still enhanced through treatment with ROCK-inhibitor. Neurites were significantly longer and denser in treated monocultures compared to treated co-cultures.

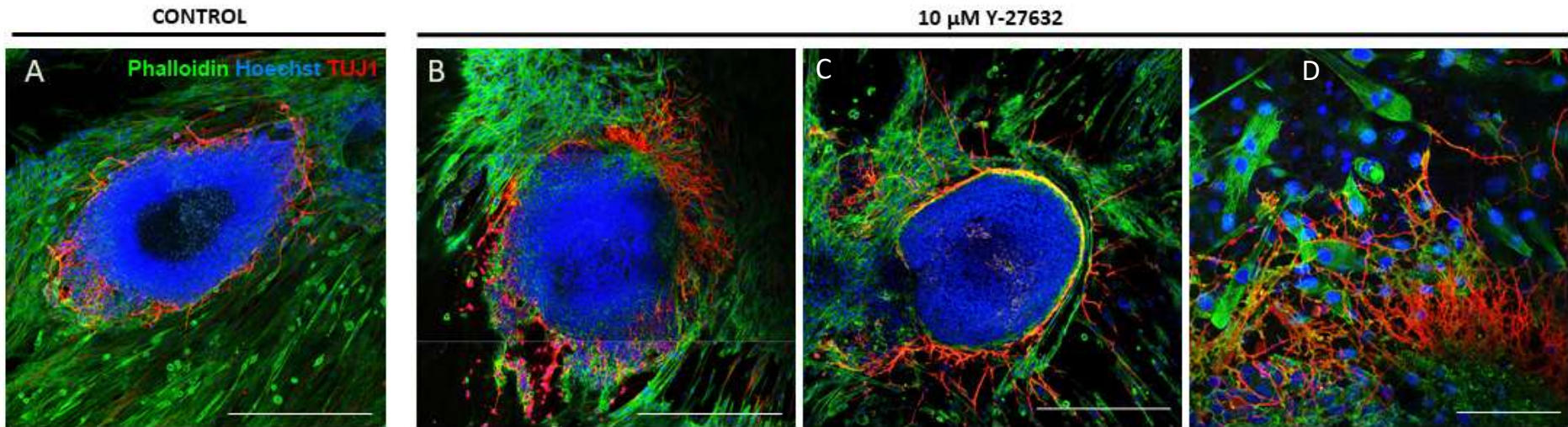


**Figure 3.3.3-1: ROCK inhibitor appears to enhance neurite outgrowth in co-culture.** Immunofluorescence shows neurites, stained with Tuj1 (red) appear longer and denser in co-culture with C2C12 myotubes after treatment with the ROCK inhibitor Y-27632 compared to the control, which contains control co-culture media, as previously outlined. Nuclei are stained with Hoechst (blue). Scale bars: A = 500 μm, B = 500 μm, C = 500 μm, D = 100 μm.

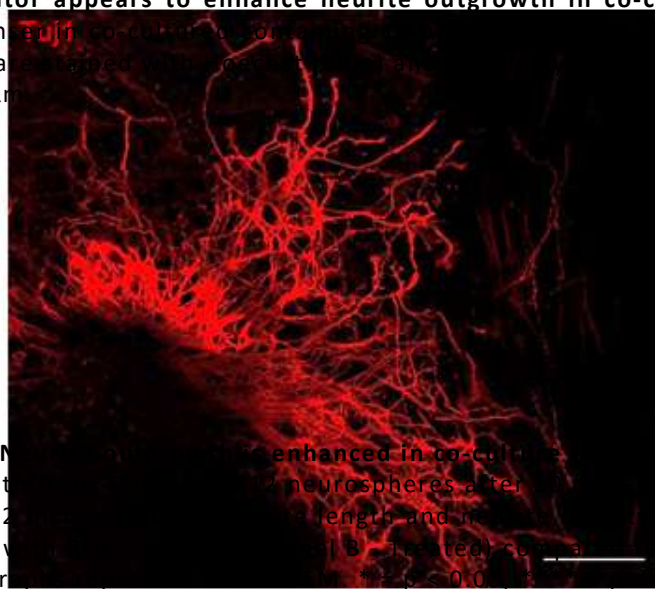
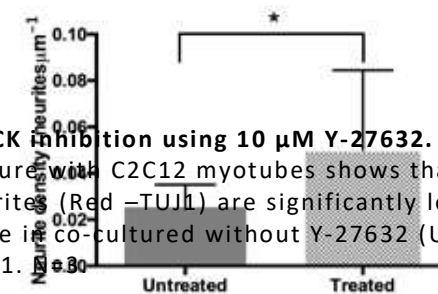
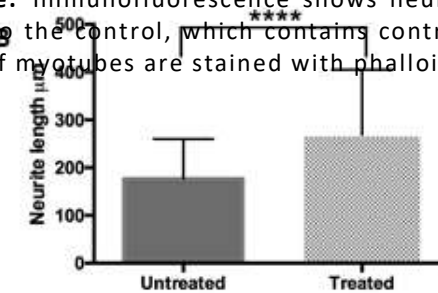


**Figure 3.3.3-2 – Neurite outgrowth is enhanced in co-culture with C2C12 myotubes after treatment with the ROCK inhibitor Y-27632.** Scale bar = 100 μm. Grayscale image. \* = p < 0.05, \*\*\*\* = p < 0.0001.



**ROCK inhibition using 10 μM Y-27632.** Quantification of neurite length and density in co-culture with C2C12 myotubes shows that selective ROCK inhibition using 10 μM Y-27632 significantly increases the length and density of neurites (Red -TUJ1) compared to those in co-culture without Y-27632 (Untreated). Scale bar = 100 μm. \* = p < 0.05, \*\*\*\* = p < 0.0001.

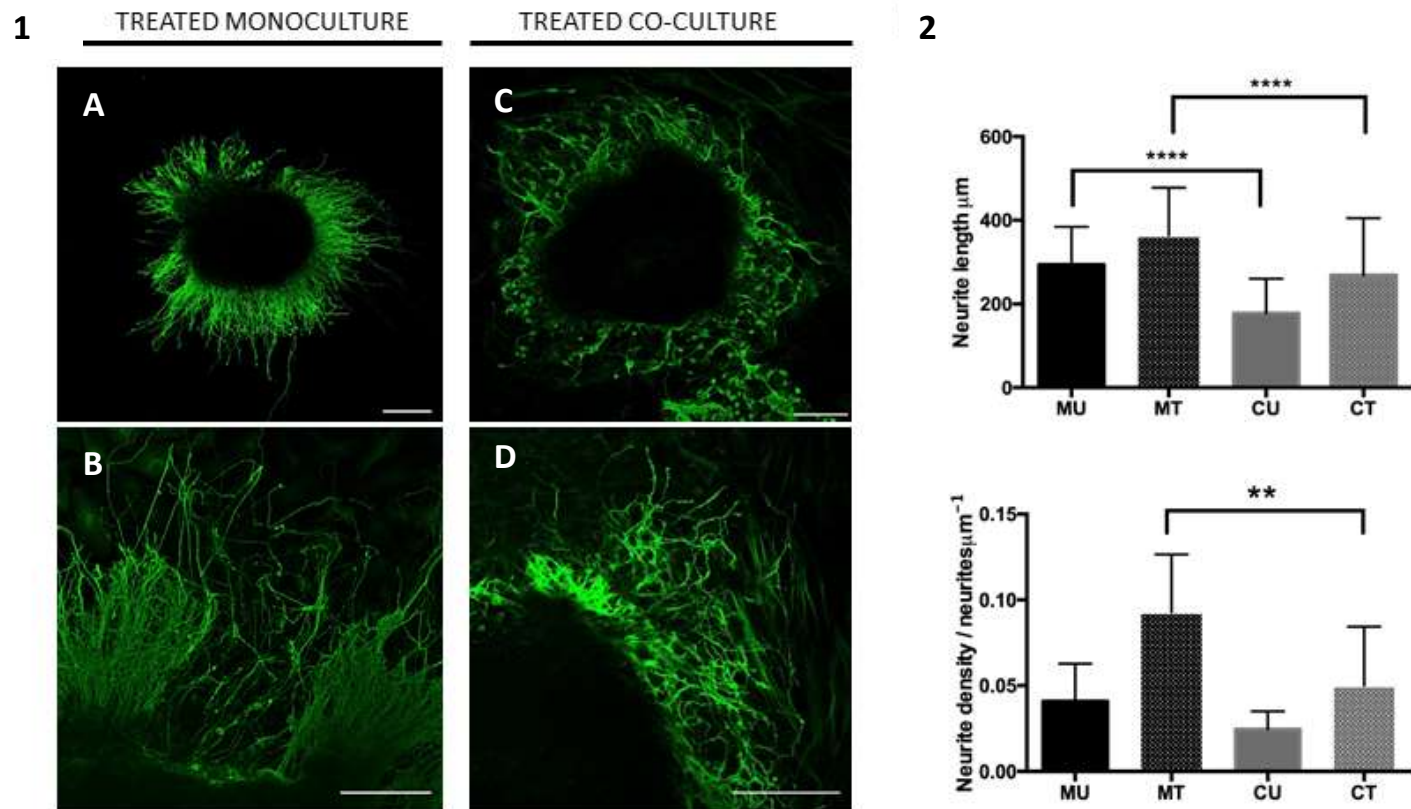


**Figure 3.3.3-3: ROCK inhibitor Y-27632 enhances both neurite outgrowth and neurite density in monoclature as well as co-culture, although not as effectively in co-culture.** Quantification of neurite outgrowth and neurite density (Panel 2) between monoclature and co-culture shows that ROCK inhibitor Y-27632 has more pronounced effect in monoclature. Neurites (TUJ1 – Green) are significantly longer and denser in treated monoclature (A+B) compared to treated co-cultures (C+D). Lower micrographs B and D show higher magnification of neurites, but are different neurospheres to those shown in A and C. MU = Mono-culture untreated; MT = Mono-culture Treated; CU = Co-culture Untreated; CT = Co-culture Treated. Scale bars: top row = 200 μm bottom row = 100 μm Graphs represent data ± SEM. \* = p < 0.05, \*\*\*\* = p < 0.0001. N=3.

### **3.3.4 Identification of neuromuscular junctions in co-culture**

Neuromuscular junctions, the chemical synapses that form between motor nerve terminals and skeletal muscle fibers, facilitate the progression of an action potential to the muscle so that it can be converted into mechanical energy, resulting in muscle contraction. To examine whether these specialised synapses form in the novel co-culture system developed herein, several techniques were employed including further immunofluorescent analysis of synapse specific structures as well as a functional assay to provide both morphological, physiological and functional evidence for the presence of neuromuscular junctions.

#### **3.3.4.1 Fundamental nuclei accumulation**

In the absence of neurons, nuclei were found at a relevantly even distribution along the length of skeletal muscle myotubes. Upon innervation by a neuron however, several nuclei cluster at myotube post-synaptic surface at the point of innervation during development of the neuromuscular junction.<sup>157</sup> This characteristic accumulation of 'fundamental nuclei' serves functionally specialised role in development and maturation of the NMJ itself.

In each of the co-culture models used in this study: dissociative neuron co-culture, neurosphere co-culture and enhanced neurosphere co-culture; fundamental nuclei accumulation can be observed at points of co-localisation, where an interaction between the neuron and myotube is thought to occur (Figure 3.3.4.1). Using immunofluorescent analysis, Figure 3.3.4.1 – A shows nuclei accumulation in a dissociation neuron culture. It was observed that neurons (TUJ-1 – red) extend longitudinally almost parallel to the C2C12 myotubes before making contact. At these points of contact (Figure 3.3.4.1 - circled), between 2-6 nuclei had accumulated and were positioned together, suggesting the presence of a neuromuscular junction at these locations.



In the neurosphere co-culture (Figure 3.3.4.1 – B+C), it was easier and less time consuming to identify neurite terminals at the myotube surface. The neurites (TUJ1 – red), radiated from the neurosphere and grew towards the myotubes (F-actin – green), where interactions between the two cell types were observed. Figure 3.3.4.1, B and C show clear examples of nuclear accumulation at points where the neurite terminal makes contact with the myotube surface. The results of a cellular response elicited by the neurite contacting the myotube are shown, whereby 4-5 nuclei have migrated and accumulated, indicating the formation of a neuromuscular junction at these points. A terminal bouton-like structure is especially apparent in Panel C (Figure 3.3.4.1) at the point of co-localisation, which is typical of the presynaptic terminal.

Nuclear accumulation also occurred in the enhanced neurosphere-myotube model, where the ROCK inhibitor Y-27632 was used to enhance neurite outgrowth in the co-culture – see D (Figure 3.3.4.1). Many neurites were seen to be radiating from the neurosphere. Circled is a point of contact between neurite and myotube. In this particular interaction, 6 nuclei have accumulated below the membrane surface, again suggesting formation of a neuromuscular junction through eliciting a cellular response to the point of contact.

### **3.3.4.2 Acetylcholine receptor accumulation**

There exist many synapse-specific structures expressed exclusively at the neuromuscular junction, some at the presynaptic nerve terminal, some within the synaptic cleft between the synapse, and others at the post-synaptic terminal (see Figure 3.3.4.2-1). At the post-synaptic terminal of a neuromuscular junction, acetylcholine receptor accumulation is characteristic at the post-junctional folds, and pivotal to neuromuscular junction functionality.<sup>156</sup> As previously discussed, acetylcholine receptors are expressed in mature C2C12 myotubes, but are found relatively evenly distributed along the length of myotubes in the absence of neural contact.

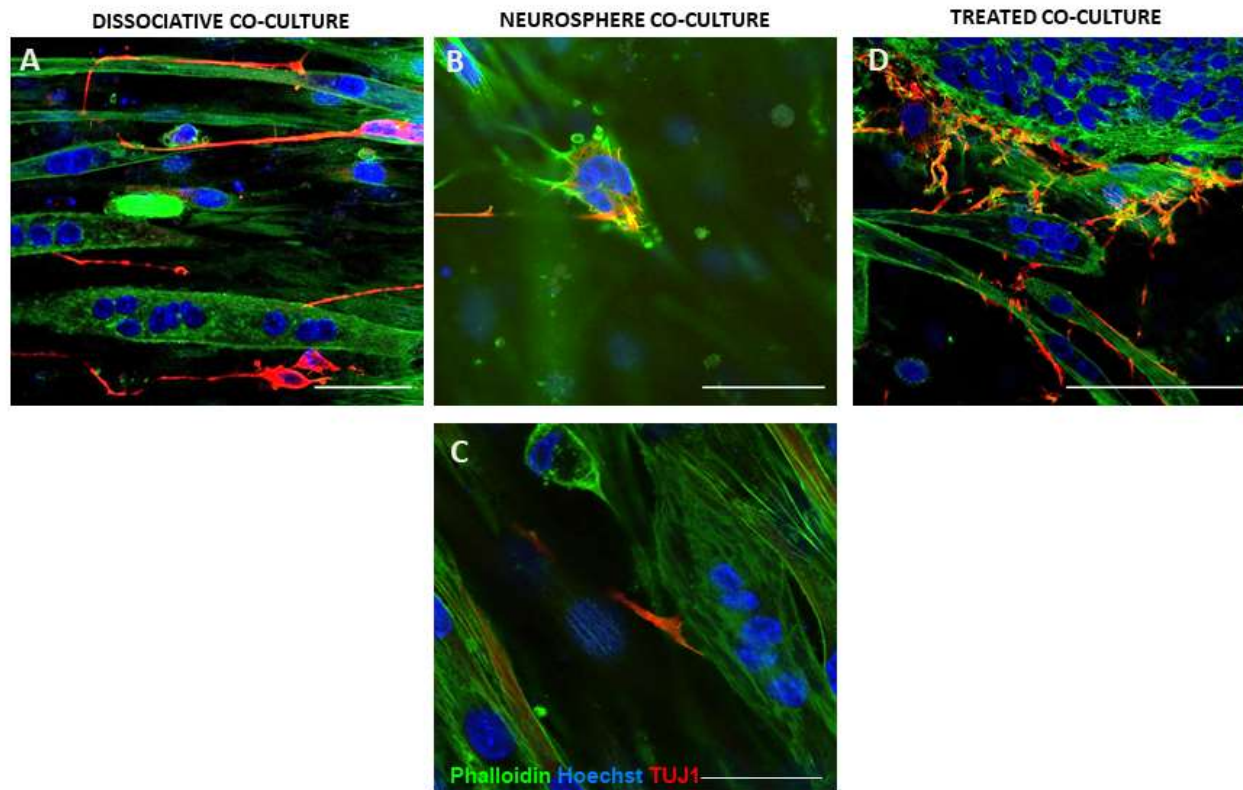


**Figure 3.3.4.1: Neuron terminals co-localise with myotubes at points where nuclei aggregation in myotubes is evident, a key feature of neuromuscular junctions.** Nuclei accumulation (Hoechst – blue) in all three types of co-culture is evident: co-culture of dissociative neurons and mature myotubes, co-culture of neurospheres and myotubes, as well as co-cultures treated with 10  $\mu$ M ROCK inhibitor Y-27632. Neurites (TUJ1 - red) appear to contact myotubes at these points. Myotubes are stained green with phalloidin. Scale bars: A, B and C = 50  $\mu$ m, D = 250  $\mu$ m

To detect whether acetylcholine receptor clusters were present in the neurosphere-myotube co-culture model at points of interaction, acetylcholine receptor stain  $\alpha$ -Bungarotoxin was used to stain co-cultures alongside TUJ1 (red - neurites), F-actin (green – myotubes), and Hoechst (blue – nuclei). Positive patches of  $\alpha$ -Bungarotoxin staining were observed at the myotube surface, in association with the neurite terminals in the co-culture system (Figure 3.3.4.2-1). Higher magnification fluorescence microscopy allowed the bouton-like structure at the nerve terminal (red) contacting the myotube surface (green) to be imaged more clearly (Figure 3.3.4.2 - A). A Z-stack image was taken, producing a cross-sectional 3D-like reconstruction of the cellular architecture at the point of co-localisation (Figure 3.3.4.2 - Arrow). This indicated that the neuron bouton terminal makes contact with the myotube, and the two structures appeared to be fused together.  $\alpha$ -Bungarotoxin (yellow) positive staining was observed in Figure 3.3.4.2 - B, where positive staining suggested the presence of acetylcholine receptor clustering. This clustering adopted the typical 'pretzel-like' shape, characteristic of that at neuromuscular junctions.<sup>141</sup>

In Figure 3.3.4.2 – panel C, both A and B have been merged to show all staining in the same field. From this, it is evident that the bouton co-localises with acetylcholine receptor clusters on myotube surface. This receptor clustering provides additional evidence to suggest the presence of neuromuscular junctions.

Further cultures were double stained using  $\alpha$ -Bungarotoxin (yellow) and TUJ1 (green) only (Figure 3.3.4.2-2). This is because  $\alpha$ -Bungarotoxin is an Alexa Fluor 594 conjugated antibody (far red), which has an excitation wavelength that overlaps slightly with the red secondary antibody used to stain neurites red with TUJ1. Although microscope settings were changed to avoid this as far as possible, a double-stain emitting the red antibody, and instead using green (TUJ1) and far red ( $\alpha$ -Bungarotoxin - changed to yellow here for visualisation purposes) was carried out to eliminate any doubts regarding overlapping

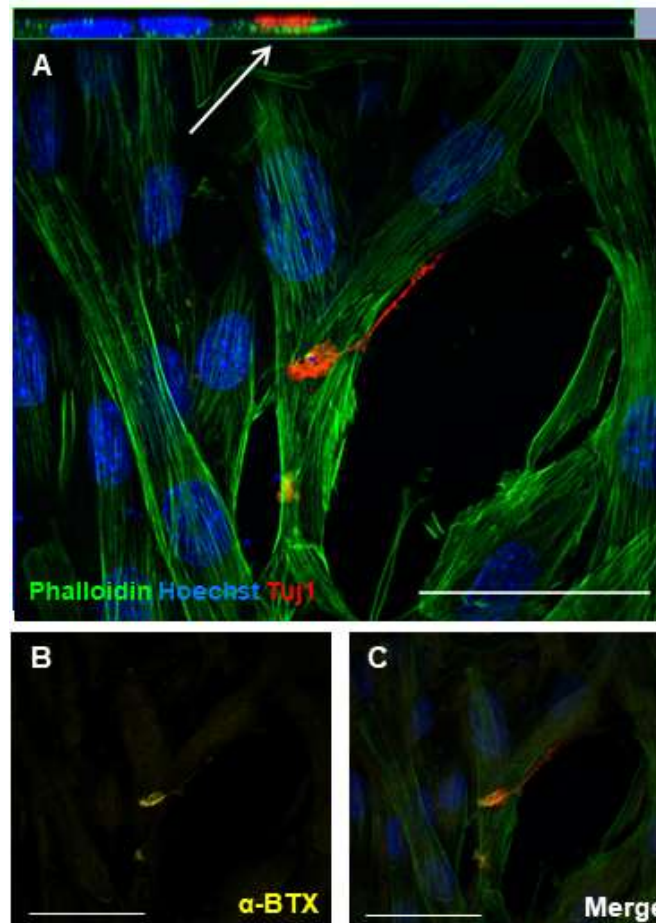


**Figure 3.3.4.2-1 Positive  $\alpha$ -bungarotoxin staining depicts acetylcholine receptor clustering at points of co-localization between neuron terminal and myotube in co-culture.** After 10 days of co-culture between TERA2.cl.SP12 derived neurospheres and C2C12 myotubes, co-localisation occurred between the two cell types. Z-stack analysis (arrow) shows contact, and  $\alpha$ -bungarotoxin staining (yellow) shows acetylcholine receptor clustering at these points of contact between neuron terminal (red: TUJ1) and myotube (green: phalloidin). Scale bars: 50  $\mu$ m.

emission spectrums. Using this double stain approach of neurosphere-myotube co-culture, a neurite extending with a growth cone at the tip was identified (Panel A - Figure 3.3.4.2-2). In Figure 3.3.4.2-2 - panel B, positive  $\alpha$ -Bungarotoxin staining is shown (+), with positive receptor clustering apparent. Once merged (Panel C - Figure 3.3.4.2-2), it is evident that the neurite is extending towards the acetylcholine receptor cluster, which was assumed to be the myotube surface edge (Figure 3.3.4.2-2 - circled), although not stained.

Dissociation neuron-myotube co-cultures were stained after 5 days of co-culture using the same immunofluorescent techniques discussed above. Figure 3.3.4.2-3 shows triple staining, where a dissociative neuron (TUJ1 – red) winds around and then extends along the length of a myotube (F-actin – green), and where a bouton-like structure can be observed at the terminal. This terminal bouton is easier observed in Figure 3.3.4.2-3 - B, where only the neurite is portrayed at a slightly higher magnification. In Figure 3.3.4.2-3 - C,  $\alpha$ -Bungarotoxin (yellow) of the same area is shown. A very distinct positive staining occurs showing acetylcholine receptor clustering is present. When combined (Figure 3.3.4.2-3 - D), we see that this acetylcholine clustering occurs at the nerve terminal on the myotube surface, where the bouton makes contact. Again, this clustering is of expected shape, size, and location, providing anatomical evidence supporting the formation of neuromuscular junctions.

Further immunofluorescence analysis of dissociative neuron-myotube co-cultures to emit any potential excitation spectrum overlap between fluorophores was also carried out (as completed for the neurosphere-myotube co-cultures). Figure 3.3.4.2-4 shows that positive acetylcholine receptor staining using  $\alpha$ -Bungarotoxin was present at the area on the myotube (not stained) where the nerve terminal bouton makes contact.

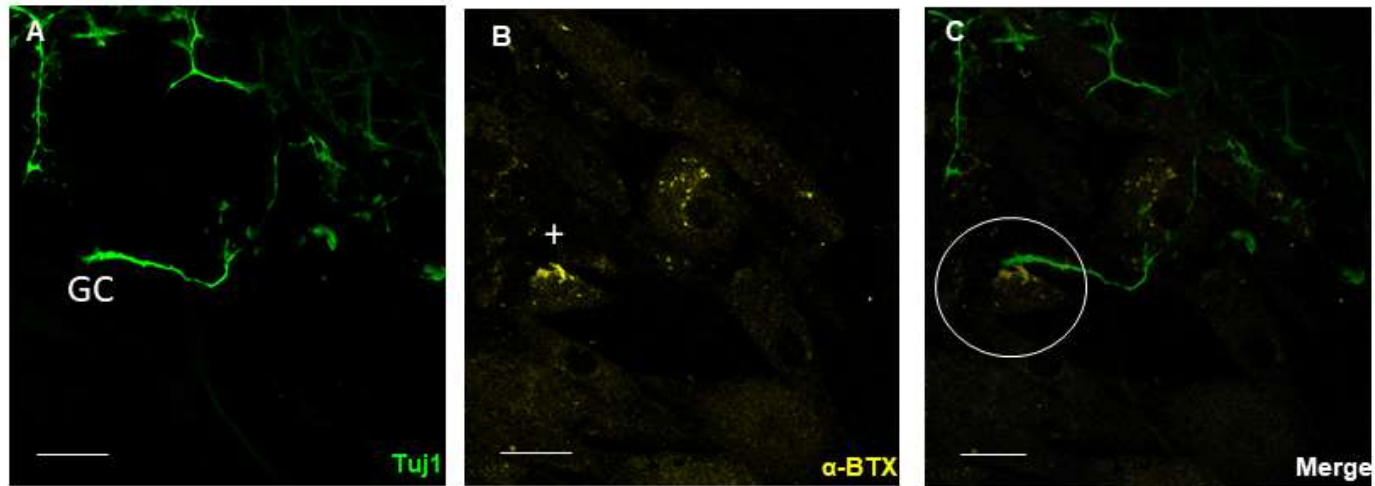


**Figure 3.3.4.2-2 – Double staining of points of co-localisation between neuron terminal and myotube reveal positive acetylcholine receptor clustering at post-synaptic membrane.**  $\alpha$ -bungarotoxin staining (yellow) shows acetylcholine receptor clustering at these points of contact between neuron terminal (green: TUJ1) and myotube (unstained) in neurosphere-myotube co-cultures after 10 days. Scale bars: 50  $\mu$ m.

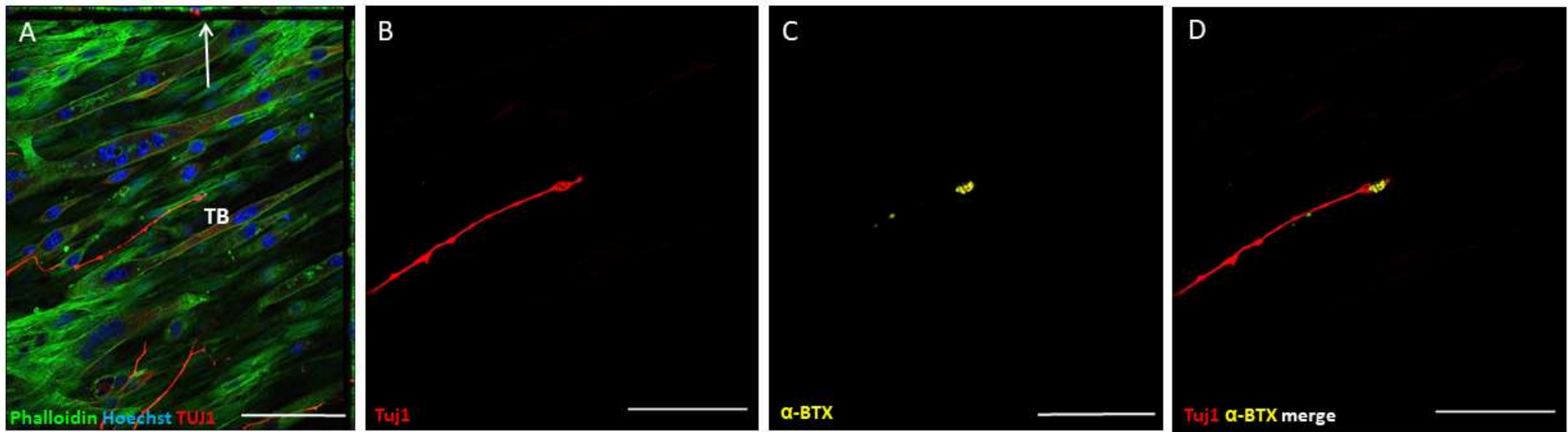


**Figure 3.3.4.2-3: Positive  $\alpha$ -bungarotoxin staining depicts acetylcholine receptor clustering at points of co-localization between neuron terminal and myotube in co-culture between dissociative TERA2.cl.SP12 derived neurons and mature myotubes.** After 5 days of co-culture between TERA2.cl.SP12 derived neurons and C2C12 myotubes, co-localisation occurred between the two cell types. Z-stack analysis (arrow) showed contact, and  $\alpha$ -bungarotoxin staining (yellow) shows acetylcholine receptor clustering at these points of contact between neuron terminal bouton (TB) and myotube. Z-stack analysis (arrow) showed contact, and  $\alpha$ -bungarotoxin staining (yellow) shows acetylcholine receptor clustering at these points of contact between neuron terminal bouton (TB) and myotube. Scale bars

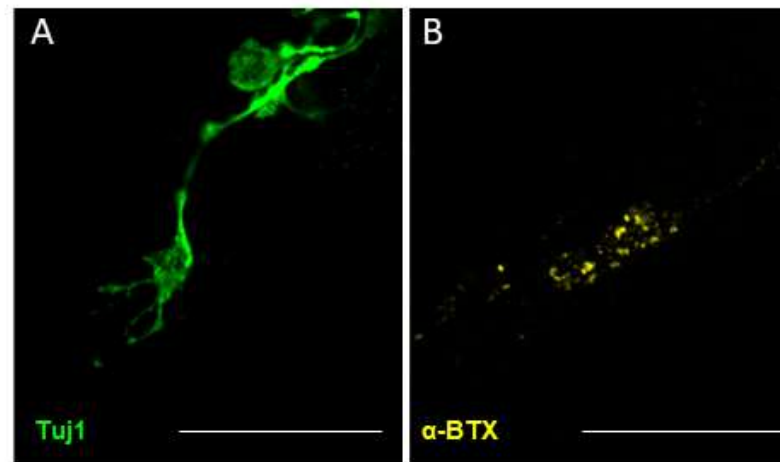


**Figure 3.3.4.2-4 – Alpha-bungarotoxin positive staining was performed to eliminate background staining (yellow) staining was performed to eliminate background staining that alpha-bungarotoxin positive patches appear at the**

111  
and alpha-  
nages show  
 $\mu\text{m}$ .

### **3.3.4.3 Functional evidence of NMJ formation**

After 10 days of co-culture, non-selective AChR agonist acetylcholine was added to co-culture media at a final concentration of 0.01  $\mu\text{M}$ . Immediately following this, phase contrast microscopy was employed to assess results of this pharmacological manipulation of co-cultures. As a negative control, 10 day old mature myotube monocultures were also subjected to the same acetylcholine concentration. No contraction was observed in the myotube monocultures after addition of acetylcholine. However, preliminary evidence of contraction was observed in co-cultures. Images and videos were captured using the 40x objective lens of the phase-contrast microscope. Figure 3.3.4.3 shows an example where a neurite and myotube twitch was observed after acetylcholine supplementation. Images were captured from the video, allowing Image J analysis. A grid was overlaid on the view before contraction, herein termed resting (Figure 3.3.4.3 - A), and after movement, to be called contraction (Figure 3.3.4.3 - B). This grid allowed movement to be visualised more clearly, and arrows were added to points of specific interest on the image – making evidence of movement more clear. Myotube movement was not obvious enough for any quantification to be carried out, and so quantification was only performed on neurite length, as this structure is pronounced in the video. Neurite length appeared to reduce by 25% during contraction.



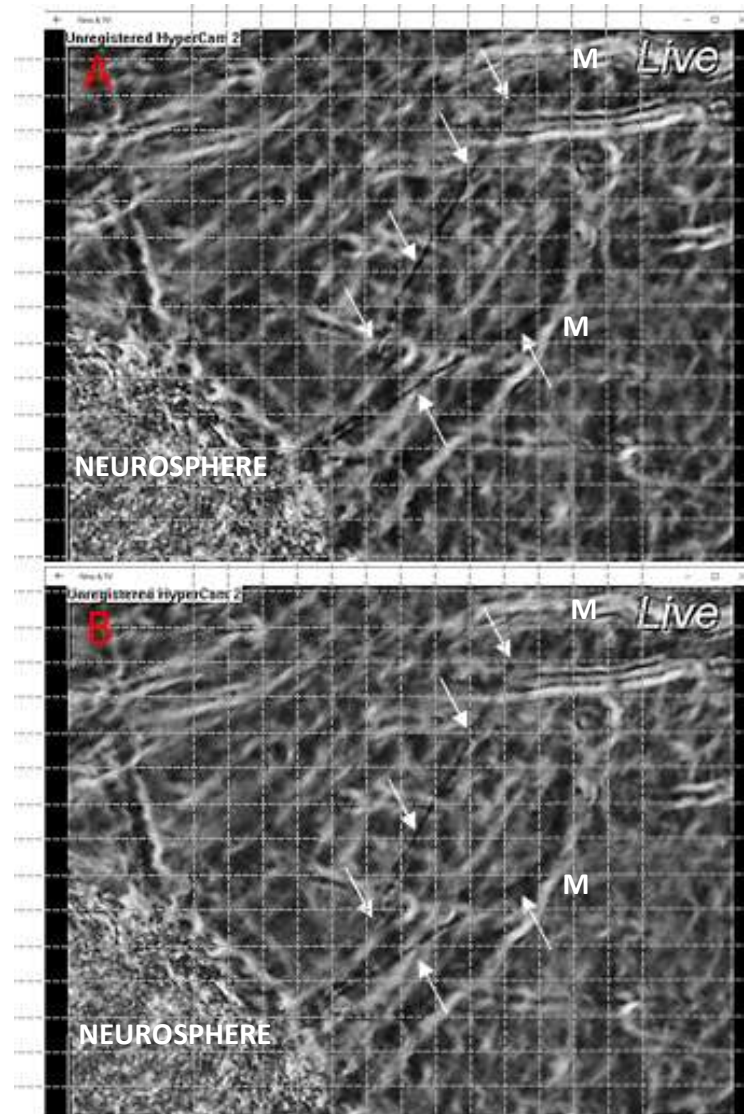


**Figure 3.3.4.3: Preliminary evidence of contraction was observed in co-culture following addition of acetylcholine.** Phase contrast microscopy was used to image/video co-cultures following addition of 0.01  $\mu\text{M}$  acetylcholine to co-culture medium. These images are taken from a video representing a point before (A) and during (B) contraction, where B was captured 0.07 seconds after A. A grid was overlaid for ease of identification of small-scale movement in the culture. Arrows identify boxes in which neurite movement is obvious when compared against each other. The neurosphere is labelled in the bottom left corner, and the myotubes to which neurites are attached are labelled M.

## 4.0 Discussion

The overall aim of this project was to use human pluripotent stem cells and an established myoblast lineage to produce a unique, robust, and reproducible co-culture model of neuromuscular junction formation. In order to do this, the project was split into three, equally important sections: first, we developed human neurons from human embryonal carcinoma TERA2.cl.SP12 stem cells through retinoid exposure. Second, mammalian skeletal muscle was developed from C2C12 myoblasts. Third, a co-culture system was designed and optimised between the aforementioned cell types, before investigating the formation of neuromuscular junctions. Through separating the project into its prerequisite developmental steps, we were able to characterize, and optimise the differentiation and resulting cell types, ultimately allowing for a co-culture model we have shown to be superior in certain elements to those already in existence. Investigation into molecular signalling pathways common to both neurite outgrowth and myogenesis was employed, allowing utilisation of mutual signalling mechanisms that benefit the co-culture design.

The *in vitro* neuromuscular junction model discussed herein, has many potential research and experimental advantages compared to existing co-culture models, as will be discussed; these are of broad interest, ranging from potential therapeutic drug screening to academic research, including investigation of signalling mechanisms and the developmental anatomy of the neuromuscular junction.

### 4.1 Producing human neurons from pluripotent stem cells

#### 4.1.1 Dissociation culture of human neurons

It is well accepted within literature that retinoic acid is a pivotal signalling molecule during embryonic patterning and embryonic development. In particular, it is a key

regulator of neural tube development and a contributor to both antero-posterior and dorsoventral patterning.<sup>19,20,21</sup> Consequently, many *in vitro* studies have used retinoic acid as a morphogen for producing neural derivatives from embryonic stem cells and embryonal carcinoma cells.<sup>192, 203, 211, 242</sup> Previous work in the laboratory has also demonstrated that retinoic acid can act as a morphogen, directing embryonal carcinoma stem cells, TERA2.cl.SP12 to produce neural derivatives.<sup>200</sup> The dissociative culture method followed, successfully utilised the ability of retinoic acid to produce neurons in monolayers.

Previous work has shown that retinoic acid induces its effects on EC cells within 24 hours, at which point, EC cells begin to lose their markers of pluripotent stem cells (SSEA-3, TRA-1-60).<sup>198</sup> It was also shown that neuroepithelial rosettes formed from EC cells in culture with retinoic acid for 2 weeks represent neural-tube like structures, similar to that of ES neural differentiation.<sup>198</sup> In this study, neuroepithelial rosettes were observed after 3 weeks of culture alongside 10  $\mu$ M retinoic acid, indicating that differentiation was progressing. Neurons removed from these rosettes were dissociated and plated for immunocytochemistry, which concludes their neural phenotype through positive staining with neuronal marker – TUJ1. Retinoic acid in its natural form however, is of limited practicality due to its rapid degradation in light and heat.<sup>212</sup> Consequently, a stable, synthetic retinoid EC23 was also used as a morphogen in the dissociative culture method of producing neurons.<sup>204</sup> Neurons produced using synthetic retinoid EC23 culminate in the same neural morphology as observed in RA cultures. Neurons stain positively for TUJ1, and form monolayers when cultured on Poly-D-lysine and laminin coated dishes. Neurons are produced when exposed to EC23 at a significantly lower concentration, 0.01  $\mu$ M as opposed to 10  $\mu$ M ATRA. Using EC23 as a morphogen however provides a more reproducible and reliable model, due to its stability and increased potency.

Neurons produced through this dissociative culture method, although stain positively for TUJ-1, are difficult to access and pinpoint particular locations of neurons. Due to their dissociative nature, once plated, they settle anywhere on the plate and their neurites readily intertwine with one another, making quantitative analysis not only time-consuming but extremely difficult, with varying neurite length. Contaminating cells can also be observed in culture with both retinoid compounds, a normal phenomenon often described in literature.<sup>206, 207, 213</sup> To identify glial contaminants, a glial marker such as myelin and GFAP could have been employed.<sup>216</sup> Nonetheless, neurons can be cultured for long periods of time using this method of dissociative neural culture, – with increasing purity of neural cultures with repeated trypsinisation steps.<sup>242</sup>

#### **4.1.2 Neurosphere formation for neurite outgrowth**

To overcome some of the limitations of the dissociative culture method discussed above, such as difficulty identifying and analysing neurons, a model of neurite outgrowth developed by Dr Kirsty Goncalves within Durham University was then used for investigating neurite outgrowth.<sup>28, 204</sup> This model produced neurospheres from TERA2.cl.SP12 embryonal carcinoma stem cells, from which neurites radiated out from the central mass when plated on laminin and Poly-D-Lysine coated culture plates. These human neurons can be visualised under phase-contrast microscopy, as this methodology allows an easier identification process of the neurons, since they project outwards from a neurosphere – a structure visible to the naked eye. As well as this, all neurons stain positively during immunocytochemical analysis for neuronal marker TUJ-1, suggesting terminal differentiation. Cultures do, however, contain contaminating cells like that of the dissociative neuron cell culture. Another advantage of this model is its use for quantification; with all neurites radiating from a central core, counting and measuring is uncomplicated, making it of significant value to studies investigating neurite inhibition of pharmaceutical enhancement of neurite outgrowth.

This culture technique proves simple in comparison to neural differentiation from embryonic stem cells as a result of the TERA2.cl.SP12 embryonal carcinoma cells having a more restricted developmental biology, and having a high propensity for producing neural derivatives.<sup>200, 194</sup> Conversely, embryonic stem cells have been used in earlier studies, involving those of mammalian development, have been used to production of neurons.<sup>217</sup> The methodology, however, is technically challenging, with requirements of conditioned medias, and are not amenable to up-scaling to meet the neural tissue.<sup>192</sup> Aggregate cultures have also been described from embryonic stem cells, but the EC-neurosphere protocol used here shares many of the important features, whilst eliminating difficult protocols and feeder cells required to produce an abundance of neural material in a robust, reproducible manner.<sup>218</sup>

#### **4.1.2.1 ROCK Inhibition enhances neurite outgrowth from neurospheres**

Neurite outgrowth from the TERA2.cl.SP12 neurosphere model can be significantly enhanced in length and density through inhibition of ROCK, a downstream effector protein in Rho-signalling. The data collected here fits with previous investigation, showing a selective inhibitor of ROCK, Y-27632, successfully enhanced the actin cycling during neurite outgrowth.<sup>219</sup> This enhancement in neurite outgrowth is a result of Rac1 and Cdc42, two molecules in the actin dynamics of the neurite that promote membrane breaching at the leading edge, which are inhibited through the mechanisms of Rho A and ROCK mediated signalling.<sup>220</sup> Neurite density is increased, but resulting neurites still do not tend to overlap one another, resulting in an enhanced, yet readily quantifiable model.

Another clear observation was the inhibition of migrating or contaminating cells surrounding the neurosphere after 10 days of neurite outgrowth, which is observed in nearly all untreated cultures. These results also align with previous data using the same neurosphere model, suggesting that the actin remodelling mechanisms affected by ROCK inhibition inhibit cell migration from the central mass neurosphere mass.<sup>204</sup> Rho A

is believed to be implicated in contraction and retraction of the actin dynamics of a cell during cellular migration, including that of squamous cancer carcinoma cells.<sup>221, 222</sup> However, the involvement of ROCK in cellular migration is yet to be identified. Consequently, the reduction in contaminating non-neuronal cells enhances the purity of neuronal culture.

The neurosphere model is hereby proven useful for investigation of signalling mechanisms involved in neurite outgrowth in development. This is of value to studying pathology of particular diseases in which neurite outgrowth is impaired, such as Alzheimer's and Parkinson's disease.<sup>204</sup>

## 4.2 Producing mammalian muscle from C2C12 myoblasts

It is known that skeletal muscle of the vertebrate embryo is derived from the paraxial mesoderm – part of the mesodermal tissue. The paraxial mesoderm is specified as a result of signalling gradients, specifically Noggin antagonisation of BMPs.<sup>56</sup> This results in the formation of somites within the paraxial mesoderm, structures containing a Myotome compartment, from which the skeletal muscle mass of the vertebrate body emanates.<sup>56</sup> The multistep process controlling muscle differentiation is governed by transcription regulators of cell fate determination, coupled with external signals influencing myogenic differentiation. These transcriptional regulators have recently been identified, but the exact function of them all, and interaction between them is yet to be fully elucidated.<sup>223</sup> The murine C2C12 myoblast cell line used to investigate myogenesis is a well-studied cell line proven to express same myogenic regulatory factors of skeletal muscle *in vivo*.<sup>65</sup> Thus, the cell line proves an extremely useful, practical tool for studying developmental biology and its associated mechanisms.

The dramatic morphological change during myogenesis, whereby small mononucleate myoblasts migrate, align, fuse, and elongate to form myotubes is also a well-documented process.<sup>224</sup> The data obtained through this study using the C2C12 cell line

fits previous data, with additional quantification of myotube number per day during the differentiation process, which is not described in current literature. Myotube number increases significantly per day, as expected, with mature myotubes obtained after 5 days of differentiation.

Myogenic regulatory factors (MRFs), are the transcriptional determinants of muscle differentiation, and include MyoD, Myf5, MRF-4, and myogenin. Each MRF becomes activated and expressed in a time-dependent manner, with positive and negative-feedback existing between them, with literature originally linking myogenin to late-stage differentiation in C2C12 differentiation.<sup>84</sup> This however, has recently been contradicted, with recent evidence showing myogenin is transiently expressed earlier than originally thought in the myogenic process, and down-regulation can result in reversal of differentiation.<sup>84, 225</sup> Instead, we looked at quantifying a more accurate terminal marker of differentiation in C2C12 tubes – Myosin Heavy Chain (MHC), a muscle-specific contractile protein whose expression is induced by MRF's during terminal differentiation of myotubes.<sup>224</sup> The data obtained shows myosin heavy chain expression increased during the process of C2C12 differentiation, with most cells expressing after the 5 days, indicative of mature myotubes. This data simulates that found in other studies, although a different method of quantification was used.<sup>225</sup> In another study quantifying MHC expression in C2C12 myotubes for example, *fusion index* was used, which looks at the number of nuclei present in myotubes in comparison to the total number of nuclei present in a field.<sup>225</sup> However, upon entering the differentiation process, the myotubes, although in monolayers, elongate around one another and so nuclei result in different planes that cannot all be visualised in the same field during immunocytochemical analysis. Accordingly, we found it more appropriate to quantify number of myotubes by number per area as they are strongly actin positive, or in the case of MHC expression, percentage expression of total myotubes present in a given field.

In the undifferentiated myoblast, only one nucleus was observed, positively staining for Hoescht. These nuclei contained numerous, prominent nuclei, as described in previous studies involving C2C12 myoblasts.<sup>232</sup> Once differentiated, the morphological characteristics of the aneural myotubes was as expected, with no acetylcholine receptor clustering or nuclei accumulation in mature myotubes – two characteristics of neuromuscular junction formation. Instead, the myotubes were multinucleate, with nuclei being of what appeared to be a random distribution, and acetylcholine receptors were also randomly distributed. Although the nuclei appeared of random distribution, one previous study found a significant difference between actual nuclei position and that of a random distribution, suggesting an intrinsic design.<sup>165</sup> On the other hand, AChR expression is comparable to that of human skeletal muscle, whereas other animals can be found to have significantly higher expression levels of the receptors.<sup>233</sup> It is possible to argue therefore that this murine cell model is a useful model for imitation of human skeletal muscle, but more reproducible.

Although well characterized and documented within the literature, C2C12 myotube cultures have a tendency to undergo apoptosis after late stage differentiation has occurred.<sup>227, 228</sup> Only a few studies have been able to maintain the myotubes for up to 10 days in culture, but the rate of differentiation was significantly slower, taking up to 8 days, rather than the 5 days reported herein.<sup>224</sup> In this study we also optimized the standard protocol allowing for cultures that can be maintained *in vitro* long-term. This is of significant value, allowing many experiments to be run in parallel with one another, whilst acting as a negative control to anything added. However, structures of a vacuole-like appearance were observed in a number myotubes, although not many. Despite this, cells remained viable and no apoptosis occurred. Further investigation into this could be of value. It may be that they are not vacuoles, but in fact membrane blebbing, which has been reported previously in some models involving C2C12 myotubes.<sup>224</sup> One study in particular that documented the membrane blebbing hypothesized the blebbing was indicative of primordial cell contraction.<sup>224</sup> Also observed in some cultures of mature



C2C12 myotubes were structures that are of a significantly wider diameter than the other cells. These giant cells, again, remain viable in culture the same as the other cells, and may only be a product of earlier differentiating cells, or myotubes better able to store nutrients. This phenomenon has also been reported in another study, but elucidation of the cause is yet to occur.<sup>224</sup>

#### **4.2.1 ROCK inhibition enhances C2C12 differentiation**

As previously mentioned, Rho A signalling activity is pivotal to the actin dynamics of many cells. Unsurprisingly, Rho ATPases including Rho A, RAC1 and Cdc42 have been hypothesised to be implicated in myoblast migration, progression of the cell cycle, as well as expression of regulatory factors.<sup>101</sup> Another study has also shown that inactivation of ROCK, a downstream effector protein in Rho signaling, is crucial for myoblast fusion during the differentiation process.<sup>100</sup> Rho activity can be found to be increased in proliferating cells, and forced expression in cells can result in a disruption of cellular fusion.<sup>100</sup> Further elucidation of the mechanisms underpinning this reveal Rho A-GTPase is implicated in M-Cadherin activity, a protein involved in myoblast fusion.<sup>103</sup> More specifically, Rho A mediates ubiquitination and degradation of M-cadherin.<sup>103</sup> Therefore, by introducing an inhibitor of ROCK into culture, C2C12 differentiation can be enhanced. Results obtained herein supply more evidence to ROCK as an inhibitory molecule in myoblast fusion and the differentiation pathway as ROCK inhibitor, Y-27632, increases the rate of differentiation. By introducing 10  $\mu$ M Y-27632 into culture, inhibition of M-Cadherin may be blocked, allowing the actin cytoskeleton to elongate. However, a more in depth analysis of actin dynamics would need to be carried out, particularly into FKHR in the nucleus, a direct substrate of ROCK.

A similar effect was noted in myosin heavy chain expression, which significantly increased in cultures treated with the ROCK inhibitor. This also indicates that myotubes mature earlier in the differentiation process, compared to the untreated cultures, proving Rho A/ROCK involvement in C2C12 differentiation. Although previous *in vitro*

C2C12 models have provided evidence for, and quantified increased differentiation through ROCK inhibition, none to our knowledge have quantified the effects on MHC expression levels and myotube maturation.

### 4.3 Modelling the Neuromuscular Junction *in vitro*

Several current *in vitro* models of neuromuscular junctions currently exist, each with their own advantages and disadvantages. Among the limitations found within these models are: biological differences to a human system; intricate and tricky culture conditions; and underdeveloped synaptic structures.

In this study, we investigated the potential of the previously discussed stem cell derived neurons form functional synapses with C2C12 myotubes, and their potential to induce contractile events. The TERA2.cl.SP12 stem cell lineage exhibits high potency for producing neural derivatives in the presence of either natural retinoid or synthetic retinoid compounds. These neural cells have previously been used in co-cultures, and are proven in their ability to form interactions.<sup>204, 206</sup> Previous investigation using these two cell types resulted in an *in vitro* co-culture model of neuromuscular junction formation, with functional and anatomical evidence showing the presence of a neuromuscular synapse between the two cell types.<sup>206</sup> In this previous work, neurons were seeded as a monolayer on top of developing C2C12 myotubes<sup>206</sup>. This approach was repeated in the initial stages of the current investigation, and this was when limitations within the co-culture system were observed. For example, as with any type of neural monolayer co-culture model, neurite-myotube interactions can be difficult to locate, and thus examine. Neurons produced by this technique also vary in length, which may also be indicative of different maturity levels, resulting in co-cultures that lack efficient and accurate quantification. This proves impractical to neurite growth analysis, studying the formation of the neuromuscular junction, and subsequent pharmacological manipulation. We also altered the protocol to culture neurons with mature myotubes rather than myoblasts.

In this study, we identified neural terminal bouton-myotube co-localisation points and upon investigation, anatomical evidence suggests the presence of neuromuscular junctions at these points of interaction.

To enhance the co-culture model to overcome some of their limitations, we developed a model utilising the ability of TERA2.cl.SP12 stem cells to form spheroid neurospheres that differentiate and undergo neurite outgrowth. Neurospheres were seeded onto fully differentiated, mature myotubes and allowed to co-culture for 10 days. During this period, we observed neurites projecting radially from the central core of neural cell mass. As anticipated, many points of co-localisation were observed between neurite growth cone/terminal bouton and myotube surface. This model system, through immunocytochemical analysis, allows for easy visualisation of different cellular structures, and as many neurites project from one central neurosphere, many neurites/connections can be analysed in a short space of time. The neurites produced in the co-culture radiate in an altered morphometric path compared to those in neurite outgrowth from neurospheres in monoculture, suggesting the system as a useful model for studying neurite guidance and docking. Neurospheres in monoculture require plating on laminin coated surfaces in order for neurite outgrowth to occur, since laminin is prominent extracellular matrix constituent pivotal to axon growth, through formation of complexing with integrin receptors that transmit signalling cues to the actin cytoskeleton, leading to neurite protrusion.<sup>237</sup> However, in the co-culture system designed here, co-culture conditions do not require being plated on a laminin coated surface as C2C12 myotubes are sufficient to support neurite and guidance. It is known that laminin constitutes the sheath overlying muscle, consisting of subunits alpha, beta and gamma. The beta-1 chain is involved in aiding neurite terminal formation, while alpha-laminin chain is involved in post-synaptic patterning. Laminin is essential for not only neurite growth but also neuromuscular junction formation, as it is involved in synaptic cleft modelling.<sup>237</sup> C2C12 cells are known to express many laminin isoforms.<sup>251</sup>

The model therefore stands as a suitable model for investigating mechanisms underpinning this.

After the 10 day co-culture period, numerous points of co-localisation can be observed between neurite terminal and the myotube surface. The positively staining neurites (TUJ1) end in a bouton-like structure, indicative of a presynaptic nerve terminal at the neuromuscular junction. The developmental biology of synapse formation observed throughout our studies matches that observed *in vivo*.

It has been revealed that during synaptogenesis, neurite terminals initially branch and make contact with a muscle fibre at several different locations.<sup>230</sup> In our model we see numerous neural branches making contact with a myotube, or myotubes. Initially, this suggested that the neuromuscular junctions formed in the co-culture system were of varying levels of maturity, or the presence of immature junctions being produced in the timeframe of the experiment. However, early in development, a plethora of motor neuron branches emanate from one axon originating at the spinal cord, resulting in muscle fibers initially being connected or innervated by numerous neurons.<sup>230</sup> Following this, all but one neurite is eliminated in a process of synapse competition and elimination.<sup>231</sup> This occurs in both the peripheral and central nervous system, both during embryogenesis and shortly after birth. It is hypothesised that this process is involved in adapting a newborn to their environment.<sup>231</sup>

This axon retraction is not asynchronous for fibres of the same muscle and occurs at different time-points during development. It can be emphasised here once again that the neurosphere design of the co-culture allows many neurites to be observed in a small area, and provides a system where numerous axons innervating a single myotube is more likely to occur, making the model valuable to investigate this process and specific molecules of interest.

In myotubes that are not in contact with neurons, nuclei exist in an approximately even distribution along the fibre. At many of the points of co-localisation between neurite terminal bouton and myotube, nuclei accumulation was clearly observed. Nuclei accumulation is characteristic at the neuromuscular junction, in which clusters of between 2 and 6 nuclei locate beneath the membrane, providing signalling cues and transcriptional profiling of proteins at the developing synapse.<sup>133, 232</sup> Our co-culture model provides further evidence that signalling cues are created by neural element inducing nuclei homing at developing NMJ, as nuclei clustering is not observed until a neural element is introduced into culture. Although apparent at many points of co-localisation, providing anatomical evidence for the presence of a neuromuscular junction, nuclei clustering was not observed at all sites of potential interaction. Literature suggests that this could be a result of the maturity of the synapse; one study in particular shows that myotubes at neuromuscular junctions devoid of fundamental nuclei clustering can still be viable and mature as nuclei may not be required for synapse maintenance once fully functional.<sup>165</sup> This may be because nuclei are involved in the initial transcriptional regulation of proteins involved in the formation of the neuromuscular junction, and once expressed, the locality of the nuclei is no longer required. For example, nuclei located proximally to developing synapse exhibit increased AChR transcription during synaptogenesis, which is then downregulated once a mature synapse is formed.<sup>163</sup>

However, much remains unclear about nuclear migration, docking, or their specialisation at the synapse. Syne-1 is a molecule of recent interest, a protein found abundantly in the nuclear envelope of myonuclei.<sup>163</sup> It would prove useful to investigate the levels of Syne-1 in nuclei in our co-culture system, and to investigate whether levels transiently increase at the point of docking, followed by a decline, causing 'undocking' of nuclei at the NMJ. Another paper outlines the idea that initially in synapse formation, resident AChRs accumulate and localise at the postsynaptic membrane prior to fundamental nuclei recruitment, postulating the idea that AChR accumulation is

involved or a pre-requisite to this process, before upregulation of AchR transcription by the nuclei once docked.<sup>225</sup> Consequently, the co-culture model could be useful to investigate the effect of neural input on myogenesis *in vitro*.

It is well documented that specialised proteins appear along the length of a muscle fibre that cluster during innervation.<sup>165</sup> In the opening stages of our investigation, we showed that C2C12 myotubes possess acetylcholine receptors, distributed somewhat randomly along the surface of mature myotubes. Upon innervation, these acetylcholine receptors migrate, and are anchored directly beneath the motor nerve terminal. Alpha-bungarotoxin staining was employed to visualise any acetylcholine receptor clustering at the points of co-localisation between neurite terminal and myotube in our co-culture staining. Positive staining indicated clustering at many of these sites, suggesting acetylcholine receptor clusters and thus post-synaptic modifications. This acetylcholine receptor clustering does not occur aneurally in humans, and occurs only upon innervation and around the same time as axon competition.<sup>234</sup> Accordingly, the model is potentially useful to study human development. A plethora of evidence is now available showing the Agrin-MUSK-raspyn receptor mediated pathways to be involved in the upregulation and synthesis of AChR's at the developing synapse; during which, agrin, which is synthesised by motor neurons, promotes anchoring of receptors.<sup>143, 144, 145</sup> As a result of this, to further elucidate and confirm neuromuscular junction formation, immunocytochemical investigation into the presence of agrin and MusK would be useful to confirm their structural presence, whilst also further consolidating the motor phenotype of the neural element.

To further confirm positive acetylcholine receptor cluster staining, a double stain of co-cultures was performed to eliminate any interference between emission spectrums between the wavelengths of the stains used. In the initial triple co-culture stain, where we used a red stain (neurites – TUJ1), a green stain (myotubes – F-actin), and a far-red stain (AChRs - alpha-bungarotoxin), there may be speculation of the red and the far red

stains overlapping. Therefore, by using a double stain consisting of a green stain for neurites and the far red for acetylcholine receptors, we eliminated any uncertainty. Although myotubes were not stained, we can confirm that the positional identity of the clusters was at the neurite terminal, on the myotube surface. We hypothesised that this was induced through neural signals as AChR clusters did not appear on uninnervated myotubes.

Anatomical evidence suggested the presence of neuromuscular junctions in our co-culture model. Subsequently, a functional assay was performed to test ability of neuromuscular junction to elicit a response in the form of contractile movement. As already mentioned, previous work has been carried out co-culturing the two cell types being used in our model, and contraction was observed in co-cultures following pharmacological manipulation.<sup>206</sup> In this previous study, contractile events were counted in co-culture after addition of agonist compounds acetylcholine (ACh), carbachol, nicotine and muscarine (Figure 5.3.11<sup>206</sup>). Antagonists including curare, and atropine were subsequently added to block contraction, providing functional evidence for neuromuscular junctions *in vitro*. From the figure, we can see that acetylcholine elicited the strongest response as more contraction was observed in acetylcholine treated cultures (B) compared to carbachol (A).<sup>206</sup> Furthermore, all agonists tested excluding acetylcholine resulted in contraction of C2C12 myotubes in the absence of neurons, whereas acetylcholine produced no contraction in monoculture. Thus, as a result of limited experimental time-frame, we chose to only examine the effect of acetylcholine on our co-culture system.

We supplemented the media of mature myotubes in monoculture with a range of acetylcholine concentrations to see if any contraction could be observed aneurally. No spontaneous contraction was observed before addition of the AChR agonist, nor did we observe any after addition at any of the concentrations. This may indicate that although acetylcholine receptors are present before neural stimulation distributed p along C2C12

myotubes, they are not present or organised in large enough quantities to elicit a contractile response.

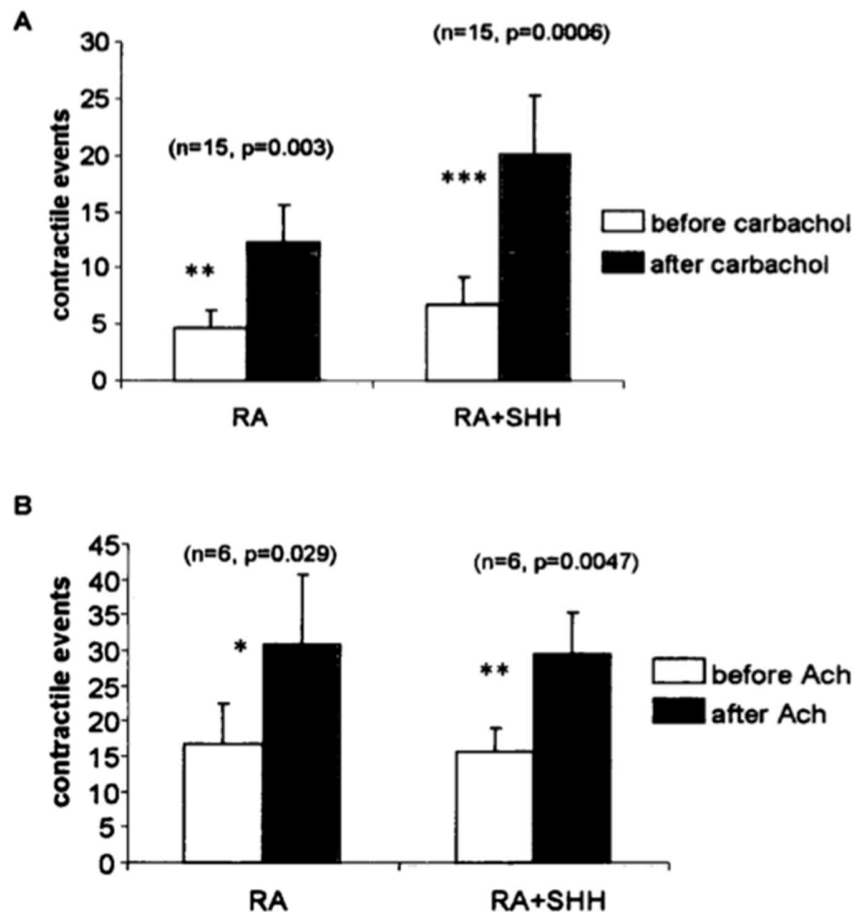


Figure 5.3.11 Quantification of contractile events stimulated by AChR antagonists ACh and carbachol. The induced RA and RA+Shh neuronal aggregates were co-cultured with myoblasts respectively in 12 well plate for 5 days before counting the contractile events. Note that there is significance (\*\*,  $p < 0.005$ ; \*\*\*,  $p < 0.001$ ) between RA and RA+Shh induced contractile events before and after carbachol (A) and also significance (\*,  $p < 0.05$ ; \*\*,  $p < 0.005$ ) before and after ACh (B). Error bars are shown as SEM. n, number of repeats.

Taken From Pan, C., 2007.

Initial evidence of contraction was observed in culture after addition of 10  $\mu$ M acetylcholine. No antagonists were added however following stimulation with acetylcholine. An alternative method of antagonising a neuromuscular junction is to block the function of acetylcholinesterase, the molecule found in the neuromuscular



junction synaptic cleft, responsible for the hydrolysis of acetylcholine to acetate and choline. Without functioning acetylcholinesterase, acetylcholine itself has been proven to be an effective blockade for contraction.<sup>40,41,235</sup> To conclude, additional investigation using pharmacological manipulation for functional assessment of our co-culture system would be beneficial to provide conclusive data. Furthermore preliminary evidence of myotube contraction using acetylcholine suggests the presence of functional neuromuscular junctions appears a result of neural stimulation rather than a myotube response, as no contraction was observed in myotube monocultures under the same conditions.

After in depth morphological and functional characterisation of the co-culture model, the model was further enhanced through introduction of selective ROCK inhibitor, Y-27632 into the culture media. Data throughout this investigation has showed the potential of Y-27632 to enhance differentiation of cell types dependent upon actin remodelling. Firstly, we applied ROCK-inhibitor Y-27632 to our neurosphere model to enhance neurite outgrowth, as ROCK, the downstream effector protein of Rho A has been shown to be involved in neurite inhibition. By inhibiting ROCK, activation of Rho GTPases Rac and Cdc42 within the neurite occurs, resulting in membrane instability at the leading edge of the neurite, allowing for membrane protrusion and extension. Following on from this, we investigated the effect of the ROCK inhibitor on the C2C12 cell line, using the same concentration of Y-27632 that we used to investigate its effect on neurite outgrowth. Our results matched, if not improved on the literature, where Rac and Cdc42 are postulated to be essential for myoblast fusion during myogenesis, meanwhile Rho A is downregulated at the onset of differentiation.<sup>109,237</sup> As a result of the aforementioned results and literature, we aimed to enhance differentiation of both cell types within our co-culture system to improve efficiency and resulting model, with the aim of increasing junctional complexes formed per model.

The data acquired from co-culture models whereby ROCK was inhibited are extremely promising, with significantly enhanced neurite outgrowth occurring. This enhanced neurite outgrowth increases the potential for an increased quantity neuromuscular junctions to form per model, since neurite density is increased. Not only this, but our enhanced co-culture model provides an exciting, unique opportunity to study the effect of ROCK inhibition on the neuromuscular junctions formed *in vitro*. Several co-culture studies using C2C12 myotubes as the skeletal muscle component for modelling the neuromuscular junction have reported immature, thin myotubes.<sup>238</sup> By inhibiting ROCK in the co-culture model presented here, this limitation can be overcome, as myotube differentiation is enhanced, and mature myotubes are obtained.

Recent scientific advancements have identified the Rho family of small guanosine triphosphatases, specifically Rac and Cdc42 as molecules involved in Agrin-induced acetylcholine receptor clustering. (49) Musk, the postsynaptic receptor tyrosine kinase for Agrin, also requires the activity of Rac and Cdc42 following Agrin activation. (48) MUSK is essential not only in the developmental biology of a neuromuscular junction, but also for their maintenance. Cdc12 has also been subject of attention following identification of its involvement in nuclear migration in myotubes, a characteristic anatomical response elicited in response to neural stimulation. Therefore, it cannot be emphasised how invaluable ROCK inhibition may prove to the future of *in vitro* models of neuromuscular junction formation, as inhibition of ROCK favours activation of Rac and Cdc42, molecules whose importance is only beginning to be elucidated in the formation and maintenance of these synapses, meanwhile aiding differentiation of both the neural and skeletal muscle components of the model.

This enhanced co-culture model, with enhanced neurite outgrowth in co-culture could provide a model better suited for high-throughput pharmacological screening or quantification. It also provides a proven platform for assessing signalling pathways, and is amenable to alterations, proven here by altered Rho signalling. All anatomical

characteristics of neuromuscular junctions previously investigated in the model were also identified in the enhanced co-culture model, including terminal presynaptic bouton formation, acetylcholine receptor clustering on the post-synaptic membrane, and nuclei accumulation at the peripheral myotube membrane, proximal to the synapse.

The model could also prove useful for studying pathology at the junction. Many pathological conditions involve the neuromuscular junction, including autoimmune as well as toxin-mediated conditions, including myasthenia gravis and botulism, respectively. However, we will focus particularly on Amyotrophic lateral sclerosis (ALS) and spinal muscular atrophy (SMA) and their relevance to the *in vitro* model we have developed. Spinal muscular atrophy, the most common genetic cause of infant death, occurs as a result of mutations in the Survival Motor Neuron 1 (*SMN1*) gene. Within the past few years, emerging evidence has shown that an upregulation of Rho A and ROCK and their involvement in cytoskeletal regulation as key contributors to the pathology of this disease.<sup>239</sup> As a result, recent pharmaceutical research included ROCK inhibitors including Y-27632.<sup>239</sup> Motor neurons are the primary tissue affected but due to the nature of motor neurons and their connection to skeletal muscle at the neuromuscular junction, thus the implication of an altered Rho A and ROCK cascade is more than likely to be more significant than currently understood; the evidence gathered in this research shows that ROCK inhibition has significant impacts on cell types undergoing differentiation or actin remodelling, and therefore will prove a very useful model for studying not just diseases of the neuromuscular junction, but motor neuron diseases in addition.<sup>239</sup>

Moreover, ROCK inhibitor Y-27632 has showed promising results in animal amyotrophic lateral sclerosis models, improving motor function.<sup>240</sup> ALS is characterised by muscle weakness emanating from motor neuron degeneration. As a result, the co-culture model described herein could provide more ethical, fully controllable conditions for pharmaceutical development and study of pathology. Furthermore, the embryonal

carcinoma cell line used here has previously been used to investigate neurite inhibition in neurodegenerative disease, including Parkinsons.<sup>28, 204</sup>

## 4.4 Conclusions

Before developing a co-culture system allowing for formation of neuromuscular junctions, we first developed and enhanced differentiation of the two cell types to be used. First, we differentiated C2C12 myoblasts into myotubes, a commonly used cell line in this kind of investigation. The C2C12 cell line can be readily differentiated easily, through low serum conditions, providing efficient and easy means of obtaining mature myotubes that express contractile apparatus, proven to be capable of contraction.<sup>241</sup> The myotubes differentiated as expected, lacking spontaneous contraction whilst possessing contractile apparatus, and expressed acetylcholine receptors distributed diffusely rather than in clusters. Meanwhile, nuclei are evenly distributed in the un-innervated myotube. We then enhanced differentiation by altering signalling mechanisms within the cell through introduction of a ROCK-inhibitor. All results obtained suggested the cell line as a good model system that will allow functional analysis of any neuromuscular junctions obtained.

Neurons were obtained from a neurosphere model from which neurites radiate outwards in culture.<sup>298</sup> The neurons from the TERA2.cl.SP12 cell line have been proven to be electrophysiological active, and capable of forming synapses with muscle in co-culture.<sup>235, 206</sup> The embryonal carcinoma cell line provides an advantageous method of obtaining neurites compared to embryonic stem cells, as easier differentiation protocols, no requirement for feeder layers/extensive, complex culture systems, and can readily be directed down a neural lineage. Neurite outgrowth can be enhanced through ROCK inhibition, which favours actin remodelling at the protruding edge of the neurite.

Following this, we developed a novel, unique, co-culture system by amalgamating both methods of differentiation into a co-culture system involving seeding the neurospheres onto mature myotubes. Anatomical characterisation of our co-culture model showed the presence of presynaptic and post-synaptic structures conducive to a functional cholinergic synapse. Preliminary functional evidence was obtained suggesting fully functional cholinergic synapse formation. Furthering on from this, the model was then enhanced by exploiting Rho A/ROCK signalling, which was proven to enhance differentiation of both cell types in monoculture. Enhanced neurite outgrowth was obtained, and it can be postulated that more neuromuscular junctions are formed per model as a result, also further work is required to investigate this hypothesis. To our knowledge, this stands as the first co-culture system that has an added element of Rho signalling manipulation, one that benefits all cell types in the co-culture. We also believe we present the first findings of nuclei clustering at the synapse in a co-culture involving the C2C12 cell line, and through simple modification of existing protocol, supply a co-culture method allowing myotubes to be maintained in culture for extended periods of time, this longevity is advantageous for pharmacological studies.

Although a heterogeneous co-culture system, results can be extrapolated to the human neuromuscular junction, although inaccuracy in biological differences will exist. The validity of any model to recapitulate *in vivo* conditions largely lies in the cell types used. Many homogenous co-culture systems are hindered by their requirement of primary human tissue, and thus large scale production of these systems is unethical, costly and unrealistic. Instead, we provide an advanced, robust and reproducible co-culture model using reliable cell lines that eliminates sample variation whilst reducing animal use, as well as providing a unique and exciting opportunity to investigate mechanisms underpinning the development, biology and pathology of the neuromuscular junction. The model provides a platform for easy identification of structures present, with potentially high-throughput neuromuscular junction formation that may provide useful

for pharmacological testing and quantification, whilst being responsive to signalling alterations.

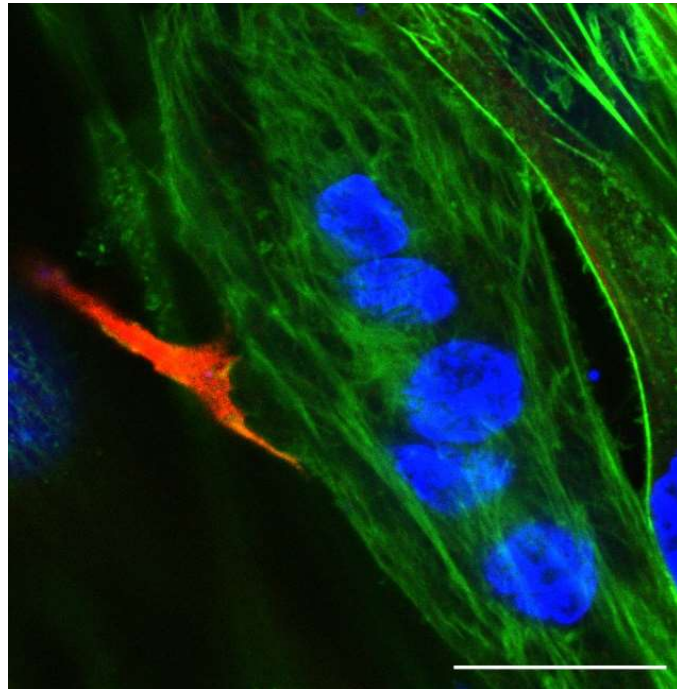


**Figure 4.4: Terminal neuron bouton contacting myotube surface where nuclei accumulation is evident.** The neuron (red,) immunofluorescently labelled with TUJ-1, appears to contact the myotube (green) at a point where nuclei (blue) accumulation has occurred. The myotube surface appears slightly raised at the point of contact. Myotube stained with phalloidin and nuclei counterstained with hoechst. Scale bar = 15  $\mu\text{m}$

## 4.5 Future Directions

The data outlined in this thesis provides a foundation for formation and study of *in vitro* neuromuscular junctions. Whilst conclusions can be made from the data, but additional investigation is required to provide unequivocal evidence, and to further build on the work presented herein. Due to the time constraints of the current project, additional further work has been suggested.

To begin with, the phenotype of the type of neurons produced was unconfirmed in our neurosphere neurite outgrowth and our co-culture model. Although we provide evidence for neuromuscular junction formation between neurites and skeletal muscle, this does not necessarily suggest the presence of motor neurons, and we cannot assume

the motor phenotypic purity of each culture. To identify motor neurons in both monoculture and co-culture, motor neuron specific markers including Lim3, Isl-3, HB-9 and ChAT should be investigated.<sup>234</sup> Nevertheless, previous work involving the stem cell line used to produce neurons throughout our studies has previously been shown to be capable of producing motor neurons.<sup>206</sup> It is well documented that Sonic hedgehog (Shh) is involved in dorso-ventral patterning of the vertebrate nervous system during embryogenesis. Here, Shh influences the fate of developing neurons, directing differential fate towards a motor phenotype.<sup>9, 10, 244</sup> This, along with many other studies which have included Shh in their differentiation media, suggests that further work should to include Shh in neurosphere differentiation protocol.<sup>206, 245, 246</sup> Previous work involving the two cell types used in co-culture have previously been differentiated using a protocol involving the use of Shh, and results showed increased contraction observed in co-cultures.<sup>206</sup> It can be hypothesised that this will increase motor neuron phenotype, and thus neuromuscular junctions formed per model in co-culture, which could easily be quantified.

To provide further evidence for neuromuscular junction presence in our *in vitro* co-culture model, additional synapse specific structures could be examined. These could include SNARE proteins, including synaptotagmins, or Agrin, Musk, or rapsyn – proteins essential in neuromuscular junction formation, specifically acetylcholine receptor clustering.<sup>123</sup> Acetylcholinesterase, the enzyme involved in acetylcholine breakdown within the synaptic cleft, is also another protein that would act as a strong indicator of neuromuscular junction formation. Other methods of microscopy could be employed to examine the anatomical structure at the neuromuscular junctions formed within our system. TEM for example, can be used to observe the ultrastructure at the neurite terminal bouton and skeletal muscle, allowing further evidence for presynaptic and postsynaptic structures to be obtained. Specifically, we would expect to observe nuclei clustering and abundant golgi-apparatus residing close to the synapse in both cell types. Golgi apparatus complexes are known to be located abundantly around especially

fundamental nuclei of the myotube, where they are involved in acetylcholine receptor synthesis and insertion into the post-synaptic active sites.<sup>247</sup> Pharmacological manipulation of co-cultures only provided preliminary evidence of functional cholinergic synapses, thus further work using additional agonists as well as antagonists would prove to be useful.

To further our characterisation of the effect of ROCK inhibition on neuromuscular junction formation *in vitro*, junctional complexes formed per model should be quantified and compared between untreated and ROCK inhibitor treated co-cultures as a method of evaluating the potential of ROCK inhibition on enhancing neuromuscular junction formation. Unfortunately, due to the time-dependent circumstances, we were unable to investigate if neuromuscular junctions were formed earlier in co-culture as a result of ROCK inhibition, something which could be easily elucidated and quantified through time-lapse studies. As well as this, as ROCK inhibition is sufficient to enhance actin remodelling, our co-culture system could be used to investigate the involvement of Rho GTPases in acetylcholine receptor clustering at the neuromuscular junction, as well as the migration of other synapse specific proteins.



## 5.0 References

1. Sadler, T.W., 2005, May. Embryology of neural tube development. *American Journal of Medical Genetics Part C: Seminars in Medical Genetics* (Vol. 135, No. 1, pp. 2-8). Hoboken: Wiley Subscription Services, Inc., A Wiley Company.
2. Ybot-Gonzalez, P., Gaston-Massuet, C., Girdler, G., Klingensmith, J., Arkell, R., Greene, N.D. and Copp, A.J., 2007. Neural plate morphogenesis during mouse neurulation is regulated by antagonism of Bmp signalling. *Development*, 134(17), pp.3203-3211.
3. Endo, Y., Osumi, N. and Wakamatsu, Y., 2002. Bimodal functions of Notch-mediated signaling are involved in neural crest formation during avian ectoderm development. *Development*, 129(4), pp.863-873.
4. Ding, J., Yang, L., Yan, Y.T., Chen, A., Desai, N., Wynshaw-Boris, A. and Shen, M.M., 1998. Cripto is required for correct orientation of the anterior–posterior axis in the mouse embryo. *Nature*, 395(6703), p.702.
5. Ding, J., Yang, L., Yan, Y.T., Chen, A., Desai, N., Wynshaw-Boris, A. and Shen, M.M., 1998. Cripto is required for correct orientation of the anterior–posterior axis in the mouse embryo. *Nature*, 395(6703), p.702.
6. Gowan, K., Helms, A. W., Hunsaker, T. L., Collisson, T., Ebert, P. J., Odom, R. and Johnson, J. E.(2001). Crossinhibitory activities of Ngn1 and Math1 allow specification of distinct dorsal interneurons. *Neuron* 31, 219-232.
7. Liem Jr, K.F., Tremml, G., Roelink, H. and Jessell, T.M., 1995. Dorsal differentiation of neural plate cells induced by BMP-mediated signals from epidermal ectoderm. *Cell*, 82(6), pp.969-979.
8. Bergsland, M., Ramsköld, D., Zaouter, C., Klum, S., Sandberg, R. and Muhr, J., 2011. Sequentially acting Sox transcription factors in neural lineage development. *Genes & Development*, 25(23), pp.2453-2464.
9. Zhu, G., Mehler, M.F., Zhao, J., Yung, S.Y. and Kessler, J.A., 1999. Sonic hedgehog and BMP2 exert opposing actions on proliferation and differentiation of embryonic neural progenitor cells. *Developmental Biology*, 215(1), pp.118-129.
10. Briscoe, J., Chen, Y., Jessell, T.M. and Struhl, G., 2001. A hedgehog-insensitive form of patched provides evidence for direct long-range morphogen activity of sonic hedgehog in the neural tube. *Molecular Cell*, 7(6), pp.1279-1291.
11. Wilson, P.A. and Hemmati-Brivanlou, A., 1995. Induction of epidermis and inhibition of neural fate by Bmp-4. *Nature*, 376(6538), p.331.
12. Roelink, H., Porter, J.A., Chiang, C., Tanabe, Y., Chang, D.T., Beachy, P.A. and Jessell, T.M., 1995. Floor plate and motor neuron induction by different concentrations of the amino-terminal cleavage product of sonic hedgehog autoproteolysis. *Cell*, 81(3), pp.445-455.
13. Ho, K.S. and Scott, M.P., 2002. Sonic hedgehog in the nervous system: functions, modifications and mechanisms. *Current Opinion in Neurobiology*, 12(1), pp.57-63.

14. Patten, I. and Placzek, M., 2000. The role of Sonic hedgehog in neural tube patterning. *Cellular and Molecular Life Sciences CMLS*, 57(12), pp.1695-1708.
15. Sun, T., Dong, H., Wu, L., Kane, M., Rowitch, D.H. and Stiles, C.D., 2003. Cross-repressive interaction of the Olig2 and Nkx2. 2 transcription factors in developing neural tube associated with formation of a specific physical complex. *Journal of Neuroscience*, 23(29), pp.9547-9556.
16. Wilson, L., Gale, E., Chambers, D. and Maden, M., 2004. Retinoic acid and the control of dorsoventral patterning in the avian spinal cord. *Developmental Biology*, 269(2), pp.433-446.
17. Zirra, A., Wiethoff, S. and Patani, R., 2016. Neural conversion and patterning of human pluripotent stem cells: a developmental perspective. *Stem Cells International*, 2016.
18. Wilson, L. and Maden, M., 2005. The mechanisms of dorsoventral patterning in the vertebrate neural tube. *Developmental Biology*, 282(1), pp.1-13.
19. Maden, M., 2007. Retinoic acid in the development, regeneration and maintenance of the nervous system. *Nature Reviews Neuroscience*, 8(10), pp.755-765.
20. Bouillet, P., Sapin, V., Chazaud, C., Messaddeq, N., Décimo, D., Dollé, P. and Chambon, P., 1997. Developmental expression pattern of Stra6, a retinoic acid-responsive gene encoding a new type of membrane protein. *Mechanisms of Development*, 63(2), pp.173-186.
21. Mark, M., Ghyselinck, N.B. and Chambon, P., 2009. Function of retinoic acid receptors during embryonic development. *Nuclear Receptor Signaling*, 7(1), pp.nrs-07002.
22. Pennimpede, T., Cameron, D.A., MacLean, G.A., Li, H., Abu-Abed, S. and Petkovich, M., 2010. The role of CYP26 enzymes in defining appropriate retinoic acid exposure during embryogenesis. *Birth Defects Research Part A: Clinical and Molecular Teratology*, 88(10), pp.883-894.
23. Concalves, K., 2017. *Development of Novel Stem Cell Based Neurite Outgrowth Models and their Application to Study Neurite Inhibition in Neurological Disorders* (Doctoral dissertation, Durham University).
24. Melton, K. R., Iulianella, A. & Trainor, P. A. Gene expression and regulation of hindbrain and spinal cord development. *Front. Biosci.* 9, 117–138 (2004)
25. Zhuang, B. and Sockanathan, S., 2006. Dorsal–ventral patterning: a view from the top. *Current Opinion in Neurobiology*, 16(1), pp.20-24.
26. Jones-Villeneuve EM, McBurney MW, Rogers KA, Kalnins VI (1982) Retinoic acid induces embryonal carcinoma cells to differentiate into neurons and glial cells. *J Cell Biol* 94(2):253–262
27. Atencia, R., García-Sanz, M., Unda, F. and Arechaga, J., 1994. Apoptosis during retinoic acid-induced differentiation of F9 embryonal carcinoma cells. *Experimental Cell Research*, 214(2), pp.663-667.
28. Clarke, K.E., Tams, D.M., Henderson, A.P., Roger, M.F., Whiting, A. and Przyborski, S.A., 2017. A robust and reproducible human pluripotent stem cell derived model of neurite outgrowth in a three-dimensional culture system and its application to study neurite inhibition. *Neurochemistry International*, 106, pp.74-84.

29. Kiryushko, D., Berezin, V. and Bock, E., 2004. Regulators of neurite outgrowth: role of cell adhesion molecules. *Annals of the New York Academy of Sciences*, 1014(1), pp.140-154.
30. Gertz, C.C., Leach, M.K., Birrell, L.K., Martin, D.C., Feldman, E.L. and Corey, J.M., 2010. Accelerated Neuritogenesis and maturation of primary spinal motor neurons in response to nanofibers. *Developmental Neurobiology*, 70(8), pp.589-603.
31. Kiryushko, D., Berezin, V. and Bock, E., 2004. Regulators of neurite outgrowth: role of cell adhesion molecules. *Annals of the New York Academy of Sciences*, 1014(1), pp.140-154.
32. Bard, L., Boscher, C., Lambert, M., Mège, R.M., Choquet, D. and Thoumine, O., 2008. A molecular clutch between the actin flow and N-cadherin adhesions drives growth cone migration. *Journal of Neuroscience*, 28(23), pp.5879-5890.
33. Brümmendorf, T. and Rathjen, F.G., 1994. Cell adhesion molecules. 1: immunoglobulin superfamily. *Protein Profile*, 1(9), pp.951-1058.
34. Williams, E.J., Furness, J., Walsh, F.S. and Doherty, P., 1994. Activation of the FGF receptor underlies neurite outgrowth stimulated by L1, N-CAM, and N-cadherin. *Neuron*, 13(3), pp.583-594.
35. Da Silva, J.S. and Dotti, C.G., 2002. Breaking the neuronal sphere: regulation of the actin cytoskeleton in neuritogenesis. *Nature Reviews Neuroscience*, 3(9), p.694.
36. Sainath, R. and Gallo, G., 2015. Cytoskeletal and signaling mechanisms of neurite formation. *Cell and Tissue Research*, 359(1), pp.267-278.
37. Schlau, M., Terheyden-Keighley, D., Theis, V., Mannherz, H. and Theiss, C., 2018. VEGF triggers the activation of Cofilin and the Arp2/3 complex within the growth cone. *International Journal of Molecular Sciences*, 19(2), p.384.
38. Tögel, M., Wiche, G. and Propst, F., 1998. Novel features of the light chain of microtubule-associated protein MAP1B: microtubule stabilization, self interaction, actin filament binding, and regulation by the heavy chain. *The Journal of Cell Biology*, 143(3), pp.695-707.
39. Kozma, R., Sarner, S., Ahmed, S. and Lim, L., 1997. Rho family GTPases and neuronal growth cone remodelling: relationship between increased complexity induced by Cdc42Hs, Rac1, and acetylcholine and collapse induced by RhoA and lysophosphatidic acid. *Molecular and Cellular Biology*, 17(3), pp.1201-1211.
40. Hall, A. and Lalli, G., 2010. Rho and Ras GTPases in axon growth, guidance, and branching. *Cold Spring Harbor Perspectives in Biology*, 2(2), p.a001818.
41. Da Silva, J.S., Medina, M., Zuliani, C., Di Nardo, A., Witke, W. and Dotti, C.G., 2003. RhoA/ROCK regulation of neuritogenesis via profilin Ila-mediated control of actin stability. *The Journal of Cell Biology*, 162(7), pp.1267-1279.
42. Da Silva, J.S., Medina, M., Zuliani, C., Di Nardo, A., Witke, W. and Dotti, C.G., 2003. RhoA/ROCK regulation of neuritogenesis via profilin Ila-mediated control of actin stability. *The Journal of Cell Biology*, 162(7), pp.1267-1279.
43. Kozma, R., Sarner, S., Ahmed, S. and Lim, L., 1997. Rho family GTPases and neuronal growth cone remodelling: relationship between increased complexity induced by Cdc42Hs, Rac1, and

- acetylcholine and collapse induced by RhoA and lysophosphatidic acid. *Molecular Cell Biology* 17:1201–1211
44. Yu, Gutekunst, Gross, & Wei. Inhibition of the Rho signaling pathway improves neurite outgrowth and neuronal differentiation of mouse neural stem cells. *Int J Physiol Pathophysiol Pharmacol.* 2013 Mar 8;11–20. □
  45. Letourneau, P.C., Condic, M.L. and Snow, D.M., 1992. Extracellular matrix and neurite outgrowth. *Current Opinion in Genetics & Development*, 2(4), pp.625-634.
  46. Edgar, D., Timpl, R. and Thoenen, H., 1984. The heparin-binding domain of laminin is responsible for its effects on neurite outgrowth and neuronal survival. *The EMBO Journal*, 3(7), pp.1463-1468.
  47. Durbeej, M., 2010. Laminins. *Cell and Tissue Research*, 339(1), p.259.
  48. Nishiuchi, R., Takagi, J., Hayashi, M., Ido, H., Yagi, Y., Sanzen, N., Tsuji, T., Yamada, M. and Sekiguchi, K., 2006. Ligand-binding specificities of laminin-binding integrins: a comprehensive survey of laminin–integrin interactions using recombinant  $\alpha 3\beta 1$ ,  $\alpha 6\beta 1$ ,  $\alpha 7\beta 1$  and  $\alpha 6\beta 4$  integrins. *Matrix Biology*, 25(3), pp.189-197.
  49. Wehrle, B. and Chiquet, M., 1990. Tenascin is accumulated along developing peripheral nerves and allows neurite outgrowth in vitro. *Development*, 110(2), pp.401-415.
  50. Magli, A., Schnettler, E., Rinaldi, F., Bremer, P. and Perlingeiro, R.C., 2013. Functional dissection of Pax3 in paraxial mesoderm development and myogenesis. *Stem Cells*, 31(1), pp.59-70.
  51. Beddington, R.S. and Robertson, E.J., 1999. Axis development and early asymmetry in mammals. *Cell*, 96(2), pp.195-209.
  52. Blake, J.A. and Ziman, M.R., 2014. Pax genes: regulators of lineage specification and progenitor cell maintenance. *Development*, 141(4), pp.737-751.
  53. Pourquié, O., Fan, C.M., Coltey, M., Hirsinger, E., Watanabe, Y., Bréant, C., Francis-West, P., Brickell, P., Tessier-Lavigne, M. and Le Douarin, N.M., 1996. Lateral and axial signals involved in avian somite patterning: a role for BMP4. *Cell*, 84(3), pp.461-471.
  54. James, R.G. and Schultheiss, T.M., 2005. Bmp signaling promotes intermediate mesoderm gene expression in a dose-dependent, cell-autonomous and translation-dependent manner. *Developmental Biology*, 288(1), pp.113-125.
  55. Wilm, B., James, R.G., Schultheiss, T.M. and Hogan, B.L., 2004. The forkhead genes, Foxc1 and Foxc2, regulate paraxial versus intermediate mesoderm cell fate. *Developmental Biology*, 271(1), pp.176-189.
  56. Tonegawa, A. and Takahashi, Y., 1998. Somitogenesis controlled by Noggin. *Developmental Biology*, 202(2), pp.172-182.
  57. Aulehla, A. and Pourquié, O., 2010. Signaling gradients during paraxial mesoderm development. *Cold Spring Harbor Perspectives in Biology*, 2(2), p.a000869.
  58. Stuart, E.T., Kioussi, C. and Gruss, P., 1994. Mammalian PAX genes. *Annual Review of Genetics*, 28(1), pp.219-238.

59. Eng, D., Ma, H.Y., Gross, M.K. and Kioussi, C., 2013. Gene networks during skeletal myogenesis. *ISRN Developmental Biology*, 2013.
60. Magli, A., Schnettler, E., Rinaldi, F., Bremer, P. and Perlingeiro, R.C., 2013. Functional dissection of Pax3 in paraxial mesoderm development and myogenesis. *Stem Cells*, 31(1), pp.59-70.
61. Buckingham, M., 1992. Making muscle in mammals. *Trends in Genetics*, 8(4), pp.144-149.
62. Buckingham, M., Bajard, L., Chang, T., Daubas, P., Hadchouel, J., Meilhac, S., Montarras, D., Rocancourt, D. and Relaix, F., 2003. The formation of skeletal muscle: from somite to limb. *Journal of Anatomy*, 202(1), pp.59-68.
63. Eng, D., Ma, H.Y., Gross, M.K. and Kioussi, C., 2013. Gene networks during skeletal myogenesis. *ISRN Developmental Biology*, 2013.
64. Meyer, D. and Birchmeier, C., 1994. Distinct isoforms of neuregulin are expressed in mesenchymal and neuronal cells during mouse development. *Proceedings of the National Academy of Sciences*, 91(3), pp.1064-1068.
65. Hernández-Hernández, J.M., García-González, E.G., Brun, C.E. and Rudnicki, M.A., 2017, December. The myogenic regulatory factors, determinants of muscle development, cell identity and regeneration. *Seminars in Cell & Developmental Biology* (Vol. 72, pp. 10-18). Academic Press.
66. Black, B.L. and Olson, E.N., 1998. Transcriptional control of muscle development by myocyte enhancer factor-2 (MEF2) proteins. *Annual Review of Cell and Developmental Biology*, 14(1), pp.167-196.
67. Davis, R.L., Weintraub, H. and Lassar, A.B., 1987. Expression of a single transfected cDNA converts fibroblasts to myoblasts. *Cell*, 51(6), pp.987-1000.
68. Bentzinger, C.F., Wang, Y.X. and Rudnicki, M.A., 2012. Building muscle: molecular regulation of myogenesis. *Cold Spring Harbor Perspectives in Biology*, 4(2), p.a008342.
69. Shen, X., Collier, J.M., Hlaing, M., Zhang, L., Delshad, E.H., Bristow, J. and Bernstein, H.S., 2003. Genome-wide examination of myoblast cell cycle withdrawal during differentiation. *Developmental Dynamics: an Official Publication of the American Association of Anatomists*, 226(1), pp.128-138.
70. Chamberlain, J.S., Jaynes, J.B. and Hauschka, S.D., 1985. Regulation of creatine kinase induction in differentiating mouse myoblasts. *Molecular and Cellular Biology*, 5(3), pp.484-492.
71. Molkentin, J.D., Li, L. and Olson, E.N., 1996. Phosphorylation of the MADS-Box transcription factor MEF2C enhances its DNA binding activity. *Journal of Biological Chemistry*, 271(29), pp.17199-17204.
72. Molkentin, J.D., Black, B.L., Martin, J.F. and Olson, E.N., 1995. Cooperative activation of muscle gene expression by MEF2 and myogenic bHLH proteins. *Cell*, 83(7), pp.1125-1136.
73. Naidu, P.S., Ludolph, D.C., To, R.Q., Hinterberger, T.J. and Konieczny, S.F., 1995. Myogenin and MEF2 function synergistically to activate the MRF4 promoter during myogenesis. *Molecular and Cellular Biology*, 15(5), pp.2707-2718.

74. Dodou, E., Xu, S.M. and Black, B.L., 2003. mef2c is activated directly by myogenic basic helix-loop-helix proteins during skeletal muscle development in vivo. *Mechanisms of Development*, 120(9), pp.1021-1032.
75. Goldman, R.D., Milsted, A., Schloss, J.A., Starger, J. and Yerna, M.J., 1979. Cytoplasmic fibers in mammalian cells: cytoskeletal and contractile elements. *Annual Review of Physiology*, 41(1), pp.703-722.
76. Wells, L., Edwards, K.A. and Bernstein, S.I., 1996. Myosin heavy chain isoforms regulate muscle function but not myofibril assembly. *The EMBO Journal*, 15(17), pp.4454-4459.
77. Brown, D.M., Parr, T. and Brameld, J.M., 2012. Myosin heavy chain mRNA isoforms are expressed in two distinct cohorts during C2C12 myogenesis. *Journal of Muscle Research and Cell Motility*, 32(6), pp.383-390.
78. John, H.A., Patrino-Georgoulas, M. and Jones, K.W., 1977. Detection of myosin heavy chain mRNA during myogenesis in tissue culture by in vitro and in situ hybridization. *Cell*, 12(2), pp.501-508.
79. Bandman, E., Bourke, D.L. and Wick, M., 1990. Regulation of myosin heavy chain expression during development, maturation, and regeneration in avian muscles: The role of myogenic and non-myogenic factors. *The Dynamic State of Muscle Fibers. Berlin: Walter de Gruyter*, pp.127-138.
80. Bader, D., Masaki, T. and Fischman, D.A., 1982. Immunochemical analysis of myosin heavy chain during avian myogenesis in vivo and in vitro. *The Journal of Cell Biology*, 95(3), pp.763-770.
81. Miller, J.B., 1990. Myogenic programs of mouse muscle cell lines: expression of myosin heavy chain isoforms, MyoD1, and myogenin. *The Journal of Cell Biology*, 111(3), pp.1149-1159.
82. Walsh, K. and Perlman, H., 1997. Cell cycle exit upon myogenic differentiation. *Current Opinion in Genetics & Development*, 7(5), pp.597-602.
83. Gilbert, S.F., Opitz, J.M. and Raff, R.A., 1996. Resynthesizing evolutionary and developmental biology. *Developmental Biology*, 173(2), pp.357-372.
84. Andrés, V. and Walsh, K., 1996. Myogenin expression, cell cycle withdrawal, and phenotypic differentiation are temporally separable events that precede cell fusion upon myogenesis. *The Journal of Cell Biology*, 132(4), pp.657-666.
85. Przybylski, R.J., MacBride, R.G. and Kirby, A.C., 1989. Calcium regulation of skeletal myogenesis. I. Cell content critical to myotube formation. *In vitro Cellular & Developmental Biology*, 25(9), pp.830-838.
86. Shainberg, A., Yagil, G. and Yaffe, D., 1969. Control of myogenesis in vitro by Ca<sup>2+</sup> concentration in nutritonal medium. *Experimental Cell Research*, 58(1), pp.163-167.
87. Park, S.Y., Yun, Y., Lim, J.S., Kim, M.J., Kim, S.Y., Kim, J.E. and Kim, I.S., 2016. Stabilin-2 modulates the efficiency of myoblast fusion during myogenic differentiation and muscle regeneration. *Nature Communications*, 7, p.10871.

88. Kherif, S., Dehaupas, M., Lafuma, C., Fardeau, M. and Alameddine, H.S., 1998. Matrix metalloproteinases MMP-2 and MMP-9 in denervated muscle and injured nerve. *Neuropathology and Applied Neurobiology*, 24(4), pp.309-319.
89. Chen, X. and Li, Y., 2009. Role of matrix metalloproteinases in skeletal muscle: migration, differentiation, regeneration and fibrosis. *Cell Adhesion & Migration*, 3(4), pp.337-341.
90. Yagami-Hiromasa, T., Sato, T., Kurisaki, T., Kamijo, K., Nabeshima, Y.I. and Fujisawa-Sehara, A., 1995. A metalloprotease-disintegrin participating in myoblast fusion. *Nature*, 377(6550), p.652.
91. Park, S.Y., Yun, Y., Lim, J.S., Kim, M.J., Kim, S.Y., Kim, J.E. and Kim, I.S., 2016. Stabilin-2 modulates the efficiency of myoblast fusion during myogenic differentiation and muscle regeneration. *Nature Communications*, 7, p.10871.
92. Bachmann, P., 1980. Motility, linear arrangement and cell-to-cell contact of myogenic cells prior to fusion. *Cell and Tissue Research*, 206(3), pp.431-440.
93. Swailes, N.T., Knight, P.J. and Peckham, M., 2004. Actin filament organization in aligned prefusion myoblasts. *Journal of Anatomy*, 205(5), pp.381-391.
94. Musa, H., Orton, C., Morrison, E.E. and Peckham, M., 2003. Microtubule assembly in cultured myoblasts and myotubes following nocodazole induced microtubule depolymerisation. *Journal of Muscle Research & Cell Motility*, 24(4-6), pp.303-310.
95. Vallenius, T., 2013. Actin stress fibre subtypes in mesenchymal-migrating cells. *Open Biology*, 3(6), p.130001.
96. Doherty, K.R., Cave, A., Davis, D.B., Delmonte, A.J., Posey, A., Earley, J.U., Hadhazy, M. and McNally, E.M., 2005. Normal myoblast fusion requires myoferlin. *Development*, 132(24), pp.5565-5575.
97. Lafreniere, J.F., Mills, P., Bouchentouf, M. and Tremblay, J.P., 2006. Interleukin-4 improves the migration of human myogenic precursor cells in vitro and in vivo. *Experimental Cell Research*, 312(7), pp.1127-1141.
98. Thomas, M., Langley, B., Berry, C., Sharma, M., Kirk, S., Bass, J. and Kambadur, R., 2000. Myostatin, a negative regulator of muscle growth, functions by inhibiting myoblast proliferation. *Journal of Biological Chemistry*, 275(51), pp.40235-40243.
99. Castellani, L., Salvati, E., Alemà, S. and Falcone, G., 2006. Fine regulation of RhoA and Rock is required for skeletal muscle differentiation. *Journal of Biological Chemistry*, 281(22), pp.15249-15257.
100. Nishiyama, T., Kii, I. and Kudo, A., 2004. Inactivation of Rho/ROCK signaling is crucial for the nuclear accumulation of FKHR and myoblast fusion. *Journal of Biological Chemistry*, 279(45), pp.47311-47319.
101. Bryan, B.A., Li, D., Wu, X. and Liu, M., 2005. The Rho family of small GTPases: crucial regulators of skeletal myogenesis. *Cellular and Molecular Life Sciences CMLS*, 62(14), pp.1547-1555.
102. Charrasse, S., Comunale, F., Grumbach, Y., Poulat, F., Blangy, A. and Gauthier-Rouviere, C., 2006. RhoA GTPase regulates M-cadherin activity and myoblast fusion. *Molecular Biology of the Cell*, 17(2), pp.749-759.

103. Charrasse, S., Comunale, F., Fortier, M., Portales-Casamar, E., Debant, A. and Gauthier-Rouviere, C., 2007. M-cadherin activates Rac1 GTPase through the Rho-GEF trio during myoblast fusion. *Molecular Biology of the Cell*, 18(5), pp.1734-1743.
104. Hollnagel, A., Grund, C., Franke, W. W., and Arnold, H. H. (2002). The cell adhesion molecule M-cadherin is not essential for muscle development and regeneration. *Molecular Cell Biology*, 22, 4760-4770.
105. Wei, L., Zhou, W., Croissant, J.D., Johansen, F.E., Prywes, R., Balasubramanyam, A. and Schwartz, R.J., 1998. RhoA signaling via serum response factor plays an obligatory role in myogenic differentiation. *Journal of Biological Chemistry*, 273(46), pp.30287-30294.
106. Stockdale, F.E. and Holtzer, H.O.W.A.R.D., 1961. DNA synthesis and myogenesis. *Experimental Cell Research*, 24(3), pp.508-520.
107. Bruusgaard, J.C., Liestøl, K., Ekmark, M., Kollstad, K. and Gundersen, K., 2003. Number and spatial distribution of nuclei in the muscle fibres of normal mice studied in vivo. *The Journal of Physiology*, 551(2), pp.467-478.
108. Metzger, T., Gache, V., Xu, M., Cadot, B., Folker, E.S., Richardson, B.E., Gomes, E.R. and Baylies, M.K., 2012. MAP and kinesin-dependent nuclear positioning is required for skeletal muscle function. *Nature*, 484(7392), p.120.
109. Cadot, B., Gache, V., Vasyutina, E., Falcone, S., Birchmeier, C. and Gomes, E.R., 2012. Nuclear movement during myotube formation is microtubule and dynein dependent and is regulated by Cdc42, Par6 and Par3. *EMBO Reports*, 13(8), pp.741-749.
110. Simon, A.M. and Burden, S.J., 1993. An E box mediates activation and repression of the acetylcholine receptor delta-subunit gene during myogenesis. *Molecular and Cellular Biology*, 13(9), pp.5133-5140.
111. Krause, R.M., Hamann, M., Bader, C.R., Liu, J.H., Baroffio, A. and Bernheim, L., 1995. Activation of nicotinic acetylcholine receptors increases the rate of fusion of cultured human myoblasts. *The Journal of Physiology*, 489(3), pp.779-790.
112. Bandi, E., Bernareggi, A., Grandolfo, M., Mozzetta, C., Augusti-Tocco, G., Ruzzier, F. and Lorenzon, P., 2005. Autocrine activation of nicotinic acetylcholine receptors contributes to Ca<sup>2+</sup> spikes in mouse myotubes during myogenesis. *The Journal of Physiology*, 568(1), pp.171-180.
113. Fambrough, D.M., 1979. Control of acetylcholine receptors in skeletal muscle. *Physiological Reviews*, 59(1), pp.165-227.
114. Entwistle, A., Zalin, R.J., Warner, A.E. and Bevan, S., 1988. A role for acetylcholine receptors in the fusion of chick myoblasts. *The Journal of Cell Biology*, 106(5), pp.1703-1712.
115. Sanes, J.R. and Lichtman, J.W., 1999. Development of the vertebrate neuromuscular junction. *Annual Review of Neuroscience*, 22(1), pp.389-442.
116. Ellman, G.L., Courtney, K.D., Andres Jr, V. and Featherstone, R.M., 1961. A new and rapid colorimetric determination of acetylcholinesterase activity. *Biochemical Pharmacology*, 7(2), pp.88-95.



117. Katz, B. and Thesleff, S., 1957. On the factors which determine the amplitude of the 'miniature end-plate potential'. *The Journal of Physiology*, 137(2), pp.267-278.
118. Padykula, H.A. and Gauthier, G.F., 1970. The ultrastructure of the neuromuscular junctions of mammalian red, white, and intermediate skeletal muscle fibers. *The Journal of Cell Biology*, 46(1), pp.27-41.
119. Frank, E. and Fischbach, G.D., 1979. Early events in neuromuscular junction formation in vitro: induction of acetylcholine receptor clusters in the postsynaptic membrane and morphology of newly formed synapses. *The Journal of Cell Biology*, 83(1), pp.143-158.
120. Iwasaki, S., Momiyama, A., Uchitel, O.D. and Takahashi, T., 2000. Developmental changes in calcium channel types mediating central synaptic transmission. *Journal of Neuroscience*, 20(1), pp.59-65.
121. Wu, H., Xiong, W.C. and Mei, L., 2010. To build a synapse: signaling pathways in neuromuscular junction assembly. *Development*, 137(7), pp.1017-1033.
122. Bello, O.D., Jouannot, O., Chaudhuri, A., Stroeve, E., Coleman, J., Volynski, K.E., Rothman, J.E. and Krishnakumar, S.S., 2018. Synaptotagmin oligomerization is essential for calcium control of regulated exocytosis. *Proceedings of the National Academy of Sciences*, 115(32), pp.E7624-E7631.
123. He, R., Zhang, J., Yu, Y., Jizi, L., Wang, W. and Li, M., 2018. New Insights Into Interactions of Presynaptic Calcium Channel Subtypes and Proteins in Neurotransmitter Release. *Frontiers in Molecular Neuroscience*, 11.
124. Isaacson, J.S., 2000. Synaptic transmission: spillover in the spotlight. *Current Biology*, 10(13), pp.R475-R477.
125. Sanes, J.R., 1982. Laminin, fibronectin, and collagen in synaptic and extrasynaptic portions of muscle fiber basement membrane. *The Journal of Cell Biology*, 93(2), pp.442-451.
126. Rotundo, R.L., Rossi, S.G., Kimbell, L.M., Ruiz, C. and Marrero, E., 2005. Targeting acetylcholinesterase to the neuromuscular synapse. *Chemico-Biological Interactions*, 157, pp.15-21.
127. Sanes, J.R. and Lichtman, J.W., 2001. Development: Induction, assembly, maturation and maintenance of a postsynaptic apparatus. *Nature Reviews Neuroscience*, 2(11), p.791.
128. Grubič, Z., Komel, R., Walker, W.F. and Miranda, A.F., 1995. Myoblast fusion and innervation with rat motor nerve alter distribution of acetylcholinesterase and its mRNA in cultures of human muscle. *Neuron*, 14(2), pp.317-327.
129. Feng, Z. and Ko, C.P., 2008. Schwann cells promote synaptogenesis at the neuromuscular junction via transforming growth factor- $\beta$ 1. *Journal of Neuroscience*, 28(39), pp.9599-9609.
130. Lanuza, M.A., Tomàs, J., Garcia, N., Cilleros, V., Just, L. and Tomàs, M., 2018. Axonal competition and synapse elimination during neuromuscular junction development. *Current Opinion in Physiology*.

131. O'Brien, R.A., Ostberg, A.J. and Vrbova, G., 1978. Observations on the elimination of polyneuronal innervation in developing mammalian skeletal muscle. *The Journal of Physiology*, 282(1), pp.571-582.
132. Thompson, W.J., 1985. Activity and synapse elimination at the neuromuscular junction. *Cellular and Molecular Neurobiology*, 5(1-2), pp.167-182.
133. Apel, E.D., Lewis, R.M., Grady, R.M. and Sanes, J.R., 2000. Syne-1, a dystrophin-and Klarsicht-related protein associated with synaptic nuclei at the neuromuscular junction. *Journal of Biological Chemistry*, 275(41), pp.31986-31995.
134. Wilson, M.H. and Deschenes, M.R., 2005. The neuromuscular junction: anatomical features and adaptations to various forms of increased, or decreased neuromuscular activity. *International Journal of Neuroscience*, 115(6), pp.803-828.
135. Tintignac, L.A., Brenner, H.R. and Rüegg, M.A., 2015. Mechanisms regulating neuromuscular junction development and function and causes of muscle wasting. *Physiological Reviews*, 95(3), pp.809-852.
136. Deschenes, M.R., Maresh, C.M. and Kraemer, W.J., 1994. The neuromuscular junction: Structure, function, and its role in the excitation of muscle. *The Journal of Strength & Conditioning Research*, 8(2), pp.103-109.
137. Fischbach, G.D., Frank, E., Jessell, T.M., Rubin, L.L. and Schuetze, S.M., 1978. Accumulation of acetylcholine receptors and acetylcholinesterase at newly formed nerve-muscle synapses. *Pharmacological Reviews*, 30(4), pp.411-428.
138. Wang, J., Fu, X.Q., Lei, W.L., Wang, T., Sheng, A.L. and Luo, Z.G., 2010. Nuclear factor  $\kappa$ B controls acetylcholine receptor clustering at the neuromuscular Junction. *Journal of Neuroscience*, 30(33), pp.11104-11113.
139. Salvaterra, P.M. and Foders, R.M., 1979. [1251] 2 $\alpha$ -bungarotoxin and quinuclidinylbenzilate binding in central nervous systems of different species. *Journal of Neurochemistry*, 32(5), pp.1509-1517.
140. Flanagan-Steet, H., Fox, M.A., Meyer, D. and Sanes, J.R., 2005. Neuromuscular synapses can form in vivo by incorporation of initially aneural postsynaptic specializations. *Development*, 132(20), pp.4471-4481.
141. Mazhar, S. and Herbst, R., 2012. The formation of complex acetylcholine receptor clusters requires MuSK kinase activity and structural information from the MuSK extracellular domain. *Molecular and Cellular Neuroscience*, 49(4), pp.475-486.
142. Sandrock, A.W., Dryer, S.E., Rosen, K.M., Gozani, S.N., Kramer, R., Theill, L.E. and Fischbach, G.D., 1997. Maintenance of acetylcholine receptor number by neuregulins at the neuromuscular junction in vivo. *Science*, 276(5312), pp.599-603.
143. Ruegg, M.A. and Bixby, J.L., 1998. Agrin orchestrates synaptic differentiation at the vertebrate neuromuscular junction. *Trends in Neurosciences*, 21(1), pp.22-27.
144. Glass, D.J. and Yancopoulos, G.D., 1997. Sequential roles of agrin, MuSK and rapsyn during neuromuscular junction formation. *Current Opinion in Neurobiology*, 7(3), pp.379-384.

145. Ferns, M., Deiner, M. and Hall, Z., 1996. Agrin-induced acetylcholine receptor clustering in mammalian muscle requires tyrosine phosphorylation. *The Journal of Cell Biology*, 132(5), pp.937-944.
146. Borges, L.S. and Ferns, M., 2001. Agrin-induced phosphorylation of the acetylcholine receptor regulates cytoskeletal anchoring and clustering. *The Journal of cell biology*, 153(1), pp.1-12.
147. Hirokawa, N. and Heuser, J.E., 1982. Internal and external differentiations of the postsynaptic membrane at the neuromuscular junction. *Journal of Neurocytology*, 11(3), pp.487-510.
148. Kleiman, R.J. and Reichardt, L.F., 1996. Testing the agrin hypothesis. *Cell*, 85(4), pp.461-464.
149. Gautam, M., Noakes, P.G., Moscoso, L., Rupp, F., Scheller, R.H., Merlie, J.P. and Sanes, J.R., 1996. Defective neuromuscular synaptogenesis in agrin-deficient mutant mice. *Cell*, 85(4), pp.525-535.
150. Hoch, W., 1999. Formation of the neuromuscular junction: agrin and its unusual receptors. *European Journal of Biochemistry*, 265(1), pp.1-10.
151. Kim, N., Stiegler, A.L., Cameron, T.O., Hallock, P.T., Gomez, A.M., Huang, J.H., Hubbard, S.R., Dustin, M.L. and Burden, S.J., 2008. Lrp4 is a receptor for Agrin and forms a complex with MuSK. *Cell*, 135(2), pp.334-342.
152. Lee, Y., Rudell, J. and Ferns, M., 2009. Rapsyn interacts with the muscle acetylcholine receptor via  $\alpha$ -helical domains in the  $\alpha$ ,  $\beta$ , and  $\epsilon$  subunit intracellular loops. *Neuroscience*, 163(1), pp.222-232.
153. Froehner, S.C., Gulbrandsen, V., Hyman, C., Jeng, A.Y., Neubig, R.R. and Cohen, J.B., 1981. Immunofluorescence localization at the mammalian neuromuscular junction of the Mr 43,000 protein of Torpedo postsynaptic membranes. *Proceedings of the National Academy of Sciences*, 78(8), pp.5230-5234.
154. Johnson, E.B., Hammer, R.E. and Herz, J., 2005. Abnormal development of the apical ectodermal ridge and polysyndactyly in Megf7-deficient mice. *Human Molecular Genetics*, 14(22), pp.3523-3538.
155. Wu, H., Lu, Y., Shen, C., Patel, N., Gan, L., Xiong, W.C. and Mei, L., 2012. Distinct roles of muscle and motoneuron LRP4 in neuromuscular junction formation. *Neuron*, 75(1), pp.94-107.
156. Wang, J., Jing, Z., Zhang, L., Zhou, G., Braun, J., Yao, Y. and Wang, Z.Z., 2003. Regulation of acetylcholine receptor clustering by the tumor suppressor APC. *Nature Neuroscience*, 6(10), p.1017.
157. Henriquez, J.P., Webb, A., Bence, M., Bildsoe, H., Sahores, M., Hughes, S.M. and Salinas, P.C., 2008. Wnt signaling promotes AChR aggregation at the neuromuscular synapse in collaboration with agrin. *Proceedings of the National Academy of Sciences*, 105(48), pp.18812-18817.
158. Fischbach, G.D. and Rosen, K.M., 1997. ARIA: a neuromuscular junction neuregulin. *Annual Review of Neuroscience*, 20(1), pp.429-458.
159. Goodearl, A.D., Yee, A.G., Sandrock, A.W., Corfas, G. and Fischbach, G.D., 1995. ARIA is concentrated in the synaptic basal lamina of the developing chick neuromuscular junction. *The Journal of Cell Biology*, 130(6), pp.1423-1434.

160. Jones, G., Herczeg, A., Ruegg, M.A., Lichtsteiner, M., Kröger, S. and Brenner, H.R., 1996. Substrate-bound agrin induces expression of acetylcholine receptor epsilon-subunit gene in cultured mammalian muscle cells. *Proceedings of the National Academy of Sciences*, 93(12), pp.5985-5990.
161. Harris, D.A., Falls, D.L., Dill-Devor, R.M. and Fischbach, G.D., 1988. Acetylcholine receptor-inducing factor from chicken brain increases the level of mRNA encoding the receptor alpha subunit. *Proceedings of the National Academy of Sciences*, 85(6), pp.1983-1987.
162. Martinou, J.C., Falls, D.L., Fischbach, G.D. and Merlie, J.P., 1991. Acetylcholine receptor-inducing activity stimulates expression of the epsilon-subunit gene of the muscle acetylcholine receptor. *Proceedings of the National Academy of Sciences*, 88(17), pp.7669-7673.
163. Englander, L.L. and Rubin, L.L., 1987. Acetylcholine receptor clustering and nuclear movement in muscle fibers in culture. *The Journal of Cell Biology*, 104(1), pp.87-95.
164. Schaeffer, L., de Kerchove d'Exaerde, A. and Changeux, J.P., 2001. Targeting transcription to the neuromuscular synapse. *Neuron*, 31(1), pp.15-22.
165. Grady, R.M., Starr, D.A., Ackerman, G.L., Sanes, J.R. and Han, M., 2005. Syne proteins anchor muscle nuclei at the neuromuscular junction. *Proceedings of the National Academy of Sciences*, 102(12), pp.4359-4364.
166. Shelton, G.D., 2002. Myasthenia gravis and disorders of neuromuscular transmission. *Veterinary Clinics: Small Animal Practice*, 32(1), pp.189-206.
167. Hirsch, N.P., 2007. Neuromuscular junction in health and disease. *British journal of anaesthesia*, 99(1), pp.132-138.
168. Verschuuren, J., Strijbos, E. and Vincent, A., 2016. Neuromuscular junction disorders. In *Handbook of Clinical Neurology* (Vol. 133, pp. 447-466). Elsevier.
169. Meriggioli, M.N. and Sanders, D.B., 2012. Muscle autoantibodies in myasthenia gravis: beyond diagnosis?. *Expert Review of Clinical Immunology*, 8(5), pp.427-438.
170. William, C., Claussen, G., Thomas, D., Fesenmeier, J.T., Pearlman, R.L. and Oh, S.J., 1993. Primary respiratory failure as the presenting symptom in Lambert-Eaton myasthenic syndrome. *Muscle & Nerve: Official Journal of the American Association of Electrodiagnostic Medicine*, 16(7), pp.712-715.
171. Lu, B., 2015. The destructive effect of botulinum neurotoxins on the SNARE protein: SNAP-25 and synaptic membrane fusion. *PeerJ*, 3, p.e1065.
172. Newsom-Davis, J., 2004. Neuromyotonia. *Revue Neurologique*, 160(5), pp.85-89.
173. Packard, M., Koo, E.S., Gorczyca, M., Sharpe, J., Cumberledge, S. and Budnik, V., 2002. The Drosophila Wnt, wingless, provides an essential signal for pre-and postsynaptic differentiation. *Cell*, 111(3), pp.319-330.
174. Pérez-García, M.J. and Burden, S.J., 2012. Increasing MuSK activity delays denervation and improves motor function in ALS mice. *Cell Reports*, 2(3), pp.497-502.

175. Vilmont, V., Cadot, B., Ouanounou, G. and Gomes, E.R., 2016. A system for studying mechanisms of neuromuscular junction development and maintenance. *Development*, 143(13), pp.2464-2477.
176. Umbach, J.A., Adams, K.L., Gundersen, C.B. and Novitch, B.G., 2012. Functional neuromuscular junctions formed by embryonic stem cell-derived motor neurons. *PLoS One*, 7(5), p.e36049.
177. Martin, N.R., Passey, S.L., Player, D.J., Mudera, V., Baar, K., Greensmith, L. and Lewis, M.P., 2015. Neuromuscular junction formation in tissue-engineered skeletal muscle augments contractile function and improves cytoskeletal organization. *Tissue Engineering Part A*, 21(19-20), pp.2595-2604.
178. Sugiyama, J.E., Glass, D.J., Yancopoulos, G.D. and Hall, Z.W., 1997. Laminin-induced acetylcholine receptor clustering: an alternative pathway. *The Journal of Cell Biology*, 139(1), pp.181-191.
179. Montanaro, F., Gee, S.H., Jacobson, C., Lindenbaum, M.H., Froehner, S.C. and Carbonetto, S., 1998. Laminin and  $\alpha$ -dystroglycan mediate acetylcholine receptor aggregation via a MuSK-independent pathway. *Journal of Neuroscience*, 18(4), pp.1250-1260.
180. Hubbard, S.R. and Gnanasambandan, K., 2013. Structure and activation of MuSK, a receptor tyrosine kinase central to neuromuscular junction formation. *Biochimica et Biophysica Acta (BBA)-Proteins and Proteomics*, 1834(10), pp.2166-2169.
181. Guo, X., Gonzalez, M., Stancescu, M., Vandenberg, H.H. and Hickman, J.J., 2011. Neuromuscular junction formation between human stem cell-derived motoneurons and human skeletal muscle in a defined system. *Biomaterials*, 32(36), pp.9602-9611.
182. Slater, C., 2017. The structure of human neuromuscular junctions: some unanswered molecular questions. *International Journal of Nolecular Sciences*, 18(10), p.2183.
183. Kishi, M., Kummer, T.T., Eglon, S.J. and Sanes, J.R., 2005. LL5 $\beta$ : a regulator of postsynaptic differentiation identified in a screen for synaptically enriched transcripts at the neuromuscular junction. *The Journal of Cell Biology*, 169(2), pp.355-366.
184. Gajsek, N., Jevsek, M., Mars, T., Mis, K., Pirkmajer, S., Breclj, J. and Grubic, Z., 2008. Synaptogenetic mechanisms controlling postsynaptic differentiation of the neuromuscular junction are nerve-dependent in human and nerve-independent in mouse C2C12 muscle cultures. *Chemico-Biological Interactions*, 175(1-3), pp.50-57.
185. Bischoff, R. and Holtzer, H., 1968. The effect of mitotic inhibitors on myogenesis in vitro. *The Journal of Cell Biology*, 36(1), pp.111-127.
186. Ríos, R., Carneiro, I., Arce, V.M. and Devesa, J., 2001. Myostatin regulates cell survival during C2C12 myogenesis. *Biochemical and Biophysical Research Communications*, 280(2), pp.561-566.
187. Goto, S., Miyazaki, K., Funabiki, T. and Yasumitsu, H., 1999. Serum-free culture conditions for analysis of secretory proteinases during myogenic differentiation of mouse C2C12 myoblasts. *Analytical Biochemistry*, 272(2), pp.135-142.
188. Langelan, M.L., Boonen, K.J., Rosaria-Chak, K.Y., van der Schaft, D.W., Post, M.J. and Baaijens, F.P., 2011. Advanced maturation by electrical stimulation: Differences in response between C2C12 and primary muscle progenitor cells. *Journal of Tissue Engineering and Regenerative Medicine*, 5(7), pp.529-539.

189. Xie, M.H., Yuan, J., Adams, C. and Gurney, A., 1997. Direct demonstration of MuSK involvement in acetylcholine receptor clustering through identification of agonist ScFv. *Nature Biotechnology*, 15(8), p.768.
190. Gajsek, N., Jevsek, M., Mars, T., Mis, K., Pirkmajer, S., Breclj, J. and Grubic, Z., 2008. Synaptogenetic mechanisms controlling postsynaptic differentiation of the neuromuscular junction are nerve-dependent in human and nerve-independent in mouse C2C12 muscle cultures. *Chemico-Biological Interactions*, 175(1-3), pp.50-57.
191. Lacazette, E., Le Calvez, S., Gajendran, N. and Brenner, H.R., 2003. A novel pathway for MuSK to induce key genes in neuromuscular synapse formation. *The Journal of Cell Biology*, 161(4), pp.727-736.
192. Jiang, J.X., Choi, R.C., Siow, N.L., Lee, H.H., Wan, D.C. and Tsim, K.W., 2003. Muscle Induces Neuronal Expression of Acetylcholinesterase in Neuron-Muscle Co-culture TRANSCRIPTIONAL REGULATION MEDIATED BY cAMP-DEPENDENT SIGNALING. *Journal of Biological Chemistry*, 278(46), pp.45435-45444.
193. Thomson, J.A., Itskovitz-Eldor, J., Shapiro, S.S., Waknitz, M.A., Swiergiel, J.J., Marshall, V.S. and Jones, J.M., 1998. Embryonic stem cell lines derived from human blastocysts. *science*, 282(5391), pp.1145-1147.
194. Andrews, P.W., Matin, M.M., Bahrami, A.R., Damjanov, I., Gokhale, P. and Draper, J.S., 2005. Embryonic stem (ES) cells and embryonal carcinoma (EC) cells: opposite sides of the same coin, pp.1526-1530.
195. Jones, T.D., Ulbright, T.M., Eble, J.N., Baldrige, L.A. and Cheng, L., 2004. OCT4 staining in testicular tumors: a sensitive and specific marker for seminoma and embryonal carcinoma. *The American Journal of Surgical Pathology*, 28(7), pp.935-940.
196. Kleinsmith, L.J. and Pierce, G.B., 1964. Multipotentiality of single embryonal carcinoma cells. *Cancer Research*, 24(9), pp.1544-1551.
197. Dawud, R.A., Schreiber, K., Schomburg, D. and Adjaye, J., 2012. Human embryonic stem cells and embryonal carcinoma cells have overlapping and distinct metabolic signatures. *PloS One*, 7(6), p.e39896.
198. Stewart, R., Coyne, L., Lako, M., Halliwell, R.F. and Przyborski, S.A., 2004. Human embryonal carcinoma stem cells expressing green fluorescent protein form functioning neurons in vitro: a research tool for co-culture studies. *Stem Cells and Development*, 13(6), pp.646-657.
199. Przyborski, S.A., Christie, V.B., Hayman, M.W., Stewart, R. and Horrocks, G.M., 2004. Human embryonal carcinoma stem cells: models of embryonic development in humans. *Stem Cells and Development*, 13(4), pp.400-408.
200. Stewart, R., Christie, V.B. and Przyborski, S.A., 2003. Manipulation of human pluripotent embryonal carcinoma stem cells and the development of neural subtypes. *Stem Cells*, 21(3), pp.248-256.
201. Horrocks, G.M., Lauder, L., Stewart, R. and Przyborski, S., 2003. Formation of neurospheres from human embryonal carcinoma stem cells. *Biochemical and Biophysical Research Communications*, 304(2), pp.411-416.

202. Clemens, G., Flower, K.R., Henderson, A.P., Whiting, A., Przyborski, S.A., Jimenez-Hernandez, M., Ball, F., Bassan, P., Cinque, G. and Gardner, P., 2013. The action of all-trans-retinoic acid (ATRA) and synthetic retinoid analogues (EC19 and EC23) on human pluripotent stem cells differentiation investigated using single cell infrared microspectroscopy. *Molecular BioSystems*, 9(4), pp.677-692.
203. Przyborski, S.A., 2001. Isolation of human embryonal carcinoma stem cells by immunomagnetic sorting. *Stem Cells*, 19(6), pp.500-504.
204. Goncalves, K.E., 2017. *Development of novel stem cell based neurite outgrowth models and their application to study neurite inhibition in neurological disorders* (Doctoral dissertation, Durham University).
205. Ostrovidov, S., Ahadian, S., Ramon-Azcon, J., Hosseini, V., Fujie, T., Parthiban, S.P., Shiku, H., Matsue, T., Kaji, H., Ramalingam, M. and Bae, H., 2017. Three-dimensional co-culture of C2C12/PC12 cells improves skeletal muscle tissue formation and function. *Journal of Tissue Engineering and Regenerative Medicine*, 11(2), pp.582-595.
206. Pan, C., 2007. *Neural differentiation from human embryonal carcinoma stem cells* (Doctoral dissertation, Durham University).
207. Lawson, M.A. and Purslow, P.P., 2000. Differentiation of myoblasts in serum-free media: effects of modified media are cell line-specific. *Cells Tissues Organs*, 167(2-3), pp.130-137
208. Lu, H., Shah, P., Ennis, D., Shinder, G., Sap, J., Le-Tien, H. and Fantus, I.G., 2002. The differentiation of skeletal muscle cells involves a protein-tyrosine phosphatase- $\alpha$ -mediated C-Src signaling pathway. *Journal of Biological Chemistry*, 277(48), pp.46687-46695.
209. Land, B.R., Podleski, T.R., Salpeter, E.E. and Salpeter, M.M., 1977. Acetylcholine receptor distribution on myotubes in culture correlated to acetylcholine sensitivity. *The Journal of Physiology*, 269(1), pp.155-176.
210. Oswald, R.E. and Freeman, J.A., 1981. Alpha-bungarotoxin binding and central nervous system nicotinic acetylcholine receptors. *Neuroscience*, 6(1), pp.1-14.
211. Strickland, S. and Mahdavi, V., 1978. The induction of differentiation in teratocarcinoma stem cells by retinoic acid. *Cell*, 15(2), pp.393-403.
212. Lehman, P.A., Slattery, J.T. and Franz, T.J., 1988. Percutaneous absorption of retinoids: influence of vehicle, light exposure, and dose. *Journal of Investigative Dermatology*, 91(1), pp.56-61.
213. Gordon, J., Amini, S. and White, M.K., 2013. General overview of neuronal cell culture. *Neuronal Cell Culture* (pp. 1-8). Humana Press, Totowa, NJ.
214. Bird, M.M., 1983. Neurons and glial cells in long term cultures of previously dissociated newborn mouse cerebral cortex. *Journal of Anatomy*, 136(Pt 2), p.293.
215. Chen, S.H., Oyarzabal, E.A. and Hong, J.S., 2013. Preparation of Rodent Primary Cultures for Neuron–Glia, Mixed Glia, Enriched Microglia, and Reconstituted Cultures with Microglia. In *Microglia* (pp. 231-240). Humana Press, Totowa, NJ.
216. Eng, L.F., 1985. Glial fibrillary acidic protein (GFAP): the major protein of glial intermediate filaments in differentiated astrocytes. *Journal of Neuroimmunology*, 8, pp.203-214.

217. Bain, G., Kitchens, D., Yao, M., Huettner, J.E. and Gottlieb, D.I., 1995. Embryonic stem cells express neuronal properties in vitro. *Developmental Biology*, 168(2), pp.342-357.
218. Reubinoff, B.E., Pera, M.F., Fong, C.Y., Trounson, A. and Bongso, A., 2000. Embryonic stem cell lines from human blastocysts: somatic differentiation in vitro. *Nature Biotechnology*, 18(4), p.399.
219. Lingor, P., Teusch, N., Schwarz, K., Mueller, R., Mack, H., Bähr, M. and Mueller, B.K., 2007. Inhibition of Rho kinase (ROCK) increases neurite outgrowth on chondroitin sulphate proteoglycan in vitro and axonal regeneration in the adult optic nerve in vivo. *Journal of Neurochemistry*, 103(1), pp.181-189.
220. Sit, S.T. and Manser, E., 2011. Rho GTPases and their role in organizing the actin cytoskeleton. *Journal of Cell Science*, 124(5), pp.679-683.
221. Ridley, A.J., 2015. Rho GTPase signalling in cell migration. *Current Opinion in Cell Biology*, 36, pp.103-112.
222. Jiang, L., Liu, X., Kolokythas, A., Yu, J., Wang, A., Heidbreder, C.E., Shi, F. and Zhou, X., 2010. Downregulation of the Rho GTPase signaling pathway is involved in the microRNA-138-mediated inhibition of cell migration and invasion in tongue squamous cell carcinoma. *International Journal of Cancer*, 127(3), pp.505-512.
223. Berkes, C.A. and Tapscott, S.J., 2005, August. MyoD and the transcriptional control of myogenesis. *Seminars in Cell & Developmental Biology* (Vol. 16, No. 4-5, pp. 585-595). Academic Press.
224. Burattini, S., Ferri, P., Battistelli, M., Curci, R., Luchetti, F. and Falcieri, E., 2004. C2C12 murine myoblasts as a model of skeletal muscle development: morpho-functional characterization. *European Journal of Histochemistry*, pp.223-234.
225. Mastroiannopoulos, N.P., Nicolaou, P., Anayasa, M., Uney, J.B. and Phylactou, L.A., 2012. Down-regulation of myogenin can reverse terminal muscle cell differentiation. *PLoS One*, 7(1), p.e29896.
226. Albuquerque, E.X., Pereira, E.F., Alkondon, M. and Rogers, S.W., 2009. Mammalian nicotinic acetylcholine receptors: from structure to function. *Physiological Reviews*, 89(1), pp.73-120.
227. Siu, P.M., Wang, Y. and Alway, S.E., 2009. Apoptotic signalling induced by H<sub>2</sub>O<sub>2</sub>-mediated oxidative stress in differentiated C2C12 myotubes. *Life Sciences*, 84(13-14), pp.468-481.
228. Shiokawa, D., Kobayashi, T. and Tanuma, S.I., 2002. Involvement of DNase  $\gamma$  in apoptosis associated with myogenic differentiation of C2C12 cells. *Journal of Biological Chemistry*, 277(34), pp.31031-31037.
229. Plantman, S., Patarroyo, M., Fried, K., Domogatskaya, A., Tryggvason, K., Hammarberg, H. and Cullheim, S., 2008. Integrin-laminin interactions controlling neurite outgrowth from adult DRG neurons in vitro. *Molecular and Cellular Neuroscience*, 39(1), pp.50-62.
230. Robinson, R., 2012. Axons compete for neuromuscular junctions. *PLoS Biology*, 10(6), p.e1001354.



231. Turney, S.G. and Lichtman, J.W., 2012. Reversing the outcome of synapse elimination at developing neuromuscular junctions in vivo: evidence for synaptic competition and its mechanism. *PLoS Biology*, 10(6), p.e1001352.
232. Brenner, H.R., Witzemann, V. and Sakmann, B., 1990. Imprinting of acetylcholine receptor messenger RNA accumulation in mammalian neuromuscular synapses. *Nature*, 344(6266), p.544.
233. Kummer, T.T., Misgeld, T. and Sanes, J.R., 2006. Assembly of the postsynaptic membrane at the neuromuscular junction: paradigm lost. *Current Opinion in Neurobiology*, 16(1), pp.74-82.
234. Fambrough, D.M., 1979. Control of acetylcholine receptors in skeletal muscle. *Physiological Reviews*, 59(1), pp.165-227.
235. Bowman, W.C., 2006. Neuromuscular block. *British Journal of Pharmacology*, 147(S1), pp.S277-S286.
236. Monnier, P.P., Sierra, A., Schwab, J.M., Henke-Fahle, S. and Mueller, B.K., 2003. The Rho/ROCK pathway mediates neurite growth-inhibitory activity associated with the chondroitin sulfate proteoglycans of the CNS glial scar. *Molecular and Cellular Neuroscience*, 22(3), pp.319-330.
237. Vasyutina, E., Martarelli, B., Brakebusch, C., Wende, H. and Birchmeier, C., 2009. The small G-proteins Rac1 and Cdc42 are essential for myoblast fusion in the mouse. *Proceedings of the National Academy of Sciences*, 106(22), pp.8935-8940.
238. Asano, T., Ishizuka, T., Morishima, K. and Yawo, H., 2015. Optogenetic induction of contractile ability in immature C2C12 myotubes. *Scientific Reports*, 5, p.8317.
239. Coque, E., Raoul, C. and Bowerman, M., 2014. ROCK inhibition as a therapy for spinal muscular atrophy: understanding the repercussions on multiple cellular targets. *Frontiers in Neuroscience*, 8, p.271.
240. Günther, R., Saal, K.A., Suhr, M., Scheer, D., Koch, J.C., Bähr, M., Lingor, P. and Tönges, L., 2014. The Rho kinase inhibitor Y-27632 improves motor performance in male SOD1G93A mice. *Frontiers in Neuroscience*, 8, p.304.
241. THELEN, M.H., SIMONIDES, W.S. and van HARDEVELD, C., 1997. Electrical stimulation of C2C12 myotubes induces contractions and represses thyroid-hormone-dependent transcription of the fast-type sarcoplasmic-reticulum Ca<sup>2+</sup>-ATPase gene. *Biochemical Journal*, 321(3), pp.845-848.
242. Coyne, L., Shan, M., Przyborski, S.A., Hirakawa, R. and Halliwell, R.F., 2011. Neuropharmacological properties of neurons derived from human stem cells. *Neurochemistry International*, 59(3), pp.404-412.
243. Wolfram, V., Southall, T.D., Günay, C., Prinz, A.A., Brand, A.H. and Baines, R.A., 2014. The transcription factors islet and Lim3 combinatorially regulate ion channel gene expression. *Journal of Neuroscience*, 34(7), pp.2538-2543.
244. Goulding, M., 1998. Specifying Motor Neurons and their Connections. *Neuron*, 21(5), pp.943-946.
245. Hu, B.Y. and Zhang, S.C., 2009. Differentiation of spinal motor neurons from pluripotent human stem cells. *Nature Protocols*, 4(9), p.1295.

246. Litingtung, Y. and Chiang, C., 2000. Specification of ventral neuron types is mediated by an antagonistic interaction between Shh and Gli3. *Nature Neuroscience*, 3(10), p.979.
247. Ralston, E., Lu, Z. and Ploug, T., 1999. The organization of the Golgi complex and microtubules in skeletal muscle is fiber type-dependent. *Journal of Neuroscience*, 19(24), pp.10694-10705.
248. McMahon, D.K., Anderson, P.A., Nassar, R.A.S.H.I.D., Bunting, J.B., Saba, Z., Oakeley, A.E. and Malouf, N.N., 1994. C2C12 cells: biophysical, biochemical, and immunocytochemical properties. *American Journal of Physiology-Cell Physiology*, 266(6), pp.C1795-C1802.
249. Taylor, J.H., Haut, W.F. and Tung, J., 1962. Effects of fluorodeoxyuridine on DNA replication, chromosome breakage, and reunion. *Proceedings of the National Academy of Sciences of the United States of America*, 48(2), p.190.
250. Teleka, S., Chijuwa, A., Senga, E. and Chisi, J.E., 2011. Cytosine arabinoside reduces the numbers of granulocyte macrophage colony forming cells (GMCFc) and high proliferative potential colony forming cells (HPP-CFC) in vivo in mice. *Malawi Medical Journal*, 23(4), pp.119-122.
251. Schuler, F. and Sorokin, L.M., 1995. Expression of laminin isoforms in mouse myogenic cells in vitro and in vivo. *Journal of Cell Science*, 108(12), pp.3795-3805.
252. Gardner, J.M. and Fambrough, D.M., 1983. Fibronectin expression during myogenesis. *The Journal of Cell Biology*, 96(2), pp.474-485.
253. Huveneers, S., Truong, H., Fässler, R., Sonnenberg, A. and Danen, E.H., 2008. Binding of soluble fibronectin to integrin  $\alpha 5\beta 1$ —link to focal adhesion redistribution and contractile shape. *Journal of Cell Science*, 121(15), pp.2452-2462.
254. Hong, W. and Lev, S., 2014. Tethering the assembly of SNARE complexes. *Trends in Cell Biology*, 24(1), pp.35-43.
255. Slater, C.R., 2017. The structure of human neuromuscular junctions: some unanswered molecular questions. *International Journal of Molecular Sciences*, 18(10), p.2183.